Deutsches Zentrum für Neurodegenerative Erkrankungen

Standort München

α- and β-secretase in Alzheimer's disease: Identity and physiological substrates

Peer-Hendrik Kuhn

Vollständiger Abdruck der von der Fakultät für Medizin der Technischen Universität München zur Erlangung des akademischen Grades eines

Doctor of Philosophy (Ph.D.)

genehmigten Dissertation.

Vorsitzender: apl. Prof. Dr. Helmuth K. H. Adelsberger

Prüfer der Dissertation:

1. Univ.- Prof. Dr. Thomas Misgeld

2. Priv.-Doz. Dr. Stefan Lichtenthaler

Die Dissertation wurde am 29.2.2012 bei der Fakultät für Medizin der Technischen Universität München eingereicht und durch die Fakultät für Medizin am 08.03.2012 angenommen.

Content

Table index

1 Introduction

1.1 Alzheimer's disease

1.1.1 History

Alzheimer's disease (AD) was first described by the psychiatrist and neurologist Alois Alzheimer in 1907 (Stelzmann et al., 1995) (Fig 1C). He described the clinical presentation of his patient Auguste Deter in the course of her mental disease (Fig 1 B). In the beginning of her disease Auguste Deter's behavior was characterized by unjustified jealousy of her husband. During disease progression her memory capabilities deteriorated and she was increasingly less oriented to time and location. Though she was able to perfectly name objects shown to her, she almost immediately forgot about these. Her procedural memory suffered as well during the course of the disease which was reflected by her ignorance to use certain objects. However, her motoric skills were perfectly normal. She could walk and use her hands properly and her motoric reflexes showed no abnormalities (Alzheimer et al., 1995; Stelzmann et al., 1995). Alois Alzheimer was in the lucky situation to be able to investigate the brain of Auguste Deter after her death. He was the first to describe the histopathological changes in the brain of Alzheimer disease patients. Using Bielschowsky's silver stain technique he illustrated neurofibrillar tangles in the brain while describing amyloid plaques as miliary foci refractory to staining (Uchihara, 2007) (Fig. 1 A).

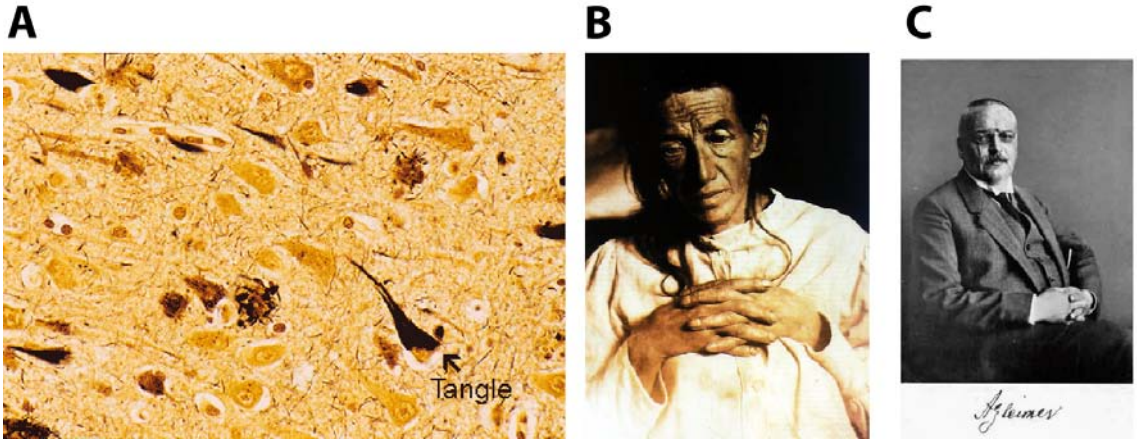

Figure 1 History of Alzheimer'S disease: (A) Bielschowsky silver stain of tangle in a brain specimen of an Alzheimer's disease patient. (B) Photograph of the first described Alzheimer's Disease (AD) patient Auguste Deter. (C) Photograph of the pyschatrist Alois Alzheimer who was the first to describe the behavioral changes of Auguster Deter during the course of AD and after her death the pathological changes in the brain of Auguste Deter. Picture Sources: http://moon.ouhsc.edu/kfung/JTY1/NeuroTest/Images/SampleR03-Tangle.gif http://hod.kcms.msu.edu/timeline.php?y=1901-1906

1.1.2 Epidemiology

Meanwhile, Alzheimer's disease is recognized as a neurodegenerative disorder which affects more than estimated 24 million people worldwide (Ballard et al., 2011). The prevalence of Alzheimer's disease is predicted to double every 20 years, affecting estimated 80 million people worldwide in 2040 (Ferri et al., 2005; Reitz et al., 2011). AD exhibits an epidemic distribution with a focus in countries of the Western world. The annual incidence rate of Alzheimer's disease increases with age, ranging from 0,4% of all people between 65 and 69 to nearly 10% of all people exceeding the age of 90. As a consequence, due to a demographic shift in favor of the elderly resulting from longer life expectancies and low birth rates, Western world populations are faced with the problem of higher numbers of Alzheimer's disease cases which are opposed by a decreasing younger population who could take care of these patients. The economic impact of dementia is displayed by €177 billion solely spent for dementia in Europe in the year 2008 (Wimo et al., 2011). The annual cost per patient with dementia is estimated at nearly €20,000.

1.1.3 Histopathology of Alzheimer's disease

Post mortem brain specimens are characterized by the three major neuropathological changes neuronal loss, tau tangles and amyloid plaques. The most important feature of Alzheimer's disease is the loss of particular cholinergic neurons (Davies and Maloney, 1976; Rasool et al., 1986; Whitehouse et al., 1982).

Tau tangles are oligomeric intracellular deposits of the microtubule binding protein Tau which has been first described as 68 kDa large protein in 1986 (Wolozin et al., 1986). Later, the gene coding for this protein was identified (Goedert et al., 1988). In healthy neurons tau binds to microtubules and promotes microtubule formation while in damaged neurons tau becomes hyperphosphorylated, dissociates from the microtubules which initiates tau tangle formation (Iqbal et al., 1986). Tau monomers start to form oligomers which in turn start to aggregate to even larger conglomerates, so-called tau tangles. These can be easily detected by light microscopy in post-mortem brain specimens after silver staining (Gallyas, 1971). Braak introduced a staging system for Alzheimer's disease which is based on the spatiotemporal formation of tau tangles which can be visualized either by a modified Gallyas silver stain or the phospho-tau specific antibody AT8 (Braak and Braak, 1997; Braak et al., 2006; Gallyas, 1971). Tau tangle formation precedes neuronal cell death. According to the Braak staging

neurofibrillar tangle (NFT) formation of the tau protein begins in pre-α projection neurons of the transentorhinal cortex to mildly affect entorhinal cortex and hippocampus in stage II. Stage III is characterized by a severe involvement of the pre-α layer in both transentorhinal and entorhinal cortex. For the first time, ghost tangles can be observed which belong to former neurons. The isocortex is still devoid of tangles or only mildly affected. In stage IV and V the layers Pre-α and Pre-β of the entorhinal cortex, CA1 of the hippocampal formation and the amygdala are severely affected by tangle formation while the number of ghost tangles increases dramatically. Stage V and VI are characterized by a complete involvement of the hippocampus and NFT formation in the isocortex. The described spatiotemporal development of tangles can be used to discriminate between different stages of Alzheimer's disease.

Amyloid plaques develop in the cortex during the course of the disease. These plaques were first identified by Konrad Bayreuther to be composed of Amyloid-β (Aβ), a small hydrophobic peptide which results from proteolytic processing of the Amyloid Precursor Protein (APP) (Glenner and Wong, 1984; Masters et al., 1985a; Masters et al., 1985b). The deposition of plaques also increases with disease progression (Braak and Braak, 1991). However, plaque formation is subject to variability among different individuals. Hence, amyloid deposits are considered to be only of limited significance for the differentiation of Alzheimer's disease stages.

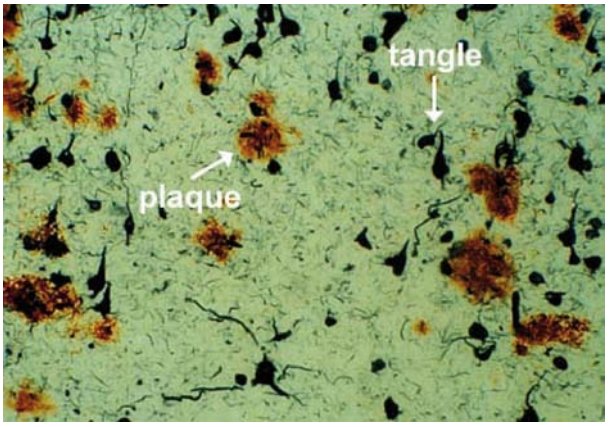

Figure 2 Representative picture of the cortex of an Alzheimer's disease brain: Visualized are extracellular senile plaques which are composed of the peptide Amyloid β (brown) and intracellular tau tangles (black) which are composed of the microtubule binding protein tau. http://ladulab.anat.uic.edu/images/ADstain.jpg

1.1.4 Familial Alzheimer's disease (FAD)

The advent of Alzheimer's disease research started with the investigation of deceased, demented Down's syndrome (DS) patients. Post-mortem analysis of brain

specimens revealed a pathology which was reminiscent to Alzheimer's disease (Jervis, 1948). The coincidental occurrence of AD pathology and triplication of chromosome 21 in DS patients caused researchers to suspect an AD risk gene on chromosome 21. In 1987 St.Georg-Hyslop identified a genetic mutation on chromosome 21 which segregated with a familial form of AD (St George-Hyslop et al., 1987). Two related articles described the mapping of the gene of the amyloid precursor protein. Finally, Goate identified an APP missense mutation which segregated with familial AD (Goate et al., 1991). The first proof for a genetic cause of FAD was provided. Until now, 26 APP mutations in 75 different families have been identified (http://www.molgen.ua.ac.be/ADMutations). The Swedish mutation of APP (APPswe) was identified in a Swedish family whose carriers developed Alzheimer's disease at a mean age of 55. The amino acid exchange from KM/DA to NL/DA makes APPSwe an improved BACE1 substrate which leads to a 6- to 8fold increase in Aβ production compared to wild type APP (Citron et al., 1992; Haass et al., 1995; Mullan et al., 1992). Further studies revealed mutations associated with an early onset of Alzheimer's disease before the age of 65 of the Presenilin 1 and Presenilin 2 gene respectively located on chromosome 14 and 1 in early-onset non-Volga German relatives (Levy-Lahad et al., 1995a; Levy-Lahad et al., 1995b; Schellenberg et al., 1992; St George-Hyslop et al., 1992; Van Broeckhoven et al., 1992). Meanwhile, 157 pathogenic Presenilin 1 mutations have been identified in 357 families thus rendering Presenilin 1 mutations the major cause of FAD http://www.molgen.ua.ac.be/ADMutations). Autosomal-dominant mutations which mostly manifest below the age of 65 are summarized under the term of FAD mutations. Though these mutations constitute less than 0.5% of all AD cases, a penetrance of close to 100% makes them a beautiful target for research to understand more about the underlying pathomolecular mechanisms (Ertekin-Taner, 2007).

1.1.5 Sporadic Alzheimer's disease

Sporadic AD has been historically defined to occur beyond the age of 60. After initial linkage studies of APP on chromosome 21 to FAD, the failure to replicate this linkage in various independent AD family collections led to the conclusion that AD might be a heterogeneous disorder. In a study that investigated both FAD and sporadic AD cases accidentally identified a novel locus on chromosome 19 which especially had a strong effect in the sporadic AD cohort (Corder et al., 1993). Concurrently, the same group identified ApoE- immunoreactivity to be associated with amyloid in both senile plaques and cerebral vessels (Schmechel et al., 1993). As ApoE mapped to the previously identified risk locus for sporadic AD, researchers started to investigate the biological and genetic association of ApoE with sporadic AD (Myers et al., 1996). Briefly after,

in-vitro assays proofed a high avidity of ApoE for Aβ while a seminal genetic study demonstrated a dose-dependent increase in AD lifetime risk and a reduced age of onset for sporadic AD in ApoE ε4 carries (Corder et al., 1993; Strittmatter et al., 1993). Moreover, this study could show that the risk was increased almost threefold in heterozygous carriers while homozygous carriers had an eightfold increased lifetime risk for AD. Since then, multiple large population or clinic-based studies established the effect of the ApoE ε4 allele as a robust genetic risk factor for sporadic AD (Myers et al., 1996). Data of a prospective study indicated that 55% of the homozygous ApoE ε4 carriers developed AD by the age of 80 compared to only 27% of heterozygous ApoE ε3/ε4 carriers and 9% of the homozygous ApoE ε3/ε3 by the age of 85. After the identification of ApoE ε4 as a risk factor for AD a first wave of first generation genome-wide association studies (GWAS) with small samples sizes tried to identify novel risk loci. Unfortunately, most of these novel identified loci lack replication until today. These were followed by a few studies with samples sizes exceeding 2000 cases and 2000 controls. While the initial studies lacked significance these studies achieved genome-wide significance due to their large sample size and identified small genetic risk factors with an odds ratio of ~1.2 such as Clusterin (CLU), PICALM and CR1 (Harold et al., 2009; Lambert et al., 2009; Seshadri et al., 2010). CLU, PICALM and CR1 could be confirmed in independent studies despite the fact that replication of GWAS hits by subsequent GWAS becomes increasingly complicated. Hence, these genes are nowadays considered to be true susceptibility loci for sporadic AD. Recently, two studies combining a very large number of samples identified five additional risk loci: EPHA1, MS4A, CD33, CD2AP and ABCA7 (Hollingworth et al., 2011; Naj et al., 2011). Meanwhile it becomes more evident that a lot of the identified risk loci are either involved in lipid metabolism, the immune system, modulation of APP processing or the clearance of Aβ. ApoE for example is necessary for efficient transport of Aβ across the blood-brain barrier (BBB). It could be shown that ApoE ε4 protein is the least efficient transporter of Aβ in a transgenic knock-in mouse model carrying two ApoE ε4 alleles (Castellano et al., 2011; Jiang et al., 2008). Maybe even more important than the Aβ transport capacity might be the transport of cholesterol in the brain. The brain is dependent on de-novo cholesterol synthesis which occurs in astrocytes and microglia. The transport of de-novo synthesized cholesterol to neurons and oligodendroglia is mediated via ApoE particles (Bu, 2009; Mahley, 1988). In a similar fashion to ApoE, clusterin can bind Aβ and thereby promotes the transport of Aβ across the BBB via a high-affinity receptor-mediated process involving transcytosis (Ghiso et al., 1993; Golabek et al., 1995; Zlokovic, 1996).

1.1.6 The Amyloid Cascade Hypothesis

From the published data it becomes evident that Aβ is still considered to be a major player in the pathogenesis of Alzheimer's disease. This assigned role resulted from the identification of Aβ as main constituent of amyloid plaques and the identification of APP and presenilin mutations increasing Aβ42 and leading to FAD (Ertekin-Taner, 2007; Glenner and Wong, 1984; Masters et al., 1985b). The major role of Aβ in the pathogenesis of Alzheimer's disease finally lead to the construction of the Amyloid cascade hypothesis which was first drafted in its entirety by John Hardy (Hardy and Higgins, 1992). In the meantime the initially constructed hypothesis has been subject to several revisions due to new research results (Haass and Selkoe, 2007; Hardy and Selkoe, 2002) (See Fig. 3). The Amyloid cascade puts Aβ into the focus of the disease by proposing disequilibrium between Aβ production and degradation which in turn leads to an accumulation of Aβ followed by its aggregation. Aβ is a very hydrophobic, amyloidogenic peptide and thus tends to the formation of oligomers, protofibrils, fibrils and finally plaques (Golde et al., 1992; Nordstedt et al., 1991). While in the beginning of modern AD research Aβ plaques were considered to be causative for neurotoxicity, this idea has been abandoned in favor of Aβ oligomers as the prime source of Aβ-mediated neurotoxcity. A seminal study could show that Aβ oligomers are neurotoxic in hippocampal slice cultures and depend on the presence of Fyn kinase (Lambert et al., 1998). It should take another four years until other groups confirmed the neurotoxic potential of Aβ oligomers in comparison to fibrils or monomers (Dahlgren et al., 2002; Walsh et al., 2002). A group around Charles Glabe extended the concept of oligomer toxicity to different amyloidogenic proteins and rescued this toxicity with an oligomer-specific antibody (Kayed et al., 2003). Moreover, they later showed that oligomers elicited membrane disruption and calcium dysregulation in cells (Demuro et al., 2005). Besides Aβ other proteins are as well involved in Aβ-mediated toxicity. Fyn kinase overexpression for example leads to increased phosphorylation of NMDA receptor subunit NR2b, increased incidences of seizures and aggravates Aβ mediated toxicity in an APP transgenic mouse model (Chin et al., 2005; Kojima et al., 1998). A more recent study could link Aβ neurotoxicitiy to the presence of microtubule binding protein tau. Though the majority of tau is localized in the axon a small proportion of tau seems to stabilize NMDA receptor units as well as Fyn kinase in the postsynaptic density of dendritic spines. In this study, Tau deficiency led to impaired Fyn signaling thus abolishing Aβ-mediated neurotoxicity (Ittner et al., 2010). This was further corroborated by a study supervised by Lennart Mucke which could show that besides Fyn and tau-mediated neurotoxicity, Aβ was also able to impair axonal transport of mitochondria and the neurotrophin receptor TrkA which was not the case in tau knockout mice

(Vossel et al., 2010). Tau hyperphosphorylation is a molecular change which meanwhile has been proven to be mediated by Aβ oligomers (Jin et al., 2011; Ryan et al., 2009). All these molecular changes precede the final death of neurons which is a major pathological hallmark in AD. Nowadays the amyloid cascade hypothesis has come under fire due to failure of drug trials and the lack of neurodegeneration in transgenic APP mouse models which generated high amounts of Aβ42 (2011; Higgins and Jacobsen, 2003). These discrepancies fostered further research. Human amyloid plaques contain high concentrations of pyroGlutamate-Aβ (pyroGlu-Aβ) while plaques in APP transgenic mice contain only very low concentrations of this form of Aβ (Hosoda et al., 1998; Iwatsubo et al., 1996; Saido et al., 1996). Pyroglutamate-Aβ is a truncated form of Aβ ranging from amino acids 3 to 42 or 11 to 42 of Aβ. The n-terminal glutamate is converted to pyro-glutamate which renders this peptide species more amyloidogenic, more neurotoxic and less prone to proteolytic degradation (Schlenzig et al., 2009). A mouse model which expressed a truncated form of Aβ which undergoes cyclization of the n-terminal glutamine to pyro-glutamate exhibited strong neurodegeneration thus providing the first model which links Aβ expression with neuronal cell death (Alexandru et al., 2011; Wirths et al., 2009). The generation of pyroGlu-Aβ depends either on truncation of Aβ1-42 to Aβ3-42 or another protease which is able to cleave at E3 of the Aβ domain. This is followed by the cyclization of glutamate by glutaminylcyclase (Cynis et al., 2008). In a follow-up study plaque formation in a mouse model carrying the Swedish mutation of APP was mitigated by pharmacological inhibition of glutamincyclase (Schilling et al., 2008).

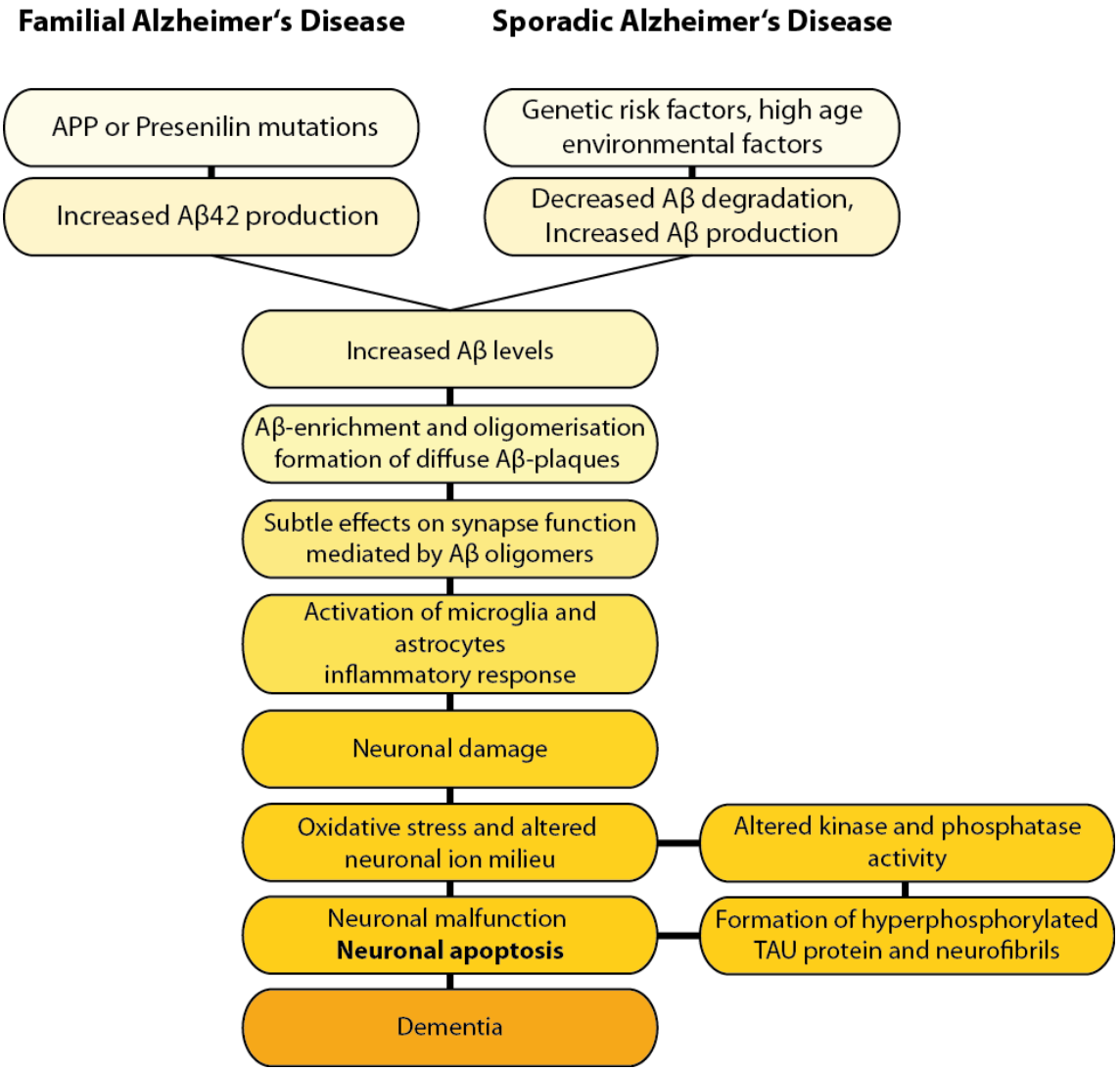

Figure 3 The concept of the amyloid cascade hypothesis: According to (Hardy and Selkoe, 2002) is depicted. The amyloid cascade hypothesis considers Aβ as the toxic agent causing neurodegeneration and finally dementia. Furthermore, the amyloid cascade considers changes in Aβ to be upstream of changes of the microtubule binding protein tau. This model proposes changes in the concentration of Aβ caused either by reduced Aβ degradation or increased Aβ generation which in the end leads to toxic Aβ oligomers that finally cause neuronal cell death.

1.2 Proteases

As the here presented data deal with proteases that besides catalyzing or preventing Aβ generation, process a plethora of other substrates, I will first introduce the general mechanism of membrane proteolysis and biological implications to later describe the proteolytic steps necessary to liberate Aβ from the Amyloid Precursor Protein (APP) as well as the involved proteases. The human genome encodes over 500 proteases, representing rougly 1.5% of the protein-coding genes (Puente et al., 2003). Proteases are intimately linked to a wide range of biological processes like protein catabolism, nutrition, protein quality control or protein maturation (Bai and Pfaff, 2011; Hook et

al., 2008; Szabo and Bugge, 2011). Two protease subclasses are membrane tethered and intramembrane cleaving proteases (see Fig. 4).

1.2.1 Regulated intramembrane proteolysis (RIP)

The term regulated intramembrane proteolysis describes the sequential proteolytic processing of membrane proteins which is subdivided into an initial cleavage of the ectodomain followed by intramembrane proteolysis of the remaining membrane stub. The majority of these proteins with some exceptions belong to the type I and type II classes of membrane proteins. The ectodomain of a typical type I membrane protein faces into the extracellular space. Ectodomain cleavage is known in the literature as ectodomain shedding and mediated by so-called sheddases (Lichtenthaler et al., 2011; Reiss and Saftig, 2009). Ectodomain shedding is considered to be the rate-limiting and regulatory step of regulated intramembrane proteolysis. Intramembrane proteolysis of the membrane-tethered stub is mediated by intramembrane cleaving proteases.

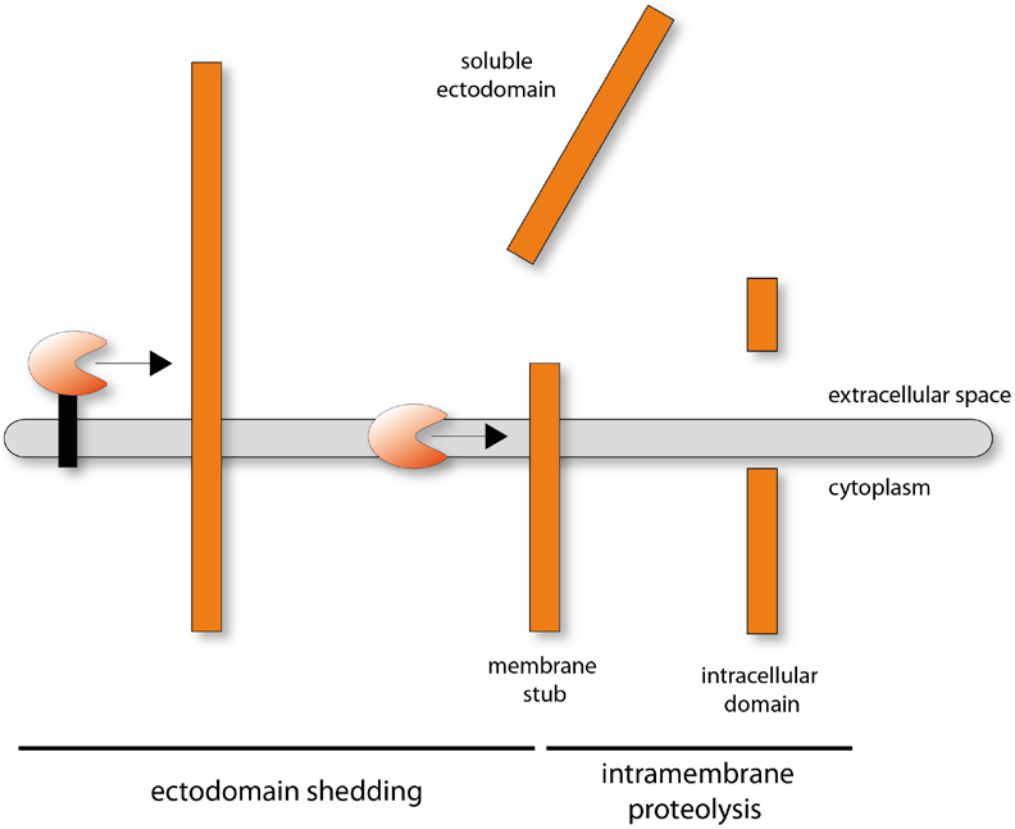

Figure 4 Regulated intramembrane proteolysis of a membrane-tethered protein: Ectodomain shedding of a membrane-tethered protein is mediated by membrane-attached proteases. After ectodomain release the remaining membrane stub is proteolytically processed by intramembrane cleaving protease.

1.2.2 Ectodomain shedding

Sheddases belong to different classes of membrane tethered proteases. Subsumed under the large family of metalloproteases are the A disintegrin and metalloprotease domain (ADAM) family and the membrane-type matrix and metalloprotease (MT-MMP) family which both account for the bulk of membrane-bound metalloproteases. The ADAM family comprises of 22 members while the MT-MMP family contains 6 members plus MMP23 which is a type-II membrane protein. Furthermore the human genome codes for the two membrane-bound aspartyl proteases BACE1 and BACE2.

1.2.2.1 The ADAM family

12 out of 22 members of the ADAM family are considered to be active as these contain the catalytic motif HEXXHXXGXXH which upon association of Zn^{2+} confers endopeptidase activity. Proteases of the ADAM family share common structural features which are an inhibitory pro-domain, a cysteine-rich domain, a disintegrin domain and a metalloprotease domain. The disintegrin domains with the exception of ADAM10 and ADAM17 are supposed to mediate integrin binding (Eto et al., 2002). The cysteine-rich domain is possibly involved in the binding of heparane sulfate class proteoglycans like, such as syndecans, exemplified by a seminal work about ADAM12 (Iba et al., 2000). The pro-domain has been shown to be indispensible for the maturation of ADAM proteins (Anders et al., 2001; Milla et al., 1999). Passing the Golgi, ADAM proteases are activated due to cleavage of the inhibitory pro-domain by proprotein convertases (Seals and Courtneidge, 2003; Srour et al., 2003). The endopeptidase activity of ADAMs enables the liberation of membrane-bound proteins. The first example of ADAM-mediated cleavage of a membrane protein has been simultanously described by two groups in 1997, identifying a membrane-bound metalloprotease as an important mediator of Tumor necrosis factor α (TNFα) relase (Black et al., 1997; Moss et al., 1997). Hence, this enzyme was called tumor necrosis factor converting enzyme (TACE). A knockout of TACE confirmed the major role of TACE in TNFα release (Peschon et al., 1998).

1.2.2.2 The MT-MMP family

Like the ADAM family MT-MMP proteases are characterized by the active site motif HEXXHXXGXXH. Besides the metalloprotease domain, MT-MMPs possess a hemopexin domain. The membrane-type matrix and metalloprotease family MT-MMP comprises of 6 members. Four of these are type-I membrane proteins (MT-MMP-1,-2,-3,-5) while two are GPI-anchored proteins (MT-MMP-4,-6). Besides these 6 membrane

bound protease, MMP23 per definition is also a membrane-bound metalloprotease as it has a type-II membrane orientation due to a signal anchor sequence (Hadler-Olsen et al., 2011). MT-MMPs are proposed to cleave a plethora of substrates like tumor necrosis factor alpha (TNFα) or Death receptor 6, CD44 or Neuropilin 1 (Suenaga et al., 2005; Tam et al., 2004). Meanwhile proteomic approaches aim at substrate identification of these proteases exploiting amine-reactive chemistry to enrich for protease cleavage-specific peptides (Kleifeld et al., 2010).

1.2.2.3 The aspartyl proteases beta-site APP cleaving enzyme 1 (BACE1) and BACE2

Identification of the aspartyl proteases BACE1 and BACE2 has been driven by AD research which aimed to elucidate the β-secretase proteolytic activity responsible for Aβ generation. BACE1 was independently identified by several groups following different approaches in 1999 (Sinha et al., 1999; Vassar et al., 1999; Yan et al., 1999). BACE1 is a 60 kDa large membrane-tethered protease which is synthesized as a preproform of the enzyme in the ER. After leaving the ER, BACE1 undergoes glycosylation at 3 out of 4 possible glycosylation sites and looses the propeptide after cleavage by a furin-like endoprotease (Capell et al., 2000). BACE1 shows maximum proteolytic activity at a pH of 4.5 and is localized in the late golgi network. The cytoplasmic domain, the dileucine motif and the transmembrane domain of BACE1 seem to be important for its normal transport. (Huse et al., 2000; Yan et al., 2001). BACE1 owes its popularity to its pivotal role in Aβ generation by APP cleavage in the juxtamembrane region (Luo et al., 2001). Meanwhile, besides APP further substrates have been proposed for BACE1 which are Neuregulin 1 type III (NRG1-III), β2 subunits of voltage-gated sodium channels, P-Selectin Glycoprotein Ligand 1 (PSGL-1), Interleukin 1 receptor type II (IL1-R2), LDL-receptor related protein (LRP), the two APP homologues Amyloid Precursor Protein like 1 and 2 (APLP1, APLP2) and the sialyltransferase ST6GAL1 (Eggert et al., 2004; Haass et al., 1992b; Hu et al., 2006; Kim et al., 2007; Kitazume et al., 2003; Kuhn et al., 2007; Li and Sudhof, 2004; Lichtenthaler et al., 2003; Sala Frigerio et al., 2010; von Arnim et al., 2005; Willem et al., 2006). Another study tried to identify novel BACE1 substrate by a quantitative mass spectrometry-driven comparison of wild type and BACE1 overexpressing tumor cells (Hemming et al., 2009). However, only for NRG1-III the physiological relevance of its proteolytic processing is really understood. BACE1 cleavage of NRG1-III releases the EGF domain and is a myelin inducing signal in the peripheral nerve system which was reflected by a hypomyelination phenotype in sciatic nerve specimens of BACE1 knockout mice (Hu et al., 2006; Velanac et al., 2012; Willem et al., 2006). Nevertheless, the role of BACE1 in

the central nervous system is far from being understood. Mice show behavioral deficits (hyperactivity, reduced anxiety levels, impaired spatial reference memory and impaired spatial reference memory) , electrophysiological abnormalities (presynaptic deficit, greater propensity for seizures) and neurochemical abnormalities like a reduced dopamine content and turnover in the striatum which cannot be explained with a lack of Neuregulin 1 type III processing (Harrison et al., 2003; Hitt et al., 2010; Hu et al., 2010; Ma et al., 2007; Wang et al., 2008; Wang et al., 2010). While BACE1 research was driven by AD research, BACE2 was almost neglected by the scientific community. Just recently, BACE2 was shown to cleave the transmembrane protein TMEM27 and thereby negatively regulating the β-cell mass in the pancreas (Esterhazy et al., 2011). Whether this anti-proliferative effect of BACE2 is exclusively due to the cleavage of TMEM27 or whether there are further BACE2 substrates in the pancreas needs further investigation.

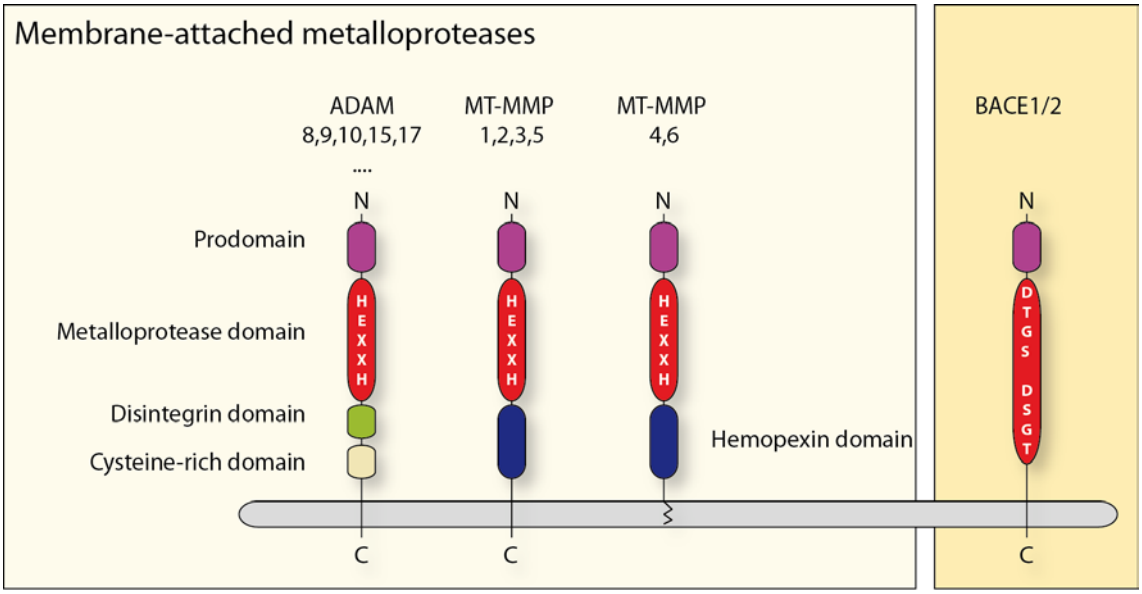

Figure 5 Schematic presentation of membrane-attached protease families: are depicted in this scheme. The members of the membrane-tethered families of metalloproteases which are the A disintegrin and metalloprotease (ADAM) family and the Membrane-type matrix metalloprotease family (MT-MMP) all contain the catalytic site motif HEXXH. While besides the metalloproteases domain the ADAM family contains a disintegrin and a cystein-rich domain, MT-MMPs are characterized by their hemopexin domain. The family of membrane-attached aspartyl proteases comprises of the proteases BACE1 and BACE2 which both contain two catalytic aspartes as active site motifs.

1.2.3 Intramembrane Proteolysis

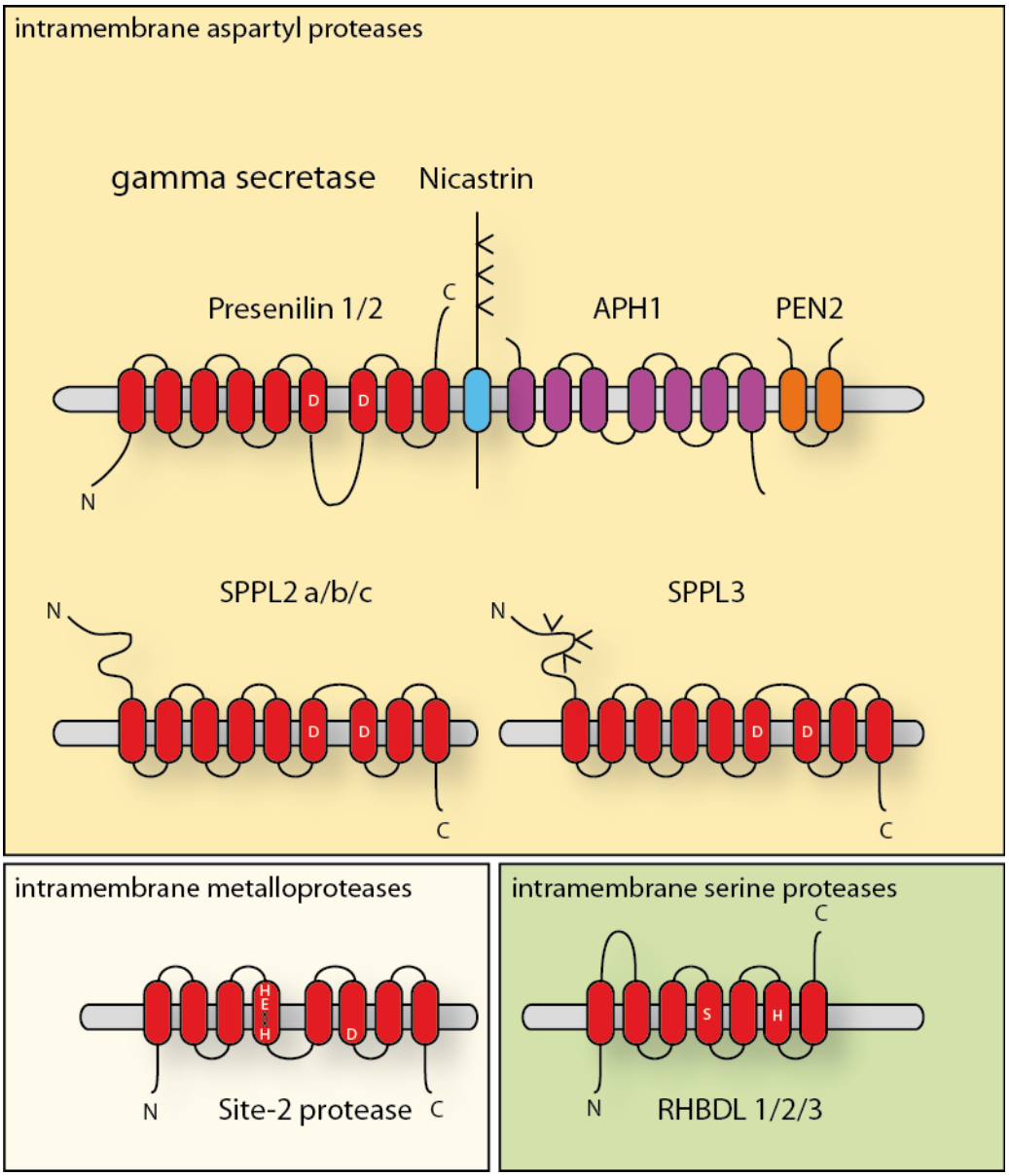

Figure 6 Schematic presentation of intramembrane cleaving proteases: All so-far known classes of intramembrane cleaving proteases are depicted. Intramembrane cleaving proteases are comprised of the aspartyl-, metallo- and serine proteases. While the aspartyl proteases SPPL2 a/b/c and SPPL3 are active on their own, gamma secretase requires besides the catalytic subunit Presenilin 1 or Presenilin 2 the structural proteins APH1, PEN2 and Nicastrin to be active. All intramembrane cleaving aspartyl proteases contain two catalytic aspartates. While gamma secreatse exclusively cleaves type-I membrane proteins, the SPPL proteases cleave type-II membrane proteins. The Site-2 protease is a metalloprotesae which is also active on its own. Rhomboid like proteases in human and rodents do not require additional proteins for their activity and possess a serine protease active-site motif.

Intramembrane proteolysis is the second step of regulated intramembrane proteolysis and describes the release of the remaining membrane stub of a protein from the

membrane. The cytoplasmic domain is released into the cytosol and can be either subject to degradation or signaling functions like nuclear signaling. Three different types of intramembrane cleaving proteases have been described so far which are aspartyl-, metallo- or serine-type intramembrane cleaving proteases (see Fig. 5). Intramembrane aspartyl proteases are represented by the gamma secretase complex and the Signal peptide peptidase like (SPPL) proteases (Fluhrer and Haass, 2007). For intramembrane cleaving metalloproteases only the Site2-protease (S2P) is so far known in humans, rodents and other species which is involved in lipid metabolism and stress response (Brown and Goldstein, 1999; Chen and Zhang, 2010; DeBose-Boyd et al., 1999). The Rhomboid family is comprised of three members which are intramembrane cleaving serine proteases (Freeman, 2009; Urban and Dickey, 2011). While gamma secretase turns over the membrane stubs of type I transmembrane proteins, the SPPL family turns over membrane stubs of type II transmembrane proteins like TNFα or Bri2 (Fluhrer et al., 2006; Friedmann et al., 2006; Martin et al., 2008).

1.2.3.1 γ-secretase

γ-secretase is a protein complex comprised of the catalytic subunits Presenilin 1 or 2 , Anterior-Phalanx defective 1 (Aph1), Presenilin Enhancer 2 (PEN2) and Nicastrin which together form an aspartyl protease activity (De Strooper et al., 1998; Esler et al., 2000; Francis et al., 2002; Wolfe et al., 1999b; Yu et al., 2000). All four components are needed to forge the active gamma secretase complex (Edbauer et al., 2003). γ-secretase cleaves exclusively the membrane stubs of a plethora of type-I membrane proteins like APP, Notch, IL-1R2, CD44, APLP1, APLP2, or Deleted in Colorectal Cancer (DCC) after ectodomain shedding (De Strooper et al., 1999; De Strooper et al., 1998; Eggert et al., 2004; Kuhn et al., 2007; Taniguchi et al., 2003). The gamma secretase complex cleaves its substrates within the membrane which was considered implausible due to the assumption that proteolysis requires the presence of water which is unlikely present in a lipid bilayer (Wolfe et al., 1999a). However, the gamma secretase complex forms a pore in the membrane with a water-filled cavity which enables gamma secretase to cleave within the membrane (Lazarov et al., 2006; Osenkowski et al., 2009; Renzi et al., 2011). Gamma secretase plays a pivotal role in the generation of Aβ by cleaving the membrane stubs of APP several times within the transmembrane domain of APP. Mutations in Presenilin 1 can shift the Aβ42/Aβ40 ratio in favor of Aβ42 and are more and more considered as loss-of-function mutations (Fluhrer et al., 2009).

Gamma secretase plays an important role in inward out signaling of cells in the context of a tissue. This was first exemplified by gamma secretase-mediated processing of the membrane tethered stub of Notch which liberates the Notch intracellular domain (NICD) that in turn translocates into the nucleus. Once in the nucleus, NICD acts as a transcription factor and determines the cellular fate of progenitor cells for their final differentiation (De Strooper et al., 1999; Gibb et al., 2011; Jorissen et al., 2010; Wen et al., 1997). Meanwhile, this has not only been shown for Notch but also for other membrane proteins which undergo RIP.

1.2.4 The Amyloid Precursor Protein (APP)

The Amyloid Precursor Protein belongs to the APP family which besides APP is comprised of the Amyloid Precursor Protein like 1 (APLP1) and 2 (APLP2). APP is ubiquitously expressed in the body. Alternative splicing of APP mRNA gives rise to tissue specific isoforms. While the most abundant form APP751 is expressed by non-neuronal tissue APP695 is exclusively expressed in neurons and APP770 is expressed by Schwann cells in the peripheral nerve system (Loffler and Huber, 1992; Sherman and Higgins, 1992). APP is a glycoprotein which is transported to the plasma membrane surface. On its way to the plasma membrane APP is posttranslationally modified via N- and O-glycosylation, sulfation and phosphorylation (Weidemann et al., 1989) and can already undergo BACE1-mediated proteolytic cleavage in the late trans-golgi network (Hartmann et al., 1997; Yan et al., 2001). Once APP has reached the plasma membrane, it has a short half-life due to proteolytic liberation by α-secretase or the metalloprotease meprin-β (Anderson et al., 1991; Jefferson et al., 2011). APP function is still far from being understood (Aydin et al., 2011). However, in recent years knockout mouse models in combination with the identification of putative APP binding partners has contributed to a better understanding of APP function *in vivo*. A recent study could confirm the binding of APP to its family members APLP1 and APLP2 in cis and in trans as well as the proposed binding to the membrane proteins Bri2 and Bri3 and the cytosolic proteins FE65 and FE65L1. Moreover, this study revealed novel binding candidates like Neurexin-1 alpha, Neurexin-2, GABA type B receptor subunit 2 (GABBR2) or Bassoon (Norstrom et al., 2010). To elucidate the function of APP, respective constitutive and conditional APP knockout mouse models have been generated (Muller et al., 1994; Wang et al., 2009b; Zheng et al., 1995). Moreover, combined knockouts with the family members APLP1 and APLP2 show functional complementation among the APP family members. While a combined knockout of APP -/- APLP1 -/- is viable, combined

knockouts of APP -/- and APLP2 -/- , APLP1 -/- and ALPP2 -/- and a triple knockout of all three proteins are lethal (Heber et al., 2000; Herms et al., 2004). APP knockout (APP-KO) mice are more sensitive to kainate-induced seizures and show reduced locomotor and exploratory activity, reduced grip strength and lower body weight as well as an altered circadian activity. Coronal brain sections of APP-KO mice show a corpus callosum agenesis and a reduced size of forebrain commissures (Muller et al., 1994; Ring et al., 2007; Zheng et al., 1995). Aged APP-KO mice present deficits in learning and spatial memory which were associated with a defect in long term potentiation (LTP). While basal glutamatergic transmission and paired-pulse facilitation seem to be unaffected, APP-KO mice exhibit a defect in paired-pulse facilitated synaptic depression which might be caused by a reduced feedback suppression of presynaptic $GABA_B$ autoreceptors (Seabrook et al., 1999; Yang et al., 2009). A lot of these described phenotypes could be rescued by the introduction of APPsα which might hint into the direction that the bigger part of APP function is mediated by the soluble ectodomain of APP (Ring et al., 2007). The underlying molecular mechanism might be explained by the interaction between APP and $GABA_B$ receptor subunit 2 (Norstrom et al., 2010). Though a lot of evidence for APP function has been gathered so far, the specific molecular mechanism how APP might regulate these processes is not understood.

1.2.5 Proteolytic Processing of the Amyloid Precursor Protein

The Amyloid Precursor Protein (APP) was one of the first membrane proteins which were known to undergo regulated intramembrane proteolysis. The APP ectodomain can be processed by three different proteases activities. Two protease activities were termed α-secretase and β-secretase before the identification of the responsible proteases while meprin-β has been just recently identified as an APP protease (Jefferson et al., 2011). For α-secretase several members of the ADAM protease family have been proposed while β-secretase was identified as BACE1. While meprin-β cleaves several times within the APP ectodomain, α- and β-secretase cleave within the APP juxtamembrane region thus driving APP ectodomain liberation. BACE1 cleaves at the N-terminus of the Aβ domain of APP which yields the soluble ectodomain APPsβ and the membrane stub C99 (Kang et al., 1987; Sinha et al., 1999; Vassar et al., 1999; Yan et al., 1999). α-secretase cleaves between Lysine-16 und Leucine-17 of the Aβ domain of APP which gives rise to the soluble ectodomain APPsα and the membrane stub C83 (Anderson et al., 1991). In case of APP α-secretase has been proposed to be ADAM9, ADAM10 and ADAM17 (Asai et al., 2003; Buxbaum et al., 1998a; Koike et al., 1999; Lammich et al., 1999; Skovronsky et al., 2000; Slack et al., 2001). α-secretase cleavage within the Aβ domain can preclude the generation of Aβ (Postina et al., 2004).

Meprin-β cleavage of APP drives N-APP generation, a fragment which has been proposed to drive neuronal apoptosis via Death receptor 6 binding (Jefferson et al., 2011; Nikolaev et al., 2009). The remaining membrane-tethered APP stubs C99 and C83 are turned over by the gamma secretase complex (Haass and Selkoe, 1993). While cleavage of C83 gives rise to the hydrophobic peptide p3 and the cytosolic APP intracellular domain (AICD), C99 cleavage by gamma secretase results in extracellular Aβ and AICD (Esch et al., 1990; Haass and Selkoe, 1993; Sisodia et al., 1990). AICD has been proposed to have a nuclear signaling function in combination with TIP60 and FE65 (Cao and Sudhof, 2001). However, this finding is heavily debated. Finally, the generation of Aβ is the starting point of the amyloid cascade (Hardy and Higgins, 1992).

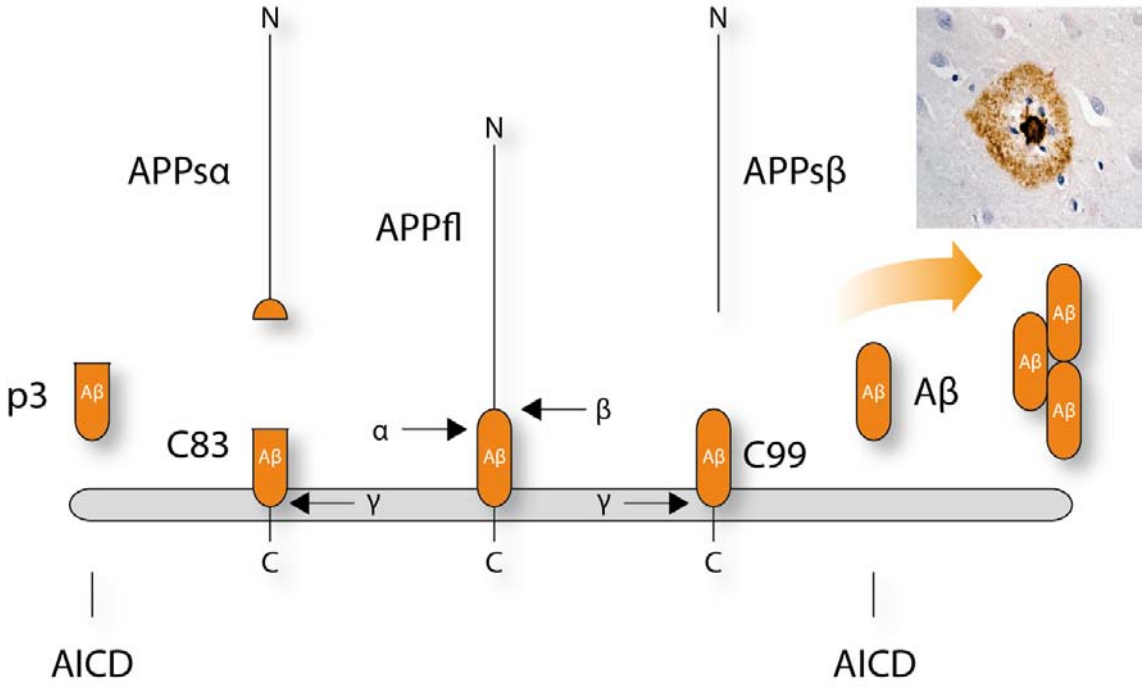

Figure 7 Scheme of APP proteolytic processing. APP full length (APPfl) is cleaved in the juxtamembrane region either by α- or β-secretase. β-secretase cleaves at the N-terminus of Aβ domain while α-secretase cleaves within the Aβ domain. β-secretase cleavage leads to the generation of the soluble APP ectodomain APPsβ and the C-terminal fragment C99 whose processing by γ-secretase gives rise to extracellular Aβ and the intracellular APP intracellular domain (AICD). α-secretase cleavage gives rise to the soluble ectodomain APPsα and the C-terminal fragment C83 whose processing by gamma secretase results in extracellular p3 fragment and AICD. Extracellular Aβ forms oligomers which finally deposit in amyloid plaques. Plaque picture source: http://idw-online.de/de/newsimage?id=58141&size=screen

1.2.6 Therapeutic strategies of Alzheimer's disease based on protease inhibition or modulation

Taking APP proteolytic processing and the amyloid cascade hypothesis into account the main aim of pharmaceutical approaches to prevent Alzheimer's disease (AD) is to lower the concentration of Aβ in the brain. Lowering Aβ can be achieved by sever-

al approaches which are based on α-secretase activation, β-secretase inhibition, γ-secretase inhibition and γ-secretase modulation. Investigation of α-secretase activation as therapeutic approach to prevent AD was motivated by the finding that α-secretase activation can lead to a competition with β-secretase which ultimately leads to a reduction of Aβ (Nitsch et al., 1992; Postina et al., 2004). Retinoic acid analogs like acitretin proofed to enhance ADAM10 trancription and lower Aβ in a mouse model. (Tippmann et al., 2009). $GABA_A$ receptor modulators and partial 5-HT_4 receptor agonists have proven to increase APPsα in cells (Marcade et al., 2008; Robert et al., 2005). Nevertheless, so far α-secretase modulation is the least developed AD therapeutic approach and is still in the preclinical phase.

Far more advanced is the inhibition of BACE1. As initial studies of BACE1 knockout mice did not reveal any overt phenotype, BACE1 was considered as a viable drug target for AD therapy. However, BACE1 is a rather difficult pharmaceutical target. The active site is rather large but the inhibitors have to be small to pass the blood-brain barrier and penetrate into the cell. First generation BACE1 inhibitors were peptidemimetics of the APP β-cleavage site in which the scissile amide bond is replaced by a non-hydrolyzable transition state analog, such as statine (Sinha et al., 1999). More recently, non-peptidergic compounds with high affinities for BACE1 have been generated (Luo and Yan, 2010). A recent clinical phase I trial proved the efficacy of an orally administered BACE1 inhibitor to lower Aβ in the brain while having no adverse effects in the acute treatment period in human patients (May et al., 2011b). However, rats treated with the same inhibitor showed retinal degeneration which consequentially led to abortion of the clinical trial. Whether long-term BACE1 inhibition has no adverse effects in humans and leads to a stabilization of the cognitive function requires further clinical studies.

In comparison to BACE1, γ-secretase is an easy pharmaceutical target with respect to the development of brain-penetrating, orally available γ-secretase inhibitors (GSI) with high potency. γ-secretase inhibitors lower Aβ in human and rodent brains (Bateman et al., 2009; Dovey et al., 2001; Siemers et al., 2007). However, target-inhibition based toxicity was observed in preclinical trials originating from the inhibition of Notch processing which could have already been anticipated from studies of Presenilin knockout mice (Searfoss et al., 2003; Shen et al., 1997). Two answers to this problem are either Notch sparing GSIs or γ-secretase modulators (GSMs). While the first case acts as a classical inhibitor sparing Notch processing, γ-secretase modulators (GSMs) shift Aβ generation to shorter, less amyloidogenic Aβ species like Aβ38 to the expense of Aβ42 (Kukar and Golde, 2008; Weggen et al., 2001). Notch-sparing GSIs and GSMs have both been tested in clinical trials. The Notch-sparing GSI BMS-

708,163 showed an *in vivo* effect by lowering Aβ in a phase-I clinical trial. Tarenflurbil (R-flurbiprofen) is an example for a first generation GSM which has been tested in a clinical phase-III trial without the observation of side-effects. However, compared to non-treated patients the cognitive decline of treated patients was not reduced which was ascribed to a low potency and bad CNS penetration of the compound (Green et al., 2009).

1.3 Click chemistry – Bioorthogonal reactions enable purification of subproteomes or investigation of posttranslational modifications

The secretome defines the entirety of secreted and shedded proteins of a given cell. While former analysis focused only on the secreted or shedded protein of interest, a novel technique should be developed which allows identification and quantification of large parts of the secretome. This is advantageous for the following reasons. First, it would enable the systematic search for protease substrates which in the end draws a more complete picture of the biology of a given protease. Second, bearing theses information in our hand, we can draw better conclusions about protease biology and potential side-effects of therapeutic protease inhibition. For a better understanding of the later described Secretome protein enrichment with Click sugars (SPECS) approach which enables identification of novel protease substrates, click chemistry and associated bioorthogonal reaction pairs will be introduced in the following paragraphs.

1.3.1 Bioorthogonal-Definition

The term bioorthogonal defines the reaction between a non-cytotoxic pair of reactive groups which is inert to the milieu of a living cell and thus allows specific labeling of proteins within the context of a living cell or whole organism (Jewett and Bertozzi, 2010).

1.3.2 Click Chemistry reactions

To allow for specific labeling of biomolecules in vivo the best strategy is to use functionalities which do not exist in nature. The first known chemical reaction in click chemistry which was applied in vivo is the Staudinger ligation (Prescher et al., 2004). The Staudinger ligation describes the reaction between an azide group and a

triarylphosphine. However, the slow kinetics of the Staudinger ligation limits its use in probing fast biochemical processes. As a consequence, chemists were looking for alternative chemical reactions which could be used for click chemistry. An alternative to Staudinger ligation is a 3+2 cycloaddition between an azide and a terminal alkyne moiety which has been developed by Huisgen. A drawback of this reaction is its dependence on heat thus rendering it inaccessible for labeling in vivo. Sharpless and coworkers developed a Cu^{I}-catalyzed rendition of the 3+2 cycloaddition between an azide and a terminal alkyne which allows labeling of biomolecules at ambient temperatures (Rostovtsev et al., 2002). However, Cu^{I} is toxic to living cells. Inspired by pioneer work of Wittig and Krebs which described the reaction kinetics between a strained cyclooctyne and phenylazide as “explosionsartig”, Bertozzi and others took advantage of this reaction to label glycoproteins on the surface of Jurkat cells (Luchansky et al., 2004; Wittig G, 1961). Though the kinetics of this reaction improved a lot compared to the reaction kinetics of a linear alkyne with an azide moiety, there was still a lot of space for improvement. This resulted in the development of new cyclooctyne variants (see Fig. 7). Increased reactivity was either achieved by the addition of electron withdrawing groups or enhancement of the ring strain of the cyclooctyne. Following the first strategy Bertozzi and coworkers improved OCT reactivity by the addition of two neighboring fluorine atoms 60fold and termed this compound Difluorcyclooctyne (DIFO) (Baskin et al., 2007). Though the reactivity compared to OCT improved a lot, DIFO synthesis is hampered by a complex 10-step synthesis procedure with only 1% yield thus rendering DIFO inaccessible to the broad scientific community. By adding two benzene groups to the cyclooctyne Boons and coworkers developed Dibenzocyclooctyne (DIBO) whose increased ring strain leads to reactivity comparable to DIFO (Ning et al., 2008). Moreover, compared to DIFO, DIBO is easier to synthesize and offers good yields. An even better solution is the monobenzocycloocytne COMBO. Here, the benzene group is positioned opposite of the alkyne bond which results in the most reactive copper-free cyclooctyne reagent so far known (Varga et al., 2011). Bicyclononyne combines better reactivity than DIBO and very good water solubility with the easiest synthesis pathway so far known for copper-free cycloaddition reagents (Dommerholt et al., 2010). Other bioorthogonal pairs are the reaction between cyclooctene and biaryltetrazine or norbonene and aryltetrazine which are easier to synthesize despite their high ring-strain (Devaraj et al., 2008; van Berkel et al., 2007). However, these reactive groups are much bigger and thus less likely to be accepted by cellular enzymes if incorporated into natural metabolites like sugars.

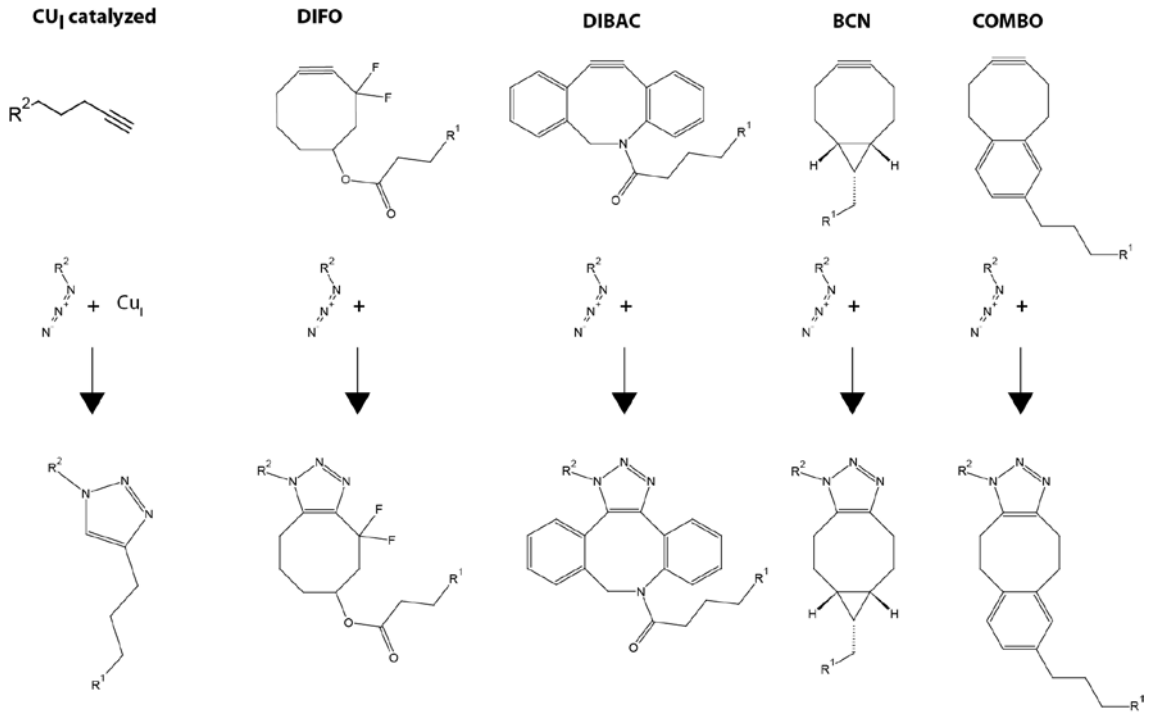

Figure 8 Strained alkynes and formed heterocycles: Shows the Copper catalyzed 2+3 cycloaddition between a terminal alkyne and an azide and the strain-promoted 2+3 cycloaddition between cycloalkynes and azides. Depicted are the different second generation cycloalkynes with increased reactivity due to electron withdrawing groups (**DIFO**) or increased strain (**DIBAC**, **BCN**, **COMBO**).

1.3.3 Click chemistry applications in molecular biology

Meanwhile click chemistry reactions have been used to visualize glycosylation, glycoproteins, lipids or farnesylation of proteins . A common strategy is the incorporation of one reaction partner in the target biomolecule which can be labeled in a subsequent reaction with an exogenously added probe. This was realized by metabolic labeling with azide- or alkynyl-bearing sugar analogs which enables N-linked, Mucin-type O-linked glycan and glycolipid labeling (Chang et al., 2009; Hang et al., 2003; Saxon and Bertozzi, 2000) (see Fig. 8). Additionally to the azide or alkyne moiety of sugar used for click chemistry labeling, the OH-groups of these sugar are peracetylated to permit their access to the cell by passive diffusion (Almaraz et al., 2011; Wang et al., 2009a). Subsequent labeling with a fluorescent or affinity probe like biotin can be achieved by linking it to an azide or alkyne moiety depending on the metabolically incorporated moiety of the biomolecule. This allows visualization of the molecule via fluorescence microscopy in the first case or its purification via streptavidin in the latter case. Both strategies allow glycoprotein labeling in cells and *in vivo* (Agard et al., 2004; Dube et al., 2006; Laughlin et al., 2008; Luchansky et al., 2004; Prescher et al., 2004).

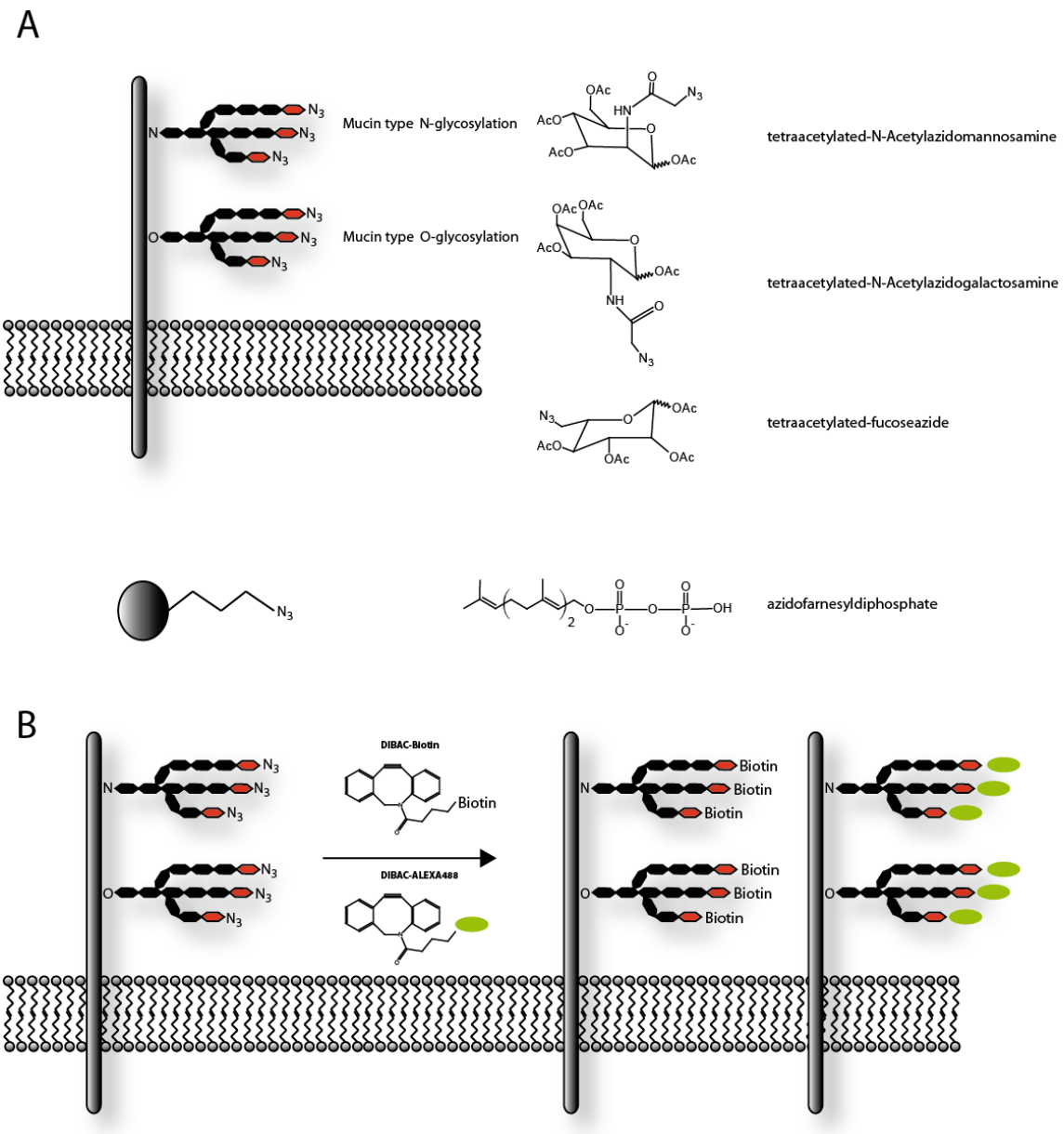

Figure 9 Metabolic labeling and labeling strategy: (A) shows the sugars N-acetylazidomannosamine, N-acetylazidogalactosamine and azidofucose for metabolic labeling of N-linked glycosylation and mucin type O-linked glycosylation. To metabolically label farnesylated protein azidofarnesyldiphosphate can be used. (B) shows the metabolic labeling of glycoproteins with azide-bearing sugars (red) and their subsequent labeling with a biotin or flurophore probe via a strain-promoted 2+3 cycloaddition.

Metabolic labeling of biomolecules in combination with subsequent click chemistry mediated attachment of affinity probes enables mass spectrometry driven identification of subproteomes like the glycoproteome or the palmitylated proteome (Hanson et al., 2007; Martin and Cravatt, 2009; Yount et al., 2010).

1.4 Goals of this work

Ectodomain shedding and intramembrane proteolysis of APP by α-, β- and γ-secretase are pivotal biological processes which are either directly or indirectly involved

in the generation of Aβ. According to the amyloid cascade hypothesis, Aβ is considered to be the key molecule in Alzheimer's disease. As Aβ is a product of APP proteolytic processing by β- and γ-secretase a lot of pharmaceutical companies are currently trying to develop inhibitors or modulators against these two enzymes. Their inhibition would prevent Aβ generation and thus interrupt the amyloid cascade. However, the knowledge about APP processing and the biology of the involved proteases are still incomplete which in the end might lead to unforeseen side-effects of future therapeutic approaches. Beyond APP processing, proteases are involved in manifold biological processes such as protein degradation, protein activation or protein release. In the nervous system, proteases have been shown to play a role in synaptic plasticity, axon pruning and outgrowth and intercellular communication (Bai and Pfaff, 2011). For these reasons, this study tries to answer two crucial questions of APP proteolytic processing.

First, which is the real α-secretase activity in primary cortical neurons? A lot of studies have been conducted in recent years to pinpoint the relevant protease representing APP α-secretase. However, these studies were either performed in non-neuronal tumor cell lines or suffered from overexpression artifacts, RNAi off-target effects and non-specific antibodies. Activation or overexpression of α-secretase has been shown to compete with β-secretase for APP as a substrate. Hence, α-secretase activation is considered as a therapeutic approach to prevent Alzheimer's disease. However, first of all the responsible protease has to be identified to enable the development of specific activators. Additionally, a lentiviral overexpression system for membrane proteins should be developed which allows the analysis of large plasma membrane proteins in primary cortical neurons and any other cell type which is hard to transfect.

Second, which substrates are proteolytically processed by BACE1 besides the APP family? The identification of BACE1 substrates has been a question in the Alzheimer field for more than a decade. Initial phenotypic studies of BACE1 knockout mice identified only mild changes. On the contrary, more recent studies of BACE1 knockout mice identified behavioral, electrophysiological and cognitive deficits. Nevertheless, the underlying proteolytic substrates of BACE1 are only partially identified. In this study a novel method should be developed which enables the proteome-wide unbiased identification of protease substrates in primary cells. Once developed the technique is supposed to identify novel substrates for BACE1 in primary cortical neurons. The identification of novel BACE1 substrates in BACE1 knockout mice will not only offer a deeper insight into the underlying biology of BACE1 but is also required to assess potential side-effects and feasibility of BACE1 inhibition as a considered therapy for Alzheimer's disease.

2 Material and Methods

2.1 DNA methods

2.1.1 Polymerase Chain reaction (PCR)

The oligos used for PCR in this study were obtained from Sigmaaldrich or Thermo. All oligos were solubilized in aqua bidest to a concentration of 100 µM. These were stored at -20°C until further usage (ddH_2O produced with a Milli Q Plus filter system, Millipore). 10 µM were used as working concentration. For a standard PCR the indicated ingredients in the following table were mixed on ice. The Polymerase was pipetted to the PCR reaction as last component.

Table 1: Set up of a PCR reaction

Substance	Amount (µl)
DNA template (100 ng/µl)	**1**
Forward oligonucleotide	**4**
Reverse oligonucleotide	**4**
dNTP (Roche)	**1**
Polymerase (PWO/TAQ)	**1**
Polymerase buffer 10x	**5**
ddH_2O	**34**
Σ=	**50**

For small or difficult to amplify PCR products Thermophilus aquaticus (TAQ) DNA polymerase was used. For longer PCR products Pyrococcus woesei (PWO) DNA polymerase was used because it produces only one mutation per 10000 base pairs due to its 3'-5' exonuclease activity. The PCR mixture was incubated in a PCR machine (Gene Amp PCR System 2700, ABI or Biorad) according to a standard-PCR program. The extension time was adjusted to the polymerization activity of the used polymerase and the length of the PCR product. Hybridisation temperature (Tα) was adjusted according to the melting temperature indicated by the manufacturer (Tm) (Tα=Tm-2°C). In case of fusion-PCRs PCR products of two preceding PCRs served as template.

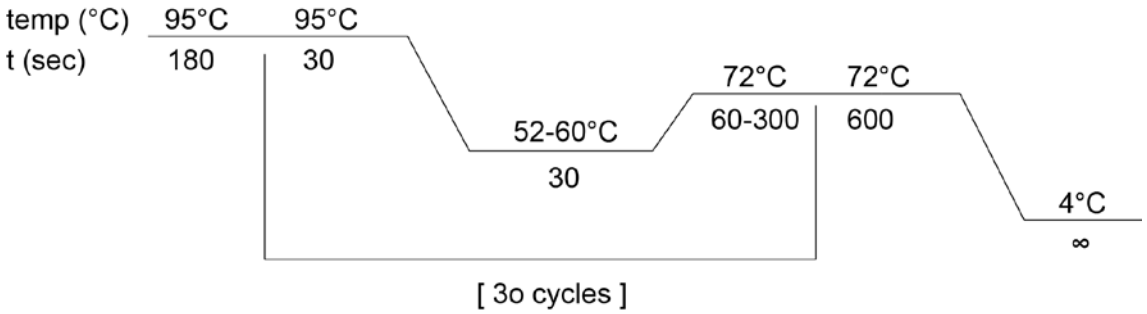

Figure 10 – PCR scheme: Depicted is a typical PCR scheme, with an initial denaturing at 95°C, an annealing step of 30 sec ranging from 52°C to 60°C depending on the primer properties and a extension step at 72°C which varies in length depending on the polymerase speed and the length of the amplified DNA fragment.

2.1.2 Restriction digest

For a restriction digest of DNA restriction enzymes of NEB and Fermentas were used. For selection of the appropriate buffer resources like **Double Digest™** provided by Fermentas or **Double Digest Finder** from NEB can be used. A standard restriction digest is indicated in the table below.

Table 2 Set up of a restriction digest

Substance	Amount (µl)
Plasmid or PCR fragment C=1 µg/µl	**1**
Restriction enzyme 1 C=10U/µl	**0,5**
Restriction enzyme 2 C=10U/µl	**0,5**
Restriction enzyme buffer (10X)	**1**
ddH_2O	**17**
Σ=	**20**

The restriction digest was incubated at 37°C for at least one hour to ensure a complete digest of the DNA. In some rare cases the incubation temperature has to be adjusted to the specific properties of the restriction enzyme. If only one restriction enzyme was used, the digested vector was treated with shrimp alkaline phosphatase (SAP) in order to prevent vector religation during subcloning of DNA fragments. Therefore 1 µl of SAP

was added to the restriction digest. If no further purification of the DNA is intended the restriction enzymes as well as shrimp alkaline phosphatase can be inactivated incubating the restriction digest at 65°C for 15 min.

2.1.3 Cloned and used DNA constructs and list of oligonucleotides

Table 3 Cloned Constructs with restriction sites and used oligonucleotides

Plasmid name	Nr.	Insert	backbone	RE sites	Templ.	Oligo I	Oligo II
plKO1.1-hsAD17-TRC68	1	-	-	-	-	-	-
plKO1.1-EGFP-hsAD10-TRC68	2	EGFP	1	BamH1/Nsi1	5	1	2
plKO1.1mod-EGFP- empty	3	Modified U6	2	Cla1/EcoR1	2	3	4
plKO2mod-EGFP- empty	4	WPRE	3	Nsi1/Kpn1	6	5	6
pEGFP-N1	5	-	-	-	-	-	-
FUGW	6	-	-	-	-	-	-
FU-Valentin	7	-	-	-	-	-	-
FUΔZeo	8	Religated	7	BSTZ17I/PME1	-	-	-
FU2ΔZeo	9	WPRE	8	EcoRI/BspEI	8	7	8
pT2d- _pA_DsRed _E1b_UAS_E1b_GW	10	-	-	-	-	-	-
FUΔZeo-DsRed-UAS-GW(DEST)	11	DsRed-UAS-GW	7	AfeI/NheI	-	-	-
FΔZeo	12	Religated	8	AfeI/SmaI	-	-	-
FΔZeo-MCSneu	13	Oligo duplex	12	XhoI/EcoRI	-	9	10
FΔZeo-GFP-MCSneu	14	GFP	13	BamH1/Nsi1	5	1	2
FΔZeo-GFP-5XUAS-GW(DEST)	15	5XUAS-GW	14	NsiI/Nhe1	-	-	-
pT2d-pA_DsRed _E1b_5XUAS_E1b_GW	17	-	-	-	-	-	-
FΔZeo-Puro -5XUAS-GW(DEST)	18	Puromycin	16	BamH1/Nsi1	19	11	12
Peak12-GFP	19	-	-	-	-	-	-
FΔZeo-Kozak-GFP-STOP-5XUAS-GW(DEST)	20	Kozak-GFP-STOP	15	BamH1/Nsi1	19	13	14
pcDNA3.1-APP-TEV-FLAG	21	APP-TEV-FLAG	22	EcoR1/Not1	22	18/16	15/19
pcDNA3.1-APP	22	-	-	-	-	-	-
FΔZeo-Kozak-Puro -5XUAS-GW(DEST)	23	Kozak-Puro	18	Xho1/ Nsi1	19	20	12
pcR8/GW/TOPO + pCS2-MCS	24	-	-	-	-	-	-
pcR8/GW/TOPO MCS neu	25	Oligo Duplex	24	-	-	21	22
pcR8/GW/TOPO-APP-TEV-FLAG	26	21	25	Hind3/Not1	-	-	-
pT2d-EXP_EF1a_Gal4VP16_pA	28	-	-	-	-	-	-
FUΔZeo-Gal4-VP16	29	Gal4-VP16	8	BamH1/Not1	28	23	24
FΔZeo-DsRed-UAS-APP-TEV-FLAG	30	26	11	Clonase	-	-	-
pCAG-Cre	31	-	-	-	-	-	-
FU2ΔZeo-iCre	32	iCre	9	Nhe1/EcoR1	31	25	26
pLKO2mod-EGFP-WPRE-hsAD10-sh6	33	Oligo Duplex	4	Mlu1/Xma1	-	29	30
plKO2mod-EGFP-WPRE-hsAD10-sh7	34	Oligo Duplex	4	Mlu1/Xma1	-	31	32
plKO2mod-EGFP-WPRE-hsAD10-sh9	35	Oligo Duplex	4	Mlu1/Xma1	-	33	34
plKO2mod-EGFP-WPRE-hsBACE1-sh1	36	Oligo Duplex	4	Mlu1/Xma1	-	35	36
plKO2mod-EGFP-WPRE-hsBACE1-sh2	37	Oligo Duplex	4	Mlu1/Xma1	-	37	38
plKO2mod-EGFP-WPRE-mmAD10-sh1	38	Oligo Duplex	4	Mlu1/Xma1	-	39	40
plKO2mod-EGFP-WPRE-mmAD10-sh2	39	Oligo Duplex	4	Mlu1/Xma1	-	41	42
plKO2mod-EGFP-WPRE-mmAD17	40	Oligo Duplex	4	Mlu1/Xma1	-	45	46
plKO2mod-EGFP-WPRE-mmAD9	41	Oligo Duplex	4	Mlu1/Xma1	-	43	44
plKO2mod-EGFP-WPRE-Control	42	Oligo Duplex	4	Mlu1/Xma1	-	27	28

Table 4 Oligonucleotides used in this study

Oligonucleotide Name	Sequence	Nr.
BamH1 BFP fw	GATCGGATCCATGGTGAGCAAGGGCGAG	1
GFP-Nsi rev II	GATCATGCATTTACTTGTACAGCTCGTCCATGC	2
U6 MluI-XmaI EcoRI rev	GATCGAATTCCCCGGGTTCCGGTTACGCGTGTCCTTTCCACAAGATATATAAAGC	3
PLVTHM RT-PCR fw	AACTCACAGTCTGGGGCATC	4
WPRE Nsi1 fw	GATCATGCATTCAACCTCTGGATTAC	5
WPRE Kpn1 rev	GATCGGTACCTCGACGGTATCGATGC	6
UBI-C promoter fw	GTTAGACGAAGCTTG	7
WPRE BspEI rev	GATCTCCGGACGATCGAGGTCGACGGTATC	8
FΔZeo-MCS neu fw	TCGAGAGGATCCAAATGCATAAAGGCCTAAGCTAGCAAG	9
FΔZeo-MCS neu rev	AATTCTTGCTAGCTTAGGCCTTTATGCATTTGGATCCTC	10
Puromycin BamH1 fw	GATCGGATCCATGACCGAGTACAAGC	11
Puromycin Nsi1 rev	GATCATGCATTCAGGCACCGGGCTTGC	12
Xho I Kozak EGFP fw	GATCCTCGAGCCACCATGGTGAGCAAGGGCGAGGAG	13
EGFP STOP Nsi1 rev	GATCATGCATTAACTACTATAACTTGTACAGCTCGTCCATGC	14
APP-TEV-FLAG fw	TTCCAAGGTGATTACAAGGATGACGATGACAAGGGTTCTGGGTTGACAAATATC	15
APP-TEV-FLAG rev	CTTGTAATCACCTTGGAAGTAGAGGTTCTCTGGTCGAGTGGTCAGTCC	16
pcDNA3.1 FP	CTCTGGCTAACTAGAGAAC	17
APP 1000 fw	AGCACCGAGAGAGAATGTCCC	18
pcDNA3.1 RP/1	CAAACAACAGATGGCTGGC	19
Puromycin Kozak XhoI fw	GATCCTCGAGCCACCATGACCGAGTACAAGC	20
pcR8 GW MCS neu fw	AGCTTGGTCTAGAGGCAATTGAAGGATCCAAGAATTCAAACGCGTAAGGTACCAAGCGGCCGCAGTAC	21
pcR8 GW MCS neu rev	TGCGGCCGCTTGGTACCTTACGCGTTTGAATTCTTGGATCCTTCAATTGCCTCTAGACCA	22
Gal4-VP16 BamH1 fw	GATCGGATCCATGAAGCTACTGTCTTC	23
Gal4-VP16 Not1 rev	GATAGCGGCCGCCGCTACATATCCAGAGC	24
iCre Nhe1 fw	GATCGCTAGCATGGTGCCCAAGAAGAAGAGG	25
iCre EcoR1 rev	GATCGAATTCTCAATCGCCCTCGAGCAGCCTCACC	26
Control fw	CGCGTCCCCCAACAAGATGAAGAGCACCAATTCAAGAGATTGGTGCTCTTCATCTTGTTGTTTTTGGAAA	27
Control rev	CCGGTTTCCAAAAACAACAAGATGAAGAGCACCAATCTCTTGAATTGGTGCTCTTCATCTTGTTGGGGGA	28
hsADAM10 sh6 fw	CGCGTCCCCAAGTTGCCTCCTCCTAAACCACTTTCAAGAGAGTGGTTTAGGAGGAGGCAACTTTTTTTGGAAA	29
hsADAM10 sh6 rev	CCGGTTTCCAAAAAAAGTTGCCTCCTCCTAAACCACTTCTCTTGAAGTGGTTTAGGAGGAGGCAACTTGGGGA	30
hsADAM10 sh7 fw	CGCGTCCCCGACATTTCAACCTACGAATTTCTCGAGAAATTCGTAGGTTGAAATGTCTTTTTGGAAA	31
hsADAM10 sh7 rev	CCGGTTTCCAAAAAGACATTTCAACCTACGAATTTCTCGAGAAATTCGTAGGTTGAAATGTCGGGGA	32
hsADAM10 sh9 fw	CGCGTCCCCGGACAAACTTAACAACAATTTCAAGAGAATTGTTGTTAAGTTTGTCCTTTTTGGAAA	33
hsADAM10 sh9 rev	CCGGTTTCCAAAAAGGACAAACTTAACAACAATTCTCTTGAAATTGTTGTTAAGTTTGTCCGGGGA	34
hsBACE1-sh1 fw	CGCGTCCCCGGTGCAAAGATTGCCTCTTGATTCAAGAGATCAAGAGGCAATCTTTGCACCTTTTTGGAAA	35
hsBACE1-sh1 rev	CCGGTTTCCAAAAAGGTGCAAAGATTGCCTCTTGATCTCTTGAATCAAGAGGCAATCTTTGCACCGGGGA	36
hsBACE1-sh2 fw	CGCGTCCCCGGGACTGTACCTGTAGGAAACTTCAAGAGAGTTTCCTACAGGTACAGTCCCTTTTTGGAAA	37
hsBACE1-sh2 rev	CCGGTTTCCAAAAAGGGACTGTACCTGTAGGAAACTCTCTTGAAGTTTCCTACAGGTACAGTCCCGGGGA	38
mmADAM10-sh1 fw	CGCGTCCGGTAGACATTATGAAGGATTATCCTCGAGGATAATCCTTCATAATGTCTATTTTTGGAAA	39
mmADAM10-sh1 rev	CCGGTTTCCAAAAATAGACATTATGAAGGATTATCCTCGAGGATAATCCTTCATAATGTCTACCGGA	40
mmADAM10-sh2 fw	CGCGTCCGGCAGACTTGGCTCTCGATAAACCTCGAGGTTTATCGAGAGCCAAGTCTGTTTTTGGAAA	41
mmADAM10-sh2 rev	CCGGTTTCCAAAAACAGACTTGGCTCTCGATAAACCTCGAGGTTTATCGAGAGCCAAGTCTGCCGGA	42
mmADAM9-sh fw	CGCGTCCGGGCTCCTGCACCTCCTTTATATCTCGAGATATAAAGGAGGTGCAGGAGCTTTTTGGAAA	43
mmADAM9-sh rev	CCGGTTTCCAAAAAGCTCCTGCACCTCCTTTATATCTCGAGATATAAAGGAGGTGCAGGAGCGGGGA	44
mmADAM17-sh fw	CGCGTCCCCGCAGCACTCCATAAGGAAACTCGAGTTTCCTTATGGAGTGCTGCTTTTTGGAAA	45
mmADAM17-sh rev	CCGGTTTCCAAAAAGCAGCACTCCATAAGGAAACTCGAGTTTCCTTATGGAGTGCTGCGGGGA	46

2.1.4 Separation of DNA fragments

TAE buffer 40 mM TRIS, 20 mM acetic acid, 1 mM EDTA (pH 8.0)

Agarose Ultra Pure agarose (Invitrogen, 15510-027)

Ethidiumbromide 1%	(Roth, 2218.1)
DNA loading buffer 4X	30% (v/v) Glycerol, 10 mM EDTA, 0,05% Orange G (w/v) (Sigmaaldrich) in ddH_2O
DNA size marker	1 kB ladder (Sigm) solubilized in DNA loading buffer
Electrophoresis Chamber	Owl Separation Systems, Inc.
DNA documentation system	Intas
Thermal printer	Mitsubishi

According to the expected size of the DNA fragment different amounts of agarose (0,5%-2,0% w/v) are cooked in TAE buffer. For fragments smaller than 500 bp agarose gels with a content of two percent are used. 40 ml of hot liquid agarose are poured into a mini chamber which can accommodate up to 10 lanes. 5 µl are added to the still liquid agarose and mixed thoroughly to ensure proper distribution. 10 µl of DNA ladder are loaded into the first lane. This allows evaluation of the size of the DNA product after gel electrophoresis. Before loading the DNA of PCR reactions or restriction digests the solution is mixed with a quarter volume DNA loading buffer of the total loading volume. This results in a higher density of the sample which allows for an easier loading procedure of the samples. After sample loading, the gel is run at 120 V for 30 min. After electrophoresis the gel is inspected under a UV screen (λ=302 nm), photos or digital pictures are taken for documentation as well as the desired DNA bands are cut out with a scalpel for subsequent processing.

2.1.5 Purification of DNA fragments out of agarose slices

For purification of DNA out of agarose slices or out of restriction digests and PCR reactions the Nucleospin® Extract Kit from Machery&Nagel is used according to the instructions of the manufacturer. The DNA captured on the column is eluted either with ddH_2O or TE buffer (5 mM TRIS, 1 mM EDTA, pH 8.0) and afterwards stored at -20°C until further work up.

2.1.6 DNA ligation

The ligation of DNA is the last step to create new plasmids. For subcloning of digested PCR products or DNA fragments which are obtained by plasmid digest, these fragments need to be attached together. For this purpose the enzymatic ligation activity of T4 ligase can be used. A typical ligation reaction mixture is indicated in the table below.

The ratio between vector and insert is critical for the success of a ligation reaction. Normally the molar ratio between vector and backbone should be one to five. The length of a DNA fragment has to be taken into account for such calculations. The example takes into account that the vector is 5000 bp long while the insert is 1000 bp long which can be calculated according the following equation and leads to the following DNA amounts (see table 5).

$Mass_{fragment}$ [ng] = 5x mass vector [ng] x $length_{fragment}$ [bp]/ $length_{vector}$ [bp]

Table 5 Set up of a Ligase reaction

Substance	Amount
Vector (digested with one or 2 restriction enzymes)	**20 ng**
Insert (digested DNA or PCR fragment)	**20 ng**
T4 DNA ligase buffer (10X)	**2 µl**
T4 DNA ligase (Roche)	**1 µl**
ddH_2O	**Ad 20 µl**
Σ	**20 µl**

2.1.7 Production of chemical competent *E.coli* bacteria

TB Medium 10 mM HEPES, 15 mM $CaCl_2$, 250 mM KCl, 55 mM $MgCl_2$ (pH 6,7)

Super Optimal Broth (SOB) 0,2% (w/v) Tryptone, 0,05% (w/v) yeast extract, 8,5 mM NaCl, 10 mM $MgCl_2$, 8,5 mM NaCl, 10 mM $MgCl_2$, 10 mM $MgSO_4$. Autoclave at 120°C and 1,2 bar for 20 min.

Luria Broth (LB) 1% (w/v) Tryptone (BD), 0,5% (w/v) yeast extract (BD), 0,5% NaCl (w/v) in dH_2O, adjust pH with NaOH to pH 7,0. Autoclave at 120°C and 1,2 bar for 20 min

LB agar plates 1% (w/v) Tryptone (BD), 0,5% (w/v) yeast extract (BD), 0,5% NaCl (w/v), 15% (w/v) Agar (BD) in dH_2O adjust pH with NaOH to pH 7,0. Autoclave at 120°C and 1,2 bar for 20 min.

Ampicillin stock solution 100 mg/ml Ampicillin (Sigma) in 80% Ethanol, filtered sterile through a 0,22 µM filter (VWR), was aliquoted and stored at -20°C until further usage.

LB-Ampicillin agar plates After autoclaving let the LB agar solution cool down to 50°C before adding Ampicillin until final concentration of 100 µg/ml (1/1000 dilution).

Shaking incubator Certomat BS-1, Braun Biotech International

Cooled centrifuge Avanti J-20XP equipped with JA-10 rotor (Beckman Coulter)

At the first day of the protocol, the desired bacterial strain is streaked out on a LB agar plate and incubated at 37°C over night. The following day 100 ml of SOB medium are inoculated with a single clone of the LB agar plate. The SOB medium is subsequently incubated in a shaking incubator at 37°C and 300 rpm.

On the day of harvest the overnight incubated SOB culture is diluted with SOB medium until the optical density at 600 nM ($OD_{600)}$ reaches 0.1. The culture is grown under continuous control of OD_{600} for another four to eight hours until the optical density reaches 0.6.

Upon reaching the appropriate density the culture is cooled down to 4°C on ice for 10 min. Afterwards the bacteria are pelletized in a cooled centrifuge (Avanti J-20XP, Beckman Coulter) equipped with a JA-10 Rotor (Beckman Coulter) at 3500 rpm for 20 min. After discarding the SOB medium, the bacterial pellet is resuspended in 4°C cold TB medium and incubated for another 10 min on ice. After a second centrifugation step (3500 rpm/20 min) the bacterial pellet was again thoroughly resuspended in 20 ml fresh TB medium, followed by addition of 7% (v/v) DMSO and a final incubation step on ice for 10 min. Finally the solution is aliquoted in 200 µl portions and frozen away at -80°C until further usage.

2.1.8 Transformation of chemical competent bacteria

Luria broth (see 2.1.6)

Luria broth agar plates (see 2.1.6)

Ampicillin stock solution (see 2.1.6)

Bacteria are thawed on ice before usage. 60 µl of chemical competent bacteria are mixed with 20 µl of a ligation reaction (2.1.5) or with 1 µl of a Clonase reaction. The

mixture is incubated for 30 min on ice, followed by a heat shock at 42°C for 1 min. Afterwards the bacteria are taken up in 320 µl Luria broth without antibiotics, followed by 30 min incubation in a shaking incubator (Certomat BS-1, Braun Biotech International). 150 µl of this mixture are finally plated on an LB agar plate with Ampicillin (100 µg/ml) which in turn is incubated at 37°C overnight. The bacterial strain for propagation of plasmids depends on the plasmid's properties.

Table 6 Bacterial strains including genotype used in this study

Name	Genotype
DH5-alpha	F^- endA1 glnV44 thi-1 recA1 relA1 gyrA96 deoR nupG Φ80d*lacZ*ΔM15 Δ(*lacZYA-argF*)U169, hsdR17(r_K^- m_K^+), λ–
DB3.1	F- gyrA462 endA1 glnV44 Δ(sr1-recA) mcrB mrr hsdS20(r_B^-, m_B^-) ara14 galK2 lacY1 proA2 rpsL20(Sm^r) xyl5 Δleu mtl1
GM2163	F^- dam-13::Tn9 (Cam^r) dcm-6 hsdR2 ($r_k^-m_k^+$) leuB6 hisG4 thi-1 araC14 lacY1 galK2 galT22 xylA5 mtl-1 rpsL136 (Str^r) fhuA31 tsx-78 glnV44 mcrA mcrB1

2.1.9 Small scale purification of plasmid DNA

Luria broth with Ampicillin (LB-AMP) (see 2.1.6)
Cooled centrifuge Multifuge 3 S-R (Heareus/Thermo)
Table top centrifuge Biofuge Pico (Heraeus/Thermo)
Shaking incubator Certomat BS-1
DNA extraction kit Nucleospin Plasmid® (Macherey&Nagel)

5 ml of LB-AMP are inoculated with a single bacterial colony of the transformation reaction streaked out and incubated at 37°C on a LB-AMP agar plate overnight. Afterwards these are inoculated at 37°C and 300 rpm in a shaking incubator. The bacterial culture is pelletized in a cooled centrifuge at 4600 rpm for 10 min. Finally the LB medium is discarded and the plasmid DNA is extracted from the bacterial pellet using a DNA extraction kit according to the instructions to the manufacturer. The DNA is solved in ddH_2O and stored at -20°C until further usage.

2.1.10 Large scale purification of plasmid DNA

Luria broth with Ampicillin (LB-AMP)	(see 2.1.6)
Cooled centrifuge	Avanti J-20XP equipped with a JA-10 rotor (Beckman Coulter)
Shaking incubator	Certomat BS-1
DNA extraction kit	Nucleobond® Xtra Midi Kit (Macherey&Nagel)
Erlenmeyer flask	

Positive bacterial colonies which are identified either by DNA sequencing or restriction digest to propagate the appropriate DNA sequence are propagated in an Erlenmeyer flask containing 250 ml LB-AMP medium at 37°C and 300 rpm in a shaking incubator. After overnight incubation the bacterial culture is pelletized in a cooled centrifuge at 6000 rpm. Afterwards the LB-AMP medium is discarded and the DNA of the bacterial pellet is extracted using a DNA extraction kit according to the instructions provided by the manufacturer. Finally the DNA is solved in ddH_2O and stored at -20°C until further usage.

2.1.11 Sequence verification of newly cloned DNA constructs

The verification of DNA sequences via sequencing was performed with DNA construct specific primers by the company GATC in Konstanz.

2.2 Cell culture methods

2.2.1 Culture and manipulation of immortalized cell lines

Cell culture media	Dulbecco's modified Eagle's medium (DMEM), High Glucose, GlutaMAX™ (Invitrogen, 61965) Dulbecco's modified Eagle's medium (DMEM), High Glucose, GlutaMAX™, Pyruvate (Invitrogen, 10569) Optimem (Invitrogen, 51985) Advanced RPMI (12633) DMEM/F12 (Lonza, BE12-7197)

Serum	Fetal calf serum (Sigma)		
Antibiotics	Penicillin/Streptomycin	1% (v/v)	(Gibco)
	Geneticin/G418	200 µg/ml	(Roche)
Non-essential amino acids	NEAA (PAA)		

Human embryonic kidney cells immortalized with the large-T antigen of the SV40 virus (HEK293-T) or immortalized with the Ebstein-Barr virus nuclear antigen (EBNA) (HEK293-E) are used as basic cell lines. Furthermore the human neuroblastoma cell line SH-SY5Y and the murine neuroblastoma cell line N2A are used in order to have immortalized cell lines of neuronal origin. Jurkat cells are used as well in this study.

2.2.1.1 Culture conditions of cells

Sterile Hood	(Hera Safe, Heraeus)
Cell culture incubator	(Hera Cell, Heraeus)
Cell culture dishes and flasks	(Nunc)
Plastic ware	(Sarstedt)
Light Microscope	(Hundt, Wetzlar)

Cells are cultured in 10 cm dishes with 8 ml cell culture medium or in 175cm^2 flasks with 12 ml cell culture medium at 37°C and 5% CO_2. Passaging and manipulation of cells is done under a sterile hood. Confluency and viability of cells is controlled under a light microcope.

2.2.1.2 Passaging of cells

PBS	140 mM NaCl, 10 mM Na_2HPO_4, KCL, 1,75 mM KH_2PO_4 pH 7,4 autoclaved at 120°C and 1,2 bar for 20 min
0,25% Trypsin-EDTA	(GIBCO, 25200)
Plastic ware	(Sarstedt)

Cell culture medium of cells is discarded using a vacuum pump attached to a waste tank. Afterwards the cells in the dish are washed with 5 ml of PBS to get rid of any remaining dead cells and excess medium. During the next step, 1 ml to 1,5 ml of Trypsin-EDTA are added to enzymatically dissociate the cells from the cell culture dish. Upon dissociation the cells are taken up in 10% Serum (v/v) growth medium and pelletized at

1000 g for 5 min at room temperature. The supernatant is discarded and cells are taken up in 10 ml fresh growth medium. Dilutions and respective growth media are indicated in the table below. For example for passaging of HEK293T cells 1/10 of the initial cell population is transferred to a new cell culture dish. The dilutions can vary depending on how dense the cells are needed.

Table 7 Cell lines including host origin and culture medium

Cell line	Species	Medium	Dilution ratio
HEK293T	Homo sapiens	DMEM+10% FCS + Pen/Strep	1/10
HEK293E	Homo sapiens	DMEM+10% FCS + Pen/Strep	1/10
N2A	Mus musculus	DMEM+10% FCS + Pen/Strep	1/5
SH-SY5Y	Homo sapiens	DMEM+15% FCS + Pen/Strep+NEAA	1/10
Jurkat	Homo sapiens	DMEM+15% FCS	1/5

2.2.1.3 Cryopreservation

Cryopreservation medium DMEM with 10% (v/v) FCS, add 10% (v/v) DMSO (FLUKA)
Cryovials (Nunc)
Cryobox (Sarstedt)
Water bath (GFL)
Centrifuge
Plastic ware/Falcon tubes (Sardstedt)

The cell pellet of an 80% confluent 10 cm dish is resuspended in 2 ml of cryopreservation medium and afterwards equally divided up into two cryovials. After slow cool down in cryoboxes cell are stored at -80°C until further usage. For long term storage cells are transferred from - 80°C to a liquid nitrogen container.
For recultivation, cells are rapidly thawed in a 37°C tempered water bath and taken up in 10 ml fresh cell specific culture medium. Afterwards cells are pelletized at 1000 rpm, the culture medium is discarded and the pellet is resuspended in fresh culture medium. Engraftment of cells was checked 10 hours after plating under a light microscope.

2.2.1.4 Liposomal transfection

For liposomal transfection of cells, DNA is mixed with Lipofectamine 2000 (Invitrogen) in a 3:1 ratio according to the instructions of the manufacturer. In more detail,

Lipofectamine 2000 is mixed with DMEM without antibiotics and incubated for 5 min. Afterwards DNA diluted in an equal volume of DMEM is added. The mixture is incubated at RT for 20 min. Afterwards, the mixture is evenly distributed on a 90% confluent cell culture dish.

2.2.2 Lentivirus production

Plasmid vectors	psPAX2, pcDNA3.1(-)-VSVG, transfer vector
Transfection medium	Optimem + 10% FCS
Packaging medium	DMEM + Pyruvate + 10% FCS
Sterile filter 0,45 µm	(VWR)
Sterile filter 0,45 µm	(Millipore, Millex, 0,45 µM, PVDF)
5 ml, 50 ml syringes	(Terumo)
Ultracentrifuge	Optima LE-80K (Beckman Coulter)
SW28 Rotor	(Beckman Coulter)
Centrifuge tubes	Ultra Clear Centr. tubes (Beckman Coulter, 344058)

For small scale production of lentiviral particles $1{,}8x10^6$ low passaged HEK293T cells are transfected with a transfection mix of 1,3 µg transfer vector, 0,75 µg psPAX2 and 0,45 µg pcDNA3.1(-)-VSVG mixed with 6,3 µl Lipofectamine 2000. Cells are seeded in 2 ml transfection medium and transfected in solution. The following day transfection medium is replaced for 2 ml of warmed packaging medium. On day 2 after transfection, the conditioned packaging medium containing lentiviral particles is filtered through a sterile filter with 0,45 µM (VWR) attached to a 5 ml syringe to remove any cellular debris. Finally, the cleared lentiviral supernatant is added to $0{,}5x10^6$ target cells. In most cases transduction success can be assessed by checking for the percentage of GFP positive cells with a fluorescent microscope.

For large scale production and generation of purified lentiviral stocks, $36x10^6$ low passaged HEK293T cells are transfected with a transfection mix containing 30 µg transfer vector, 20 µg psPAX2 and 10,8 µg pcDNA3.1(-)-VSVG and 136 µl of Lipofectamine 2000. Cells are mixed with the transfection mix in a 50 ml Falcon tube. $9x10^6$ transfected cells are seeded in 9 ml per 10 cm dish. The following day the transfection medium is exchanged for 8.5 ml of warm packaging medium without detaching the cells. On day 2 after transduction, the medium is collected and filtered through a 0,45 µM sterile filter (Millipore, these have better quality than VWR and therefore can filter higher volumes before clocking). 36 ml of medium are filled into one ultra clear tube fitted into a swinging bucket of the SW28 rotor. After balancing by the addition of medium the rotor is

centrifuged at 22000 rpm and 4°C for 2 hours. Afterwards the medium is carefully removed with a vacuum pump without disturbing the white fragile pellet at the bottom of the tube. Immediately after medium removal, the pellet is covered with 250 µl of TBS-5+BSA buffer and incubated for 4 hours in the fridge followed by resuspension, a clarying spin at 3000 rpm in a cooled table top centrifuge and aliquoting into desired volume amounts. The potency of the purified virus can be assessed by testing different concentrations of the virus on the same number of cells.

Table 8 Cell lines generated via lentiviral transduction

Cell line	Construct	Target cells
SHSY5Y-ADAM10-hs7-shRNA	plKO2mod-EGFP-WPRE-hsAD10-sh7	SHSY5Y
SHSY5Y-ADAM10-hs9-shRNA	plKO2mod-EGFP-WPRE-hsAD10-sh9	SHSY5Y
SHSY5Y-Control-shRNA	plKO2mod-EGFP-WPRE-Control	SHSY5Y
HEK293T-BACE1-shRNA1	plKO2mod-EGFP-WPRE-hsBACE1-sh1	HEK293T
HEK293T-BACE1-shRNA2	plKO2mod-EGFP-WPRE-hsBACE1-sh2	HEK293T
HEK293T-Control-shRNA	plKO2mod-EGFP-WPRE-Control	HEK293T
SHSY5Y-APP-TEV-FLAG + Gal4-VP16	FUΔZeo-Gal4-VP16 + FΔZeo-DsRed-UAS-APP-TEV-FLAG	SHSY5Y

2.2.3 Isolation and culture of primary cortical neurons

Culture medium Neurobasal medium (Invitrogen, 21103049), supplemented with 2% (v/v) B27 DMEM (Invitrogen, 17504044), 0,5mM Glutamine, 1% Pen/Strep (v/v)

Plating medium DMEM, High Glucose, Glutamax™ supplemented with 10% (v/v) FCS, 1% Pen/Strep (v/v)

Digestion medium 9,7 ml DMEM, High Glucose, Glutamax™, 0,01 g Cysteine neutralized with 27 µl 1 M NaOH (S2770, Sigma), 200U Papain (P3125, Sigma) (ca. 300 µl) (mix in the indicated order)

Preparation medium Hank's balanced salt solution (HBSS) with Calcium and Magnesium (Invitrogen, 24020)

Dissociation medium DMEM, High Glucose, Glutamax™ supplement with 10% FCS (v/v)

Coating medium 25 µg/ml Poly-D-Lysine (Sigmaaldrich)

Instruments	Appropriate surgical scissors and forceps (Fine Science tools, FST)
Plastic ware	15 cm dishes, T175 flasks and 6well plates (Nunc)

The day before preparation of neurons, plates are covered with coating medium. On the day of preparation before starting with the extraction of neurons, necessary media are prepared and kept at 37°C until further usage. The pregnant mouse with E15/E16 embryos is killed by cervical dislocation. The fur of the abdomen and thorax region is disinfected with 80% Ethanol. After disinfection, a small incision is cut into the fur leaving a cranial and a caudal skin leaflet. Pulling both in opposite directions allows for easy displacement of the skin. A second cut into the peritoneum gives access to the abdominal cavity with the embryos. The embryonic containing uterus is detached from the blood supply and directly put into a 15 cm dish on ice filled with 20 ml of 4°C HBSS. In the next step, embryos are removed out of the uterus, the head is detached from the corpus by carefully cleaving it off. Next, the skin is removed from the head and the dura mater is opened at the lambda and carefully removed under protection of both hemispheres. After detachment of the brain from the head, the pia mater is removed from both hemispheres starting from the circle of willis. Next, the hemispheres are incubated in the digestion medium at 37°C for 15 min. Afterwards the digested hemispheres are carefully triturated with a 2 ml syringe attached to a pelleus ball. The dissociated neurons are transferred to a new falcon tube to get rid of non-dissociated brain pieces. The neuron suspension is centrifuged at 800 rpm for 5 min. Finally, the neuron pellet is again dissociated in plating medium. Neurons are counted and appropriate numbers are seeded according to the plate size (indicated in the table below). After 4 hours the plating medium is exchanged for the culture medium.

Table 9 Typical numbers of neurons seeded in different well-sizes

Number of plated neurons	Plate type
100.000	96well plate
500.000	24well plate
1.500.000	6well plate
20.000.000	T175 Flask

2.2.4 Lentiviral infection of primary cortical neurons

Purified lentiviral stocks
96well plate with neurons

Before starting with the actual experiments, the potency of purified lentiviral stocks has to be determined by adding different dilutions of virus on the same amount of neurons. This is done in a 96Well format. Two days after infection, the transduction efficiency is assessed by counting the percentage of GFP positive cells in one high power field (HPF). The final working concentration is the neighboring lower dilution of the dilution which yields 100% transduction efficiency in order to have a safety margin which guarantees 100% transduction efficiency in every experiment.

2.2.5 Compound treatment of cells including primary neurons

Cells like neurons are treated with the following compounds:

Table 10 Compounds used in this study

Substance	Source	Solvent	Concentration
TAPI-1	Peptides International	DMSO	25 µM
C3 (β-Secretase inhib. IV)	Calbiochem	DMSO	2 µM
tetraacetyl-*N*-azidoacetyl-mannosamine	Katarzyna Koroniak	DMSO	50 µM
tetraacetyl-*N*-azidoacetyl-galactosamine	Katarzyna Koroniak	DMSO	50 µM
DBCO-PEG12-Biotin	Click chemistry tools	DMSO	20 µM

Cells are treated with TAPI-1 and C3 over night and with tetraacetyl-*N*-azidoacetyl-mannosamine or tetraacetyl-*N*-azidoacetyl-galactosamine for 48 hours.

2.3 Protein analysis methods

2.3.1 Cell lysis

PBS 140 mM NaCl, 10 mM Na_2HPO_4*2 H_2O, 1,4 mM KH_2PO_4, 2,7 mM KCL in ddH_2O

STEN-lysis buffer 150 mM NaCl, 50 mM TRIS, 2 mM EDTA, 1% NP40 (USBiological)

STET-lysis buffer 150 mM NaCl, 50 mM TRIS, 2 mM EDTA, 1% Triton-X100 (Merck)

Standard lysis protocol

Supernatant is transferred from the well to a 1,5 ml cup and subjected to a clarifying spin at 15000 rpm for 1 min. The supernatant is transferred to a fresh 1,5 ml cup without disturbing the pellet and frozen at -20°C until further analysis. Afterwards the cells are washed once with ice-cold PBS to get rid of most of the serum proteins. Cells are lysed on ice with a cell number and dish size adjusted volume of 4°C cold lysis buffer for 15 minutes (see table). Afterwards remaining cells are resuspended with a pipette. Finally, the lysate is transferred to a 1.5 ml cup and subjected to a clarifying spin at 15000 rpm at 4°C. The clarified lysate is transferred to a new 1.5 ml cup without disturbing the pellet. Afterwards the pellet is discarded and the clarified lysate is frozen away at -20°C. Protein concentration is determined with the BC assay (see 2.3.3).

Table 11- Lysis volume

Type of dish	Amount of lysis buffer
24Well plate	300 µl
6 cm plate	500 µl
10 cm plate	1000 µl

2.3.2 Extraction of soluble and insoluble fraction of brain tissue

DEA Lysis Buffer	0,2% Diethylamine (v/v)**,** 50 mM NaCl**,** (final pH is 10, doesn't need to be adjusted!!)**,** 2 mM EDTA
TRIS buffer	0,5 M TRIS pH 6,8
Cleaning solutions	MetOH (100%), PBS (140 mM NaCl, 10 mM Na_2HPO_4*2 H_2O, 1,4 mM KH_2PO_4, 2,7 mM KCL)
Triton lysis buffer	150 mM NaCl**,** 50 mM Tris**,** 2 mM EDTA**,** pH 7,5**,** 1% Triton-X100 (v/v)
Waste container	For wash solutions
Potter	which can be attached to a motorized potter device
2 ml Cups	Sarstedt
1,5 ml Cups	Sarstedt
1,5 ml Cups	Beckman Coulter
TLA-55 rotor	Beckman Coulter
Ultracentrifuge	Beckman Coulter

All protocol steps should be done on ice eg. 4°C

Label tubes according to your samples. Prealiquot 220 µl TRIS buffer into the 2 ml cups which afterwards get filled with the brain homogenate. Fix the piston to the motorized potter device. 2 ml of DEA lysis buffer is added to one frozen P7-P brain in the potter. The piston is dipped into the cylinder of the potter. Subsequently, the motor is started and the brain is homogenized until no bigger particles can be observed in the cylinder. The homogenate is transferred to the previously prepared 2 ml eppendorf cup. Afterwards piston and cylinger are cleaned with ice-cold Methanol (100%), followed by two washes with PBS. The whole sequence is repeated until all samples are homogenized.

The resulting neutralized homogenates are kept on ice in the meantime. During the next step, the homogenates are centrifuged at 5000 rpm for 10 min at 4°C in a cooled table-top centrifuge. The 2,2 ml of milky yellow homogenate are carefully split on two 1,5 ml cups suitable for ultracentrifugation without disturbing the pellet followed by ultracentrifugation at 55000 rpm for 30 minutes at 4°C. While the supernatants are centrifuged the remaining pellet in the 2 ml tubes is carefully sucked dry followed by the addition of 1 ml PBS buffer. Afterwards the pellets are centrifuged again at 14000 rpm for five minutes. Any remaining soluble fraction is removed during this step. Finally the pellets are solubilized in triton lysis buffer and intermittent vortexing for one hour. In the meantime the ultracentrifugation should be done. Transfer the soluble clear fraction to new eppendorf cups without disturbing the pellet. This will yield the DEA soluble fraction of your brain. After completion of the lysis incubation of your pellets in the 2 ml cups centrifuge again at 15000 rpm for 10 min. Finally transfer the supernatant to a fresh eppendorf cup. This will yield the insoluble, detergent soluble membrane fraction of the brain.

2.3.3 Protein measurement

Bicinchinonic acid (BC) Assay	BC Assay Solution A and B (Uptima, UP95424A)
ELISA reader	Powerwave XS, Biotek
96well microtiter plates	Nunc

For standard measures of the protein concentration of lysates obtained from primary or immortalized cells, solution A and Solution B are mixed in a 50:1 ratio. 10 µl of lysate are mixed with 200 µl of AB mixture in a 96 microtiter plate followed by 30 minutes incubation at 37°C. Afterwards absorption of the purple color reaction is measured with an ELISA reader at 562 nm wave length according to the instructions of the manufac-

turer. Using different defined concentrations of bovine serum albumin as a reference standard allows determination of the sample protein concentration.

2.3.4 SDS gel electrophoresis

4x Laemmli buffer	0,25 M TRIS pH 6,8 adjusted with HCL, 8% SDS (w/v) 40% Glycerin (v/v), 1 spatula bromphenol blue solved in ddH_2O
4x Lower TRIS buffer	1,5 M TRIS **pH 8,8** adjusted with HCL, 0,4% SDS (w/v)
4x Upper TRIS buffer	0,5 M TRIS **pH 6,8** adjusted with HCL, 0,4% SDS (w/v)
10x TRIS-Glycine	0,24 M TRIS base (w/v), 0,2 M Glycine (w/v) (Roth), dH_2O, 1% SDS (w/v) ad 5 l (for 10X TRIS/Glycine)
TEMED	(N,N,N',N'-Tetramethylethylendiamin, Roth)
Ammoniumpersulfate	(APS, Sigma): 10% (w/v) solved in ddH_2O
Gel running system	Mini-Protean system (Biorad)
Power supply	Powerpac 300 (Biorad)
Gel cast equipment	Plates, gel racks (Biorad)
MW marker	See blue plus 2 (Invitrogen)

In this work, proteins are separated under denaturing conditions in 1,5 mm thick gels (7,5 ml of separation gel, 2,5 ml of stacking gel) . For gel electrophoresis the Mini-Protean system of Biorad is used according to the instructions of the manufacturer. The amounts indicated in the table below are sufficient to cast two polyacrylamide gels.

Table 12 - Volumes for the composition of two TRIS-glycine polyacrylamide gels

	8% Gel	**10% Gel**	**12% Gel**	**15% Gel**
Separation gel				
Acrylamid 40% (Serva)	7,8 ml	6,66 ml	6 ml	4 ml
ddH_2O	4,2 ml	5,33 ml	6 ml	8 ml
4X Lower TRIS	4 ml	4 ml	4 ml	4 ml
APS	30 µl	30 µl	30 µl	30 µl
TEMED	30 µl	30 µl	30 µl	30 µl
∑=	**16 ml**	**16 ml**	**16 ml**	**16ml**
Stacking gel				
Acrylamid 40% (Serva)	1,3 ml	1,3 ml	1,3 ml	1,3 ml
Aqua bidest	6,5 ml	6,5 ml	6,5 ml	6,5 ml
4X Upper TRIS	2,5 ml	2,5 ml	2,5 ml	2,5 ml
APS	30 µl	30 µl	30 µl	30 µl
TEMED	30 µl	30 µl	30 µl	30 µl
∑=	**10,3 ml**	**10,3 ml**	**10,3 ml**	**10,3 ml**

For separation of the investigated proteins different amounts of protein are loaded on the gel which never exceed 50 µg. For loading of protein, the protein lysate is mixed with 4X Laemmli buffer and cooked for 5 min at 95°C. After loading, the sample enters the gel at 80 V until it reaches the separation gel. This can be controlled by the visible separation of the molecular weight marker. Subsequently, proteins in the sample are separated at 120 V until the bromphenol blue containing running front reaches the end of the gel.

2.3.5 Separation of proteins with low molecular weight

Acrylamide solution	49,5% Acrylamide (w/v) (Serva), 3% Bis-Acrylamide (w/v) (Serva) in ddH_2O
Gel buffer	3 M TRIS/HCL, 0,3% (w/v) SDS
Glycerol	32% Glycerol in ddH_2O (v/v)
Anode buffer	1 M TRIS/HCL pH 8,9
Cathode buffer	0,1 M TRIS/HCL, 1 M Tricine (Biomol), 0,1% SDS (w/v)

For separation of low molecular weight proteins the discontinuous two step gel system according to Schägger is used (Schagger and von Jagow, 1987). All solutions are set up before casting of gels. Before casting the gels, APS is added to both separation gel solutions. First, the second separation gel solution is poured into the casting chamber. Directly afterwards, the casting chamber is tilted to a 60° angle and the first separation gel solution is carefully layered over the second separation gel solution. This results in a uniform gradient. The separation gel is covered with a layer of isopropanol to form a straight edge between separation and stacking gel. After polymerization, isopropanol is removed and the separation gel is covered with the stacking gel solution with the desired gel comb. The volumes indicated in the following table are sufficient for two 1,5 mm thick gels. The gel running buffers are indicated above. Proteins enter the gel at 80 V until these arrive in the separation gel. This can be visually controlled by separation of the molecular weight marker. Upon arrival, the voltage is set to 120 V until the bromphenol blue containing running front reaches the end of the gel.

Table 13 - Volumes for the composition of two TRIS-TRICINE polyacrylamide gels

	Sep. Gel (2. phase)	Sep. Gel (1. phase)	Stacking gel
Acrylamide sol.	3,5 ml	1,5 ml	0,5 ml
Gel buffer	3,5 ml	2.5 ml	1,55 ml
Aqua bidest	-	3,5 ml	4,2 ml
Glycerine	3,5 ml	-	-
10% APS	32,5 µl	35 µl	25 µl
TEMED	3,25 µl	4 µl	5 µl
∑	**10,5 ml**	**7,5 ml**	**6,7 ml**

2.3.6 Coomassie staining of SDS gels

Staining solution 50% (v/v) Ethanol, 10% acetic acid (v/v), 2% (w/v) Coomaassie Blue-R (FLUKA,27816), in ddH_2O

Destaining solution ddH_2O

Horizontal shaker Kleinschüttler KM2 (Edmund Bühler GmbH)

Slab gel dryer Slab gel dryer system (Savant)

15 cm dishes plastic ware (Sarstedt)

After separating the proteins on a SDS-polyacrylamide gel, proteins in the gel can be either stained directly in the gel with different dyes or subjected to Western blot. For staining proteins directly with Coomassie, the gel is removed from the glass plates, rinsed twice with 20 ml of ddH_2O to get rid of salts and SDS which interfere with the staining procedure. Afterwards the gel is put into a 15 cm dish and incubated for 30 min in 15 ml of staining solution. The staining step is followed by three intensive washes with 20 ml ddH_2O to thoroughly remove the staining solution. The initial wash procedure is followed by several 30 min wash steps with ddH_2O under gentle agitation on a horizontal shaker under exchange of the destaining solution between every wash step. For documentation gels are dried at 50°C with the slab gel dryer system (Savant) over night.

2.3.7 Western Blot

Mini-Protean-Blotting System	(Biorad)
Whatman papers	**(**Schleicher&Schuell)
PVDF membranes	(Millipore)
Nitrocellulose membranes, pore size 0,45 µm	(Whatman,1040196)
Sponges and transfer cassette	(Biorad)

Transfer-Buffer 10X	0,24 M TRIS, 0,2 M Glycine (Roth), dH_2O ad 5l
PBS-Tween	140 mM NaCl, 10 mM Na_2HPO_4*2 H_2O, 1,4 mM KH_2PO_4, 2,7 mM KCL, 1% Tween-20 (Merck) (v/v), dH_2O ad 1l
Milk blocking-buffer	5% skim milk powder (Töpfer) (w/v) solved in PBS-Tween
I-Block	Combine 1 g I-Block powder (Tropix), 500 µl Tween-20, PBS ad 0,5 l. Heat the solution in the microwave (prevent cooking of the solution) until all visible particles are dissolved. I-Block can be stored at 4°C until usage.

Horizonal shaker Typ 3005	**(GFL)**
ECL-System	**(General Electric)**
ECL-Plus-System	**(General Electric)**

For Western Blot separated proteins in the polyacrylamide gel have to be transferred to a membane which is able to bind and immobilize proteins. Therefore a sandwich (From bottom to top: sponge, 2 layers of whatman paper, polyacrylamide gel, membrane, 2 layers whatman, sponge whatman) is build and fixed in a transfer cassette according to the instructions of the provider. The membrane is orientated to the anode as the due to the SDS negatively charged proteins migrate to it. The transfer is done at 400 mV for 65 min. After the transfer remaining unspecific protein binding sites of the membrane are blocked by incubating the membrane in either milk-blocking buffer or I-block depending on the antibody for 30 min on a horizontal shaker at 200 rpm and room temperature (RT). The block step is followed by two short washes with 20 ml PBS-T and incubation of the membrane with the primary antibody for one hour (The incubation time can be longer depending on the binding kinetic of the antibody to its antigen). Afterwards, the primary antibody is collected into its harboring tube and the membrane is washed twice with 20 ml PBS-Tween to get rid of any remaining primary antibody and more important of the preservative sodium azide which would otherwise interfere with the horse radish peroxidase activity of the secondary antibody.

The secondary antibody is diluted in PBS-T + 0,5% BSA 1:5000-1:10000 depending on the secondary antibody and the antigen. This dilution is incubated for 45 min on the membrane. Finally, the membrane is washed five times with PBS-T to remove unbound secondary antibody or nonspecifically bound antibody. For development of the Western Blot either ECL (enhanced chemiluminescence) or ECL Plus in case of weak signals are used according to the instructions of manufacturer.

2.3.8 Antibody list

PBS	140 mM NaCl, 10 mM Na_2HPO_4*2 H_2O, 1,4 mM KH_2PO_4, 2,7 mM KCL in ddH_2O
6% BSA	6% bovine serum albumin (Sigmaaldrich) (w/v), solved in 100 ml ddH_2O
PBS-Tween	PBS, 0,05% Tween®20 (Merck, 817072) (v/v)
Sodium azide stock	10% Sodium azide (NaN_3) (w/v)

All antibodies are diluted in PBS-T + 0,6% BSA + Sodium azide (0,05% w/v)

Table 14 Antibodies

antibody	Epitope	Dilution	Host	Source
Anti-Sez6	Sez6 ectodomain	1:2000	Rabbit	Jenny Gunnersen
Anti-L1CAM-555	L1CAM ectodomain	1:1000	Rat	Peter Altevogt
Anti-CHL1	CHL1 ectodomain	1:1000	Goat	R&D Systems, AF2147
Anti-Contactin-2	Contactin-2 ectodomain	1:1000	Goat	R&D Systems, AF4439
Anti-APLP2	APLP2 ectodomain	1:5000	Rabbit	Calbiochem, 171617
Anti-APLP1	APLP1 ectodomain	1:1000	Rabbit	Proteintech, 12305-AP
Anti-APP-22C11	APP ectodomain	1:1000	Mouse	Konrad Bayreuther
Anti-APP 2C11	Cytoplasmic domain	1:10	Mouse	Elisabeth Kremmer
Anti-sAPPβ 8C10	ISEVKM	1:10	Rat	Elisabeth Kremmer
Anti-sAPPβ 192wt	C-terminus of APPsβ	1:1000	Rabbit	Dale Schenck
Anti-sAPPα 14D6	YEVHHQ	1:10	Mouse	Elisabeth Kremmer
Anti-sAPPα 7A6	YEVHHQ	1:10	Mouse	Elisabeth Kremmer
Anti-N-Cadherin C32	C-terminus of N-Cadherin	1:1000	Mouse	BD Bioscience, 610921
Anti-N-Cadherin	Ectodomain of N-Cadherin	1:1000	Rabbit	Cell Signaling, 4061
Anti-PTPRF	Cytoplasmic Domain	1:1000	Mouse	Neuromab, N165/38
Anti-ADAM10	ADAM10 c-terminus	1:1000	Rabbit	Calbiochem 422751
Anti-BACE1-3D5	BACE1	1:1000	Mouse	Bob Vassar
Anti-FLAG M2	DYKDDDDK	1:2000	Mouse	Sigmaaldrich, F1804
Anti-β-Actin	β-Actin	1:10000	Mouse	Sigmaaldrich
Anti-Ac. β-Tubulin	Acetylated β-tubulin	1:10000	Mouse	Sigmaaldrich, T8535

2.3.9 Detection and Quantification

Image System	LAS-4000 (GE Healthcare, formerly owned distributed by Fujifilm)
ECL detection System Western	

2.3.10 Analysis of immunoprecipitated peptides with matrix-assisted laser desorption ionization (MALDI) mass spectrometry

STED-wash buffer	150 mM NaCl, 50 mM TRIS, 2 mM EDTA, 0,1% n-Dodecyl-β-D-maltoside (DDM) (Calbiochem,)
STE-buffer	150 mM NaCl, 50 mM TRIS, 2 mM EDTA
FLAG-M2 agarose	Agarose with immobilized FLAG-M2 antibody (Sigmaaldrich)
ddH_2O	
target plate	MALDI target plate (Applied Biosystems)
MALDI mass spectrometer	MALDI DESTR (Applied Biosystems)
Software Data Explorer	(Applied Biosystem)
Software GPMAW	(Lighthouse)

For determination of the APP-cleavage site of ADAM10, a construct was cloned which contains TEV cleagage site followed by a FLAG-epitope tag upstream of the juxtamembrane region of APP. APP-TEV-FLAG is stably expressed in SHSY5Y cells. One T-175 flask is conditioned with 7 ml medium over night. Conditioned medium of 3 confluent T-175 flasks is cleared through a 0,45 µM filter. 21 ml of the overnight conditioned medium are subjected to immunoprecipitation (IP) with 40 µl of FLAG-M2 agarose for two hours on a rotary shaker at 4°C. Afterwards, the FLAG-M2 beads are sequentially washed two times with STED-wash buffer, two times with STE buffer and finally two times with ddH_2O. The captured peptides are eluted from the FLAG-M2 agarose with 40 µl Glycine pH 2.5 for 15 minutes on ice followed by transfer of the acidic eluate to a new 1,5 ml cup. In the following step the eluate is neutralized with 200 µl of 100 mM TRIS pH 8.0. Add 2,4 µl DTT of 0,1 M DTT stock solution, 1,2 µl of 0,1 M EDTA and 1 µl of TEV protease in the indicated order. Incubate the mixture at 4°C on a rotary shaker over night. Dilute the mixture with 15 ml PBS in a falcon tube. Add 10 µl of FLAG-M2 agarose. Incubate for two hours on a rotary shaker. Centrifuge at 4600 rpm in Heareus Cryofuge to spin down the FLAG-M2 agarose. Finally wash the

beads sequentially two times with STED wash buffer, two times with STE buffer and 3 times with ddH_2O. Elute the captured peptides with 20 µl of a 20/20/1 (v/v) mixture of Chromasolv grade water/ACN/TFA saturated with α-cyano matrix. Spot 1 to 2 µl on a hydrophobic target plate and let the spots dry. Afterwards peptides are measured in linear mode and reflector mode with a mass range from 500 m/z to 4000 m/z, a low mass gate of 500 m/z, 100 spectral counts per measurement with a MALDI DESTR.

2.3.11 Secretome protein enrichment with click sugars (SPECS)

Ultrafiltration spin columns	Vivaspin 20 (Satorius Stedim Biotech,VS2022)
Dialysis buffer	PBS (see 2.3.8)
Biotin-Click reagent	DBCO-PEG12-biotin conjugate (A105P12-25, Click chemistry tools)
Wash buffer	PBS + 2% (w/v) SDS
Elution buffer	62.5 mM TRIS pH 6.8, 2% (w/v) SDS, 7,5% (v/v) Glycerol, 2,5% (v/v) β-Mercaptoethanol, 48% (w/v) Urea
Biotin stock	100 mM D-Biotin solved in DMSO
Streptavidin beads	High Capacity Streptavidin Agarose (Thermo, 20361)
Sterile filter 0,45 µm	(Millipore, Millex, 0,45 µM, PVDF)

48 hours conditioned media of HEK293T cells or primary neurons labeled with the desired N-acetylazido amino sugar are filtered into a precooled ultrafiltration spin column through a 0,45 µM sterile filter attached to a 50 ml syringe. Afterwards the columns (normally is a control and treatment condition) are centrifuged at 4600 rpm for 50 min in a 4°C cold centrifuge (Haereus Biofuge 3 S-02). After centrifugation the flow is discarded and the retentate is filled up with 20 ml PBS. This procedure is repeated 3 times in order to get rid of any free n-acetylazido amino sugar. In the last repetition instead of filling up the retentate with 20 ml PBS. 1 ml of PBS + 5% (v/v) DMSO + 2,5 µl of DBCO-PEG12-Biotin (50 mM) is added to the retentate and incubated at 4°C in the fridge over night in order to perform the click reaction between the incorporated n-acetylazido amino sugar and the strained alkyne moiety of the Biotin reagent. The following day the biotinylated retentate is diafiltrated another four times against PBS as described above. After the fourth centrifugation step, the retentate is taken up in 9,5 ml of PBS + 2% SDS which is in turn added on a polyprep column loaded with 300 µl Streptavidin beads. After the load is run through the Streptavidin bead, the flow through

is run through the beads a second time and finally discarded. The binding step is followed by 3 sequential wash steps with 10 ml PBS+2% to remove nonspecifically bound proteins. After the wash procedure bound proteins are eluted by cooking up Streptavidin beads with 150 µl of Elution buffer + 5 µl 100 mM Biotin (final concentration 3 mM). Eluted proteins are separated on 8% Tris/Glycine gel (2.3.5) and afterwards stained with Coomassie (2.3.6).

2.3.12 Preparation of peptides for mass spectrometric measurement

ABC buffer	100 mM NH_4HCO_3 (Sigmaaldrich,A6141) solved in LC-MS grade H_2O Chromasolv (Sigmaaldrich,39253)
DTT buffer	10 mM DTT (Sigmaaldrich, 43817) in ABC buffer
IAA buffer	55 mM Iodoacetamide (Sigmaaldrich, I1149) in ABC buffer
ACN	Acetonitrile (A9551, Fischer Scientific)
Extraction buffer (ExBu)	2 volumes ACN + 1 volume of 5% FA (Sigmaaldrich, 56302) (v/v) in LC-MS grade H_2O
Trypsin	Sequencing-grade Trypsin (Promega, V5111)
Digestion buffer	0**,**1 µg/µl Trypsin (w/v) in 90% (v/v) ABC buffer and 10% (v/v) CAN (this solution can be kept at -80°C until further usage

Peptides of proteins are extracted by tryptic digest from polyacrylamide gels. All solutions except from the extraction buffer have to be prepared freshly just before use. First, the protein of interest is separated on an ordinary Tris/Glycine gel (2.3.4) which is afterwards stained with Coomassie (2.3.7). Before starting with the excision of gel slices, clean scapel and spatula with isopropanol or methanol (technical grade) and check the equipment for dust. Cut out bands and further cut these into 1 mm^3 cubes. Transfer the cubes into a 96well plate. Add 150 µl of ACN to the gel cubes and incubate these on a horizontal shaker (Edmund Bühler GmbH, KM-2) at 200 rpm, at room temperature (RT) for 10 min. The gel pieces should become completely dehydrated and white. If this is not the case, discard the ACN and repeat the whole step. In the next step, add 50 µl of DTT buffer and incubate at 55°C for 30 min. This leads to a reduction of all cysteine residues. Let the reaction cool down to RT, add 150 µl ACN and let it incubate on a horizontal shaker for 10 min. Afterwards, discard all liquid and cover the gel cubes with sufficient IAA buffer and incubate these for 20 min in the dark. This step leads to an alkylation of all reduced cysteine residues. Discard IAA buffer and shrink gel pieces

again by addition of 150 µl of ACN and incubation for 10 min on a horizontal shaker. Remove all liquid and add 50 µl of 4°C cold trypsin buffer and incubate gel cubes on ice for 30 min. Check if solution is absorbed, if yes, add more trypsin buffer until the gel cubes are slightly covered. Incubate gel cubes overnight at 37°C. Add 100 µl of extraction buffer to the gel pieces and incubate them on a horizontal shaker at 37°C for 15 min. Transfer liquid into 0,5 ml vials. Repeat this procedure at least two times and until the gel pieces are completely dry (normally 3 rounds of extraction are needed). Lyophilize peptides in a speed vac. Lyophilized peptides can be kept at -20°C until further usage.

2.3.13 Online HPLC and measurement of peptides with an LTQ-Velos-Orbitrap

Mass spectromter	LTQ-Velos-Orbitrap (Thermo)
Liquid chromatography	Proxeon Easy-NLC II (Thermo)
Running media	**A** H_2O with 0,1% FA LC-MS CHROMASOLV®, ≥99.5% (GC) (Sigmaaldrich, 34673) **B** ACN with 0,1% FA LC-MS CHROMASOLV®, ≥99.5% (GC) (Sigmaaldrich, 34668)
In-house made Columns	15 cm columns (New Objective, FS360-75-8-N-S-C15) packed with C18 AQ 2,4 µm resin (Dr. Maisch GmbH)

Peptides are loaded and eluted online from a 15 cm long in-house made column with a gradient created by a nano-HPLC directly attached to the ESI source of the mass spectrometer according to the following parameters. (10-25% **B** 50 min, 25-45% **B**, 20 min, 45-95% **B** 2 min, 4 min 95% **B**). The whole gradient takes 75 min. A full ms scan recorded in profile mode with a mass range from 300 m/z to 2000 m/z, a resolution of 30.000 and a target value of 1.000.000, is followed by data dependent collision induced dissociation (CID) in the ion trap of the 14 most intense ions with an isolation width of 2 Da. A target value of 10.000, enabled charge state screening, a monoisotopic precursor selection, 35% normalized collision energy, an activation time of 10 ms, wide band activation and a dynamic exclusion list with 30 s exclusion time are applied. Corresponding samples are measured alternating between samples of the control and treatment condition.

2.3.14 Analysis of mass spectrometric raw data with the MaxQuant Suite

Raw Files are loaded into the MaxQuant Suite. In order to quantify the protein amount in a treatment condition relative to a control condition, raw files of both conditions are loaded into the MaxQuant suite and defined as treatment or control sample in the experimental design file. The MaxQuant Suite contains the peptide search algorithm termed Andromeda similar to commercial peptide search algorithms like Mascot or Sequest. All three programs allow identification of proteins based on the comparison of fragmentation spectra and their parent mass with masses deposited in virtual databases. MaxQuant is used with the following parameters. The database mouse IPI FTMS data are deisotoped before analysis. Water loss, ammonia loss, methionine oxidation and N-terminal acetylation as variable modifications and cysteine alkylation as fixed modification are taken into account for peptide searches. Only those peptides are identified that have less than 20 ppm of deviation from the in silico predicted mass for FTMS and 0,5 Da for ITMS (Iontrap). For label-free quantification (LFQ) the option Match between runs with a 3 min window as well as LFQ are enabled. Only unique peptides are considered for quantification.

2.3.15 Construction of protein filters using SWISS PROTdatabases in excel

For this purpose tab delimited files from all annotated proteins with the SWISSPROT annotations glycosylation, signal peptide, GPI-anchor, signal-anchor or transmembrane domain are loaded into excel. These tables allow filtering of the ouput tables of MaxQuant for all kind of glycosylated membrane proteins or secreted glycoproteins.

2.4 Methods for RNA analysis

2.4.1 RNA extraction

QIAshredder (Qiagen, 79654)
RNeasy Mini Kit (Qiagen, 74104)

RNA is isolated from cells homogenizing the cells with the QIAshredder kit according to the instructions of the manufacturer. RNA is purified with a spin column from the RNeasy kit according to the instructions of the manufacturer.

2.4.2 Reverse transcription

Purified RNA is reverse transcribed with the High Capacity Reverse transcription kit (ABI) according to the instructions of the manufacturer.

2.4.3 qRT-PCR

qRT-PCR machine 7500 Fast Realtime PCR (ABI)
qRT-PCR master mix
cDNA (see 2.4.2)

Quantitative real time PCR (qRT-PCR) is performed with a qRT-PCR machine according to the SYBR Green method using a predefined master mix and reverse transcribed RNA as template. All samples are amplified and measured in duplicates on a 96-well plate according to the protocol indicated below. qRT-PCR primers are designed using Primer 3Plus and afterwards checked for specificity with a melt curve as well as an analytical agarose gel and for efficiency by amplifying a standard dilution curve. In the ideal case a primer pair would lead to an efficiency of two which indicates a perfect DNA duplication in every cycle and one single defined melt curve peak without any side peaks. The yield of a specific RNA is measured by calculating the ∆ct value between a reference cell and the cell of interest. Furthermore, standards like GAPDH or β-actin are included in the analysis to correct for differences in the amount of pipetted template.

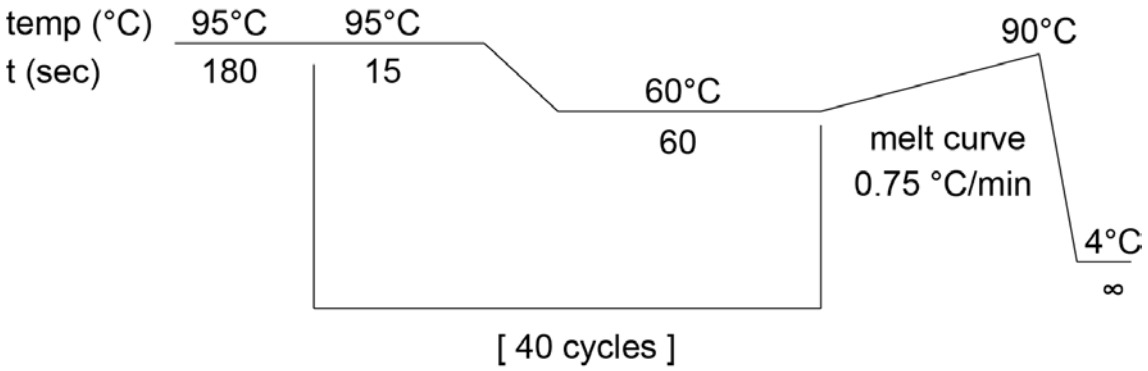

Figure 11 Diagram of a typical qRT-PCR reaction to quantify the RNA content in a sample. Primers are designed to be compatible to this qRT-PCR method.

3 Results

3.1 Construction of potent lentiviral shRNA and lentiviral overexpression vectors

One aim of this thesis was the elucidation of the α-secretase identity in primary cortical neurons which represent the most relevant *in vitro* culture system to study processes involved in Alzheimer's disease pathogenesis.

Using lipotransfection, only about 1% of all neurons are transfected. While in single cell experiments this efficiency is desirable, it renders biochemical experiments impossible. Viruses are a viable alternative to lipotransfection offering almost 100% efficiency in gene delivery (Zufferey et al., 1997). Adeno-associated viruses (AAV) and pseudotyped lentiviruses both enable efficient gene delivery to neurons. Both have their specific disadvantages and advantages.

For the transduction of neurons in this thesis, lentiviruses were used due to a higher packaging capacity, easier purification and higher transduction efficiency *in vitro*.
The basis of all viral shRNA vectors was the plKO1.1 vector developed by the RNAi consortium (TRC). This vector cannot be obtained with a multiple cloning site which allows subcloning of shRNA coding oligo duplexes. To allow for subcloning, a multiple cloning site bearing the restriction sites MluI/XmaI was subcloned in the right distance downstream to the TATA box of the U6 promoter (see Fig. 11). In a second step, the puromycin (Puro) coding sequence (CDS) was exchanged for the green fluorescent protein (GFP) CDS as a fast visual read out for the transduction efficiency of primary cortical neurons was needed. The Woodchuck Hepatitis Virus posttranscriptional response element (WPRE) was subcloned downstream of the GFP CDS as it improves expression of GFP in primary cortical neurons (Paterna et al., 2000; Zufferey et al., 1999). The final vector was termed plKO2mod-EGFP-WPRE and is the basis of all knockdown constructs used in this thesis. Oligo duplexes coding for potent shRNA sequences according to the prediction algorithm of the TRC consortium were subcloned into the plKO2mod-EGFP vector. Immortalized mouse neuroblastoma cells (N2A) were infected to screen for potent murine shRNA sequences. Potent shRNAs could be found against murine ADAM9, ADAM10 and ADAM17 respectively (see 3.2). Lentiviral stocks were generated for one non-targeting control shRNA and six different targeting shRNAs as pointed out in the material and methods section (see 2.2.2).

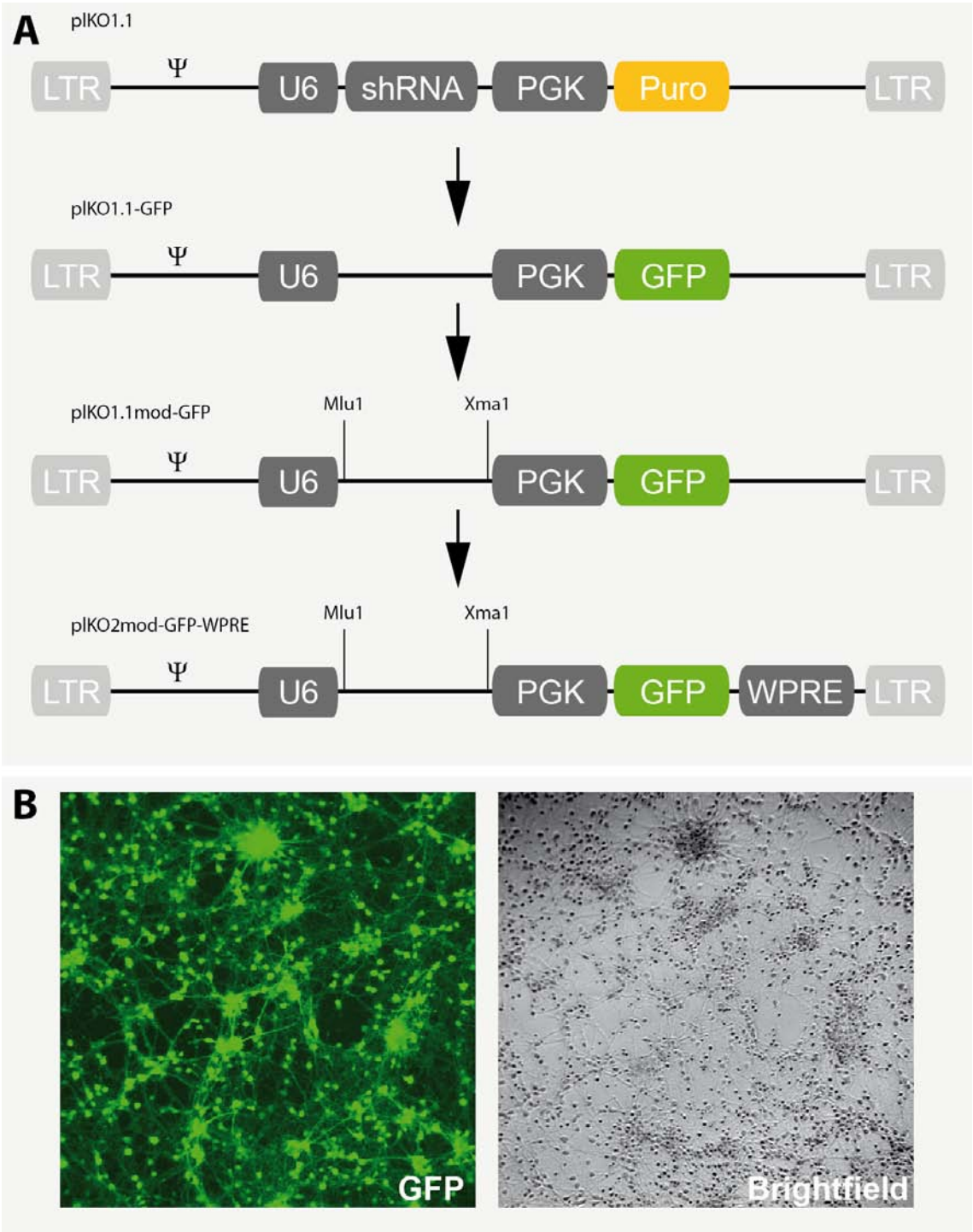

Figure 12 Cloning strategy lentiviral RNAi vectors and application example: (**A**) Origin construct and cloning strategy to obtain the pIKO2mod-EGFP-WPRE-empty vector which is the basis vector for shRNA mediated RNAi experiments in this study. (**B**) Typical high power-field of neurons infected with an shRNA vector which codes for GFP driven by the PGK promoter and an shRNA driven by the U6 promoter.

Furthermore, during my thesis the lentiviral knockdown and overexpression systems were used in a collaborative study to knock down Nicalin and Nomo or to overexpress the new component TMEM147 of the Nicalin/Nomo/TMEM147 complex (Dettmer et al., 2010).

Lentiviral particles are generated in HEK293T cells by triple transfection of vectors coding the structural virus proteins as well as a transfer plasmid which contains the genetic information to be transduced into the target cell line. In principle, the generation of lentiviral particles is no problem as long as the expression of the transgene of interest does not interfere with cell viability or virus generation. Translation of the lentiviral RNA in the packaging cells is in particular a problem in case of plasma membrane proteins and proapoptotic proteins. Their overexpression leads to impaired maturation of lentiviral particles in the first case or apoptosis of packaging cells in the latter case. Both events interfere with the virus production. This was exemplified by the attempt to generate lentiviral particles of the type-I orientated plasma membrane protein APP containing a TEV protease cleavage site followed by a FLAG epitope tag (APP-TEV-FLAG) with a normal transfer vector. Almost no infectious particles were generated. The reason for a lack of infectious lentiviral particles is the competition between the envelope glycoprotein of the vesicular stomatitis virus (VSVG) and the transmembrane protein of interest for the pseudotyping of the lentiviral particle surface. Upon expression of APP-TEV-FLAG the intended pseudotyping of the lentiviral particle with VSVG is impaired which leads to impaired infectivity of the lentiviral particles (Fig 13).

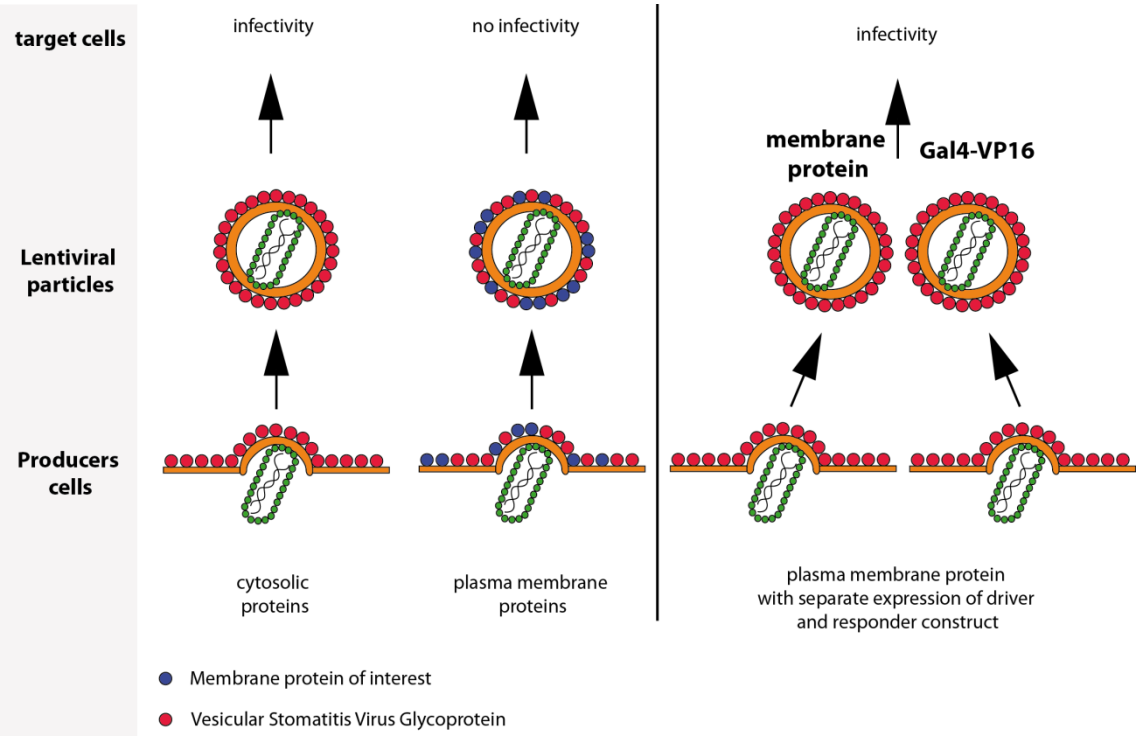

Figure 13 Problem of lentivirus generation in case of membrane proteins and a solution to this problem: Shows the problem of transmembrane transgenes for lentiviral production. Lentiviral vectors are RNA vectors and thus their RNA is also translated in the packaging cells besides being incorporated into lentiviral particles. Plasma membrane proteins can compete with the viral envelope protein VSV-G during pseudotyping of lentiviral particles which in the end leads to a low concentration of VSV-G on the surface of a lentiviral particle and thus to low infectivity. To circumvent this problem, this study introduces a novel vector system which makes use of the Gal4-UAS system and shields the translation of the gene of interest by the placement of a second transgene upstream of the UAS element. Hence, lentiviral particles can be generated which transport transmembrane transgenes RNA and are still infectious.

This problem can only be solved by a system which fulfills two criteria. First, the expression cassette should be silent in the packaging cells. Second, transgene expression should start upon infection of the target cells. Completion of both criteria can be achieved by usage of a promoter which is only active in the presence of a transcription factor which is not present in mammalian cells. Therefore, the Gal4-UAS system was implemented in the context of a lentiviral vector. This system consists of a responder virus which contains one or two genes of interest under the control of a unidirectional or bidirectional UAS element dependent on the number of transgenes and a driver virus which expresses the fusion protein Gal4-VP16 under control of the Ubiquitin-C promoter (UBC). The fusion protein Gal4-VP16 consists of the yeast transcription factor Gal4 binding to the UAS element and the Herpes simplex protein VP16 which recruits the mammalian transcription machinery. Lentiviridae are RNA viruses which transport genetic information in form of RNA. This has very important implications for the production of lentiviral particles. As the whole RNA including long terminal repeats (LTR), packaging signal and expression cassette is expressed to be incorporated into the lentiviral particle, translation of the first open reading frame (ORF) of this RNA occurs in both packaging and target cells. Though the UAS element is silent in the target cells, the first open-reading frame (ORF) will still be translated. To suppress the translation of the gene of interest (GOI) in the packaging cells another coding sequence (CDS) of GFP, DsRed or Puromycin was placed upstream of the UAS element. The placement of another CDS upstream of the UAS element blocks translation of the gene of interest in packaging cells as the ribosome scans over the RNA and will mainly translate the first encountered CDS (Fig 14). A Gateway^{TM} cassette was placed downstream of the UAS element to accelerate the cloning process of transgenes of interest.

This system in the end not only enables transmembrane protein expression but also the expression of proapoptotic transgenes which would lead to cell death in a normal lentiviral transfer vector.

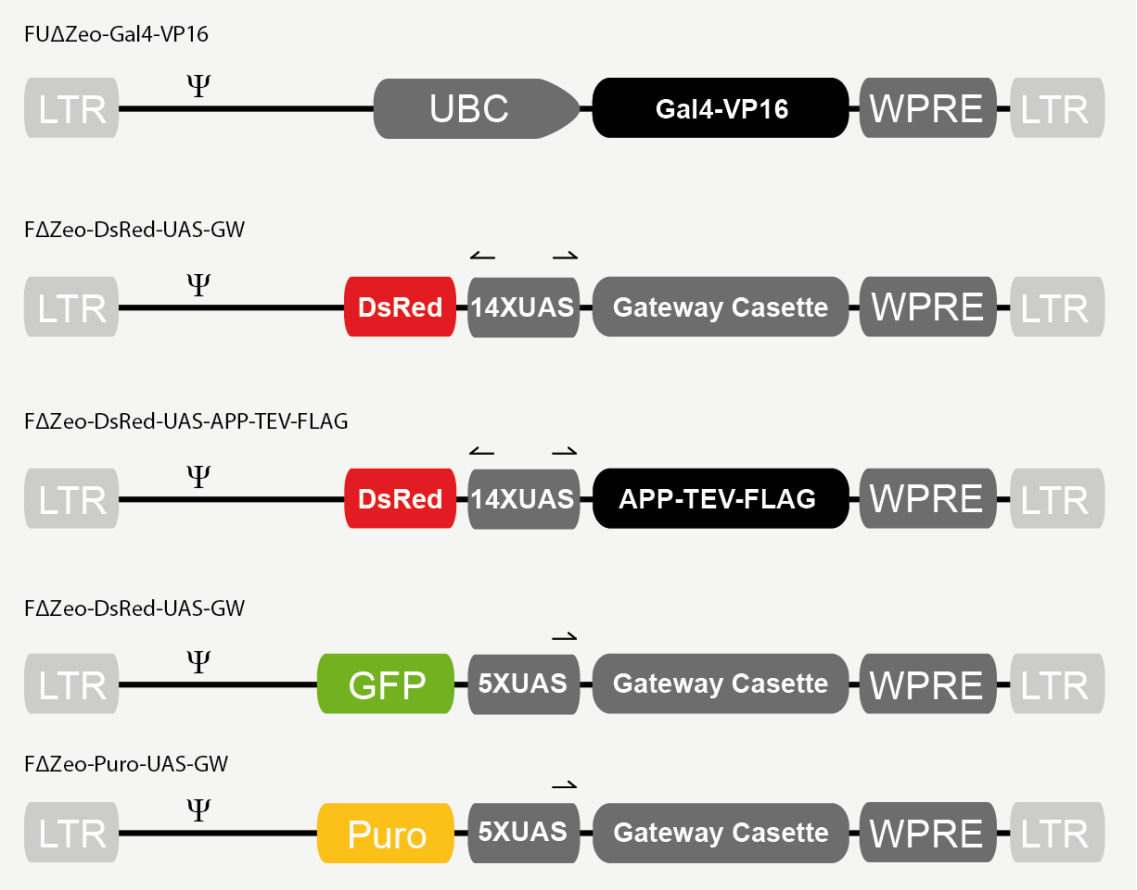

Figure 14 Design of the Gal4-UAS based lentiviral vectors: This figure shows the design of the GAL4-UAS-based lentiviral vectors used for the expression of plasma membrane transgenes. FUΔZeo-Gal4-VP16 is the driver virus which expresses the transcriptional activator GAL4-VP16. Follow by the bidirectional system which contains a reporter and the gene of interest in opposite directions and finally the unidirectional system with GFP or puromycin which act as a translational block of the gene of interest in the packaging cells by being translated themselves.

Both the RNAi expression and the GAL4-VP16-UAS based overexpression system were used in this study to generate APP-TEV-FLAG overexpressing SHSY5Y (5Y) cells. Additionally, these cells were expressed either a control shRNA or ADAM10 targeting shRNAs and GFP. Therefore 5Y cells were first cotransduced with the Gal4-VP16 expressing driver virus and the APP-TEV-FLAG and DsRed expressing responder virus (Fig 14A). Afterwards cells were FACS-sorted with a MoFlo (Beckman Coulter) according to their expression of DsRed in collaboration with Joachim Ellwart (Helmholtz). Afterwards these cells were infected with lentiviral vectors expressing GFP as transduction control and either a Control shRNA or an ADAM10 targeting shRNA (Fig 14B). Finally, these cells were used to determine the cleavage site of α-secretase and to investigate its dependency on the presence of the metalloprotease ADAM10 (See 3.4).

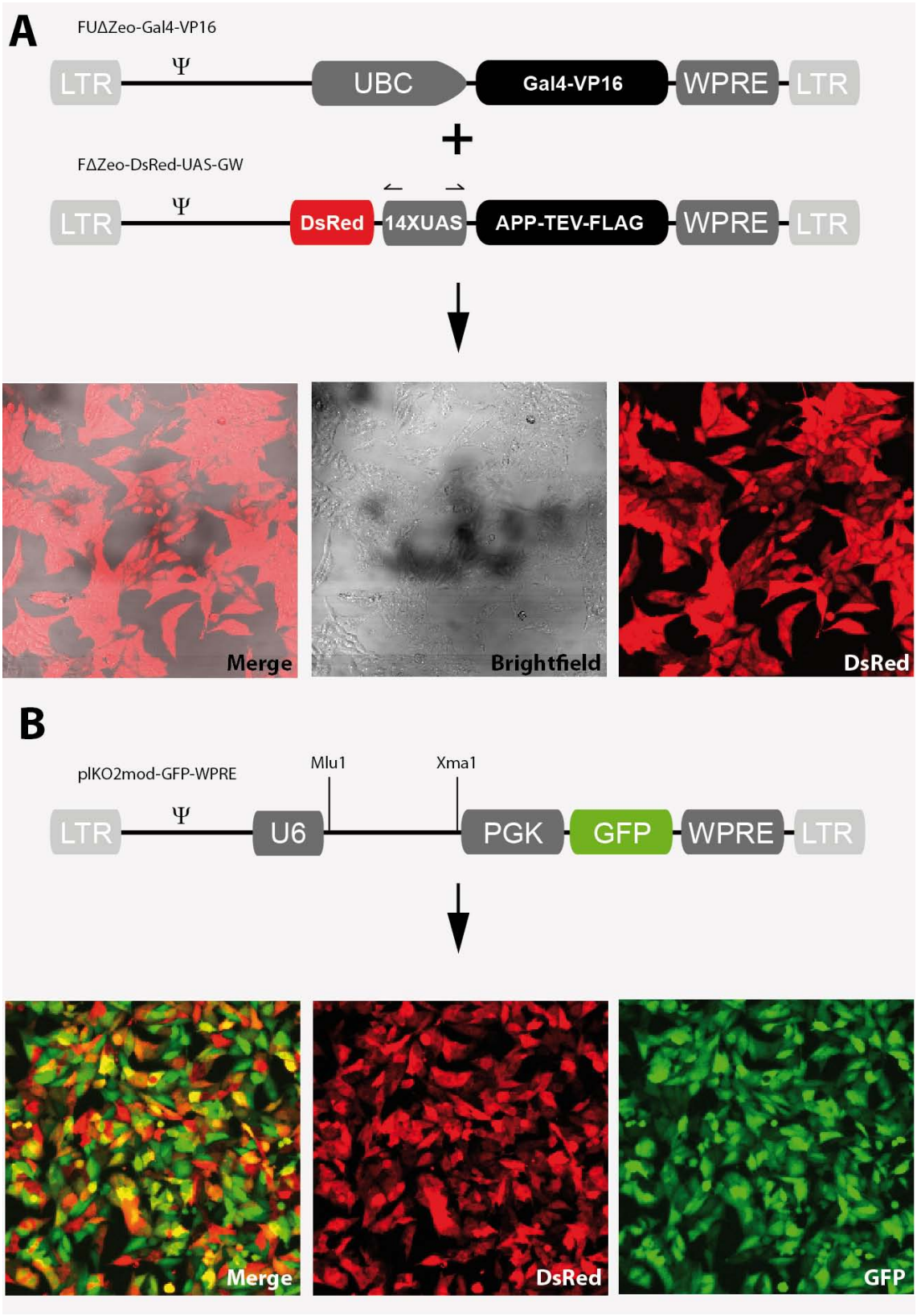

Figure 15 Strategy to generate APP-TEV-FLAG: Cells which were transduced with APP-TEV-FLAG and DsRed. Cells were sorted according their DsRed expression with MoFlo FACS sorter in collaboration with Joachim Ellwart. Afterwards cells were infected with the pIKO2mod vector which expressed GFP and either a control shRNA or an ADAM10 specific shRNA. These cells were generated to later perform the determination of the APP ADAM10 cleavage site.

3.2 ADAM10 is the physiological α-secretase in primary cortical neurons

Several ADAM proteases have been proposed as the physiological relevant alpha secretase. Furthermore, alpha secretase has been proposed to compete with β-secretase BACE1 for APP as a substrate thus partially preventing the generation of Aβ. However, the results of these experiments were hampered by usage of tumor cell lines, siRNA off-target effects, or protease overexpression and lead to the conclusion that ADAM9, ADAM10 and ADAM17 are all involved in APP processing and somehow can compensate for each other. To clarify these ambiguous results we investigated the role of different ADAM proteases in primary cortical neurons. For this purpose, 1.5 million E15/E16 neurons were infected after 3 days in vitro (div) with lentiviruses coding for shRNAs against ADAM9, ADAM10 and ADAM17 in order to determine the identity of α-secretase in primary cortical neurons. Infectivity of different dilutions of the purified lentiviral stock was determined by the percentage of GFP fluorescent neurons in one high power field. The working dilution of every virus stock was the parent dilution of the minimal dilution needed to infect all neurons. Usage of the parent dilution ensures for almost 100% infectivity in every single experiment. Two days after infection medium was replaced completely. Finally, cell culture supernatant as well as neuronal lysates were analyzed at 7 div, two days after the medium change. The neuronal supernatant was analyzed for the α-secretase specific APP species APPsα. APPsα was detected by the in-house made antibody 7A6 specifically recognizing murine APPsα. Furthermore APPsβ, Amyloid-β (Aβ) and the total amount of shedded APP ectodomain were detected in the conditioned medium while the lysate was analyzed for full length APP, β-actin as a loading control and ADAM10 to check for knockdown efficiency.

First, the effect of ADAM9 and ADAM17 knockdown in primary cortical neurons was analyzed. The mRNA amount of ADAM9, ADAM10 and ADAM17 was analyzed via qRT-PCR to analyze knockdown efficiency on the one hand and to exclude off-target effects of the targeting shRNA on the other proteases. Both the ADAM9 and the ADAM17 shRNA led to a robust knockdown of the targeted protease (Fig 17 C). In case of ADAM9 knockdown, only a very mild increase of ADAM10 and ADAM17 mRNA was observed while ADAM17 knockdown also led to a mild reduction of ADAM9 (Fig. 16 C). However, these mild off-target effects as well as the ADAM9 and ADAM17 targeting knockdowns lead to no significant reduction in APPsα as well as total secreted APP (APPs-total) (Fig. 16 A). The quantification of six independent experiments is shown in Fig. 16 B**.** Furthermore, the levels of full length APP (cell. APP) and ADAM10 were not changed by expression of ADAM9 or ADAM17 in the Western Blot (Fig. 16 A).

The lacking reduction of APPsα indicate that ADAM9 and ADAM17 play only a minor role in APP processing in primary cortical neurons.

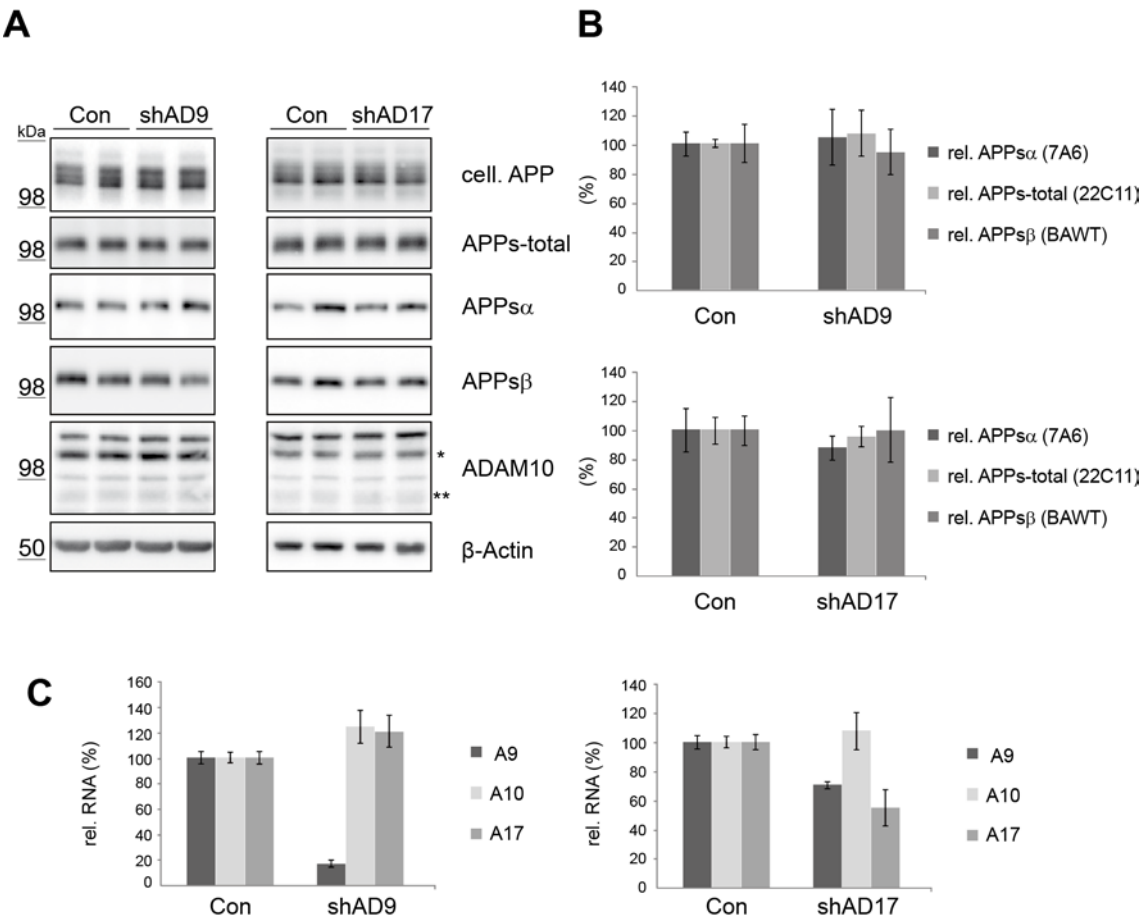

Figure 16 Dependence of neuronal APP alpha secretase in primary cortical neurons on ADAM9 and ADAM17: shows the analysis of APP processing in ADAM9 and ADAM17 knockdown neurons. (**A**) ADAM10 was unaffected in both ADAM9 and ADAM17 knockdown neurons. All APP species including the soluble species were unaffected by ADAM9 and ADAM17 knockdown. (**B**) Quantification for APPsα, APPsβ and APPs-totalof six independent experiments is shown. (**C**) qRT-PCR confirmed the knockdown efficiency of the different shRNAs.

In sharp contrast, APPsα was completely abolished in condition media of neurons infected with two different ADAM10 targeting shRNAs (see Fig. 17 A). Parallel to the reduction in APPsα, a mild concomitant increase of APPsβ and Amyloid-β could be observed in the conditioned media of neurons infected with the ADAM10 targeting shRNAs. This effect was more pronounced in case of shRNA-I (sh-I) than for shRNA-II (sh-II). Furthermore, a slight accumulation of the mature band of APP full length (cell. APP) could be observed in the lysate for sh-I while sh-II additionally led to an increase of the lower immature band (see Fig. 17 A). An immunoblot against ADAM10 showed clear reduction of ADAM10 protein upon ADAM10 knockdown. This result was independently confirmed by qRT-PCR for ADAM10. While ADAM10 mRNA was reduced to less than 10%, ADAM9 and ADAM17 mRNA were unaltered or slightly increased (see

Fig. 17 C). This experiment provides strong evidence for ADAM10 being the sole, long sought, alpha secretase activity in primary cortical neurons. Furthermore, the results suggest competition of ADAM10 and BACE1 for APP as a substrate as upon ADAM10 knockdown, the BACE1-specific product APPsβ as well as gamma secretase dependent Aβ are increased.

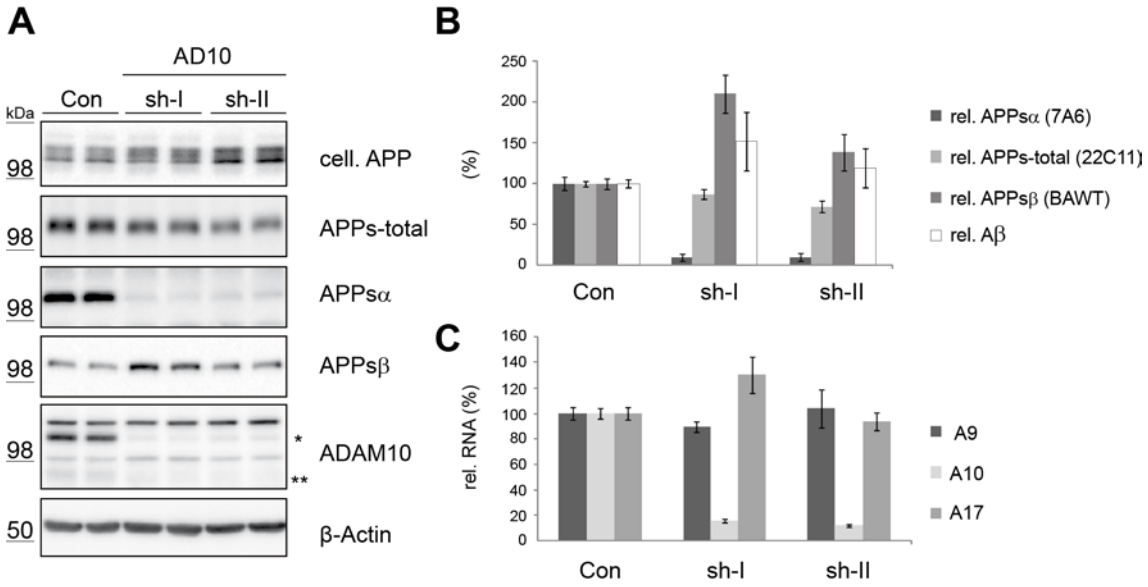

Figure 17 ADAM10 knockdown in neurons abolishes APPsα: Shown is the analysis of APP processing in ADAM10 knockdown neurons. (**A**) Two different shRNA both led to an almost complete abolishment of ADAM10 expression as can be seen by the reduction of the proform (*) and the mature form of ADAM10 (**). This coincided with a strong reduction of APPsα and an increase in APPsβ and Aβ while APPs-total was only mildly reduced. (B) Quantifiaction of APP species of 8 independent experiments. (**C**) qRT-PCR shows that ADAM10 expression is strongly reduced while ADAM9 and ADAM17 expression is almost unaffected.

3.3 A Cre-mediated conditional knockout of ADAM10 independently confirms ADAM10 as the sole APP alpha secretase in primary cortical neurons

To independently confirm ADAM10 being the sole APP alpha secretase, a conditional *in vitro* ADAM10 knockout mouse model was used. For the generation of Cre-expressing lentiviral particles, Cre was subcloned into a lentiviral vector and lentiviral particles were generated as pointed out (2.1.3). Alpha secretase dependent processing of APP was investigated in more detail isolating A10Δ/Δ E15/E16 neurons from a conditional ADAM10 knockout mouse model (Gibb et al., 2010) in which exon 9 of both ADAM10 loci is flanked by loxP sites. $1.5x10^6$ neurons were seeded per well. After two days *in vitro* (div) neurons were infected with Cre-coding virus. Cre-driven recombination of flanking loxP sites deletes exon 9 which in turn leads to a loss of ADAM10 coding mRNA by non-sense mediated RNA decay. Two days after infection, medium was

exchanged for fresh medium and neurons were cultured for another two days. Western Blots against ADAM10 confirmed the almost complete knockout of ADAM10 upon Cre infection while infection with a Control virus had no effect on ADAM10 expression (ADAM10 Lys). As further controls, the ADAM10-specific APP cleavage product (APPsα) as well as the BACE1-specific cleavage product APPsβ were analyzed in collaboration with Dr. Alessio Colombo. APPsα was completely abolished in the ADAM10 knockout which is in line with the performed ADAM10 knockdown experiments in primary cortical neurons (3.2). Simultaneously, APPsβ was unchanged which is contrary to the observed increase of APPsβ in ADAM10 knockdown neurons (see Fig. 17). This result strongly indicates that the increase in APPsβ and Aβ in case of ADAM10 knockdown is an off-target effect of the ADAM10 targeting shRNAs. APPs-total was only mildly reduced. Loss of ADAM10 expression upon Cre virus infection and the coincidental reduction of APPsα both confirm ADAM10 as the sole alpha secretase in primary cortical neurons.

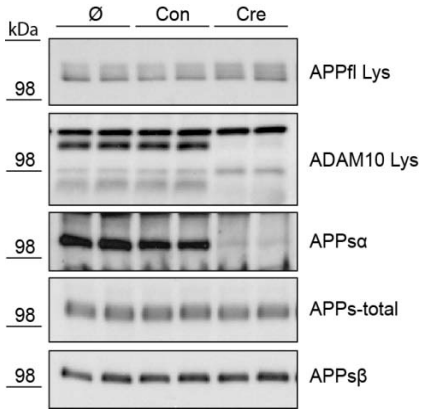

Figure 18 Cre-mediated knockout of ADAM10 abolishes APPsα: Shows the analysis of APP processing in neurons isolated from a conditional ADAM10 knockout model which were either infected with an empty control virus or a Cre-expressing virus. APPsα as well as ADAM10 were almost completely abolished up infection with Cre while APPs-total was slightly reduced. However, in contrast to ADAM10 knockdown APPsβ was unaffected.

3.4 ADAM10 cleaves between Lysine 16 and Leucine 17 of the Amyloid β domain of APP

To independently confirm the results about ADAM10 as APPα secretase I used MALDI-TOF mass spectrometry which is an excellent technique to determine the mass of small peptides which for example allows the determination of the cleavage site of a protease like ADAM10 in the APP juxtamembrane region. The Maldi-Tof Destr (ABI) can be used in linear or reflector mode. The reflector mode increases the resolution by focusing ionized peptides in an opposing electrical field but is limited to peptides up to 5000 Da. The penetration depth into the opposing field correlates with the energy of the

peptides. This means the higher the energy, the higher the penetration depth of the peptide into the electrical field. This in turn results in an isotopic resolution of the measured peptides. Size and glycosylation of the ectodomain of the amyloid precursor protein (APP) prevent usage of the reflector mode and thereby the direct detection of the cleavage site of ADAM10. To circumvent this problem, I made use of an approach which combines the use of a Tobacco Etch Virus (TEV) cleavage site followed by a FLAG-epitope tag. Both were positioned 17 amino acids upstream of the BACE1 cleavage site of APP as it was already known from previous studies that alpha secretase cleaves closer to the plasma membrane (see Fig. 19 A). Sequential FLAG-immunoprecipitation and TEV-protease digest followed by another FLAG-immunoprecipitation lead to the purification of the C-terminal peptide of APP defined by the N-terminal TEV protease cleavage site and the C-terminal cleavage site by either BACE1 or ADAM10. First, we tested whether the processing of APP-TEV-FLAG is not altered upon the insertion of the TEV-protease cleavage site and the FLAG epitope. APP-TEV-FLAG was expressed with the Gal4-UAS system in SHSY5Y (5Y) cells (see Fig 14). Cells were FACS-sorted with a MoFlo according their DS-Red Expression to obtain a homogenous population (in collaboration with Joachim Ellwart) (see Fig. 15). To investigate the effect of ADAM10 on APP-TEV-FLAG ectodomain shedding, FACS-sorted 5Y cells were lentivirally transduced with constructs expressing a control shRNA or two different ADAM10 targeting shRNAs. (see Fig. 19 B). Finally, these different cell lines were compared to each other for APP-TEV-FLAG ectodomain shedding. APP-TEV-FLAG was expressed equally in all three cell lines. In sharp contrast, total levels of APP-TEV-FLAG ectodomain, ADAM10 mediated sAPPα as well as the FLAG positive APP ectodomain were reduced under both ADAM10 knockdowns (sh7, sh9) compared to the control (Con) (see Fig 19 B). A representative quantification of three independent experiments is shown in Fig. 19 **C**. For mass spectrometric analysis, APP-TEV-FLAG expressing control cells were compared to APP-TEV-FLAG expressing ADAM10 knockdown cells with the hairpin hs9 after a 4 hour or an overnight incubation period. The overnight incubation period yielded one prominent peak at 4695.24 Da which would speak for ADAM10 cleavage at glutamine 15 of the Aβ domain of APP. Besides the prominent peak at 4695.24 Da, a small peak could be detected at 4824.43 Da which would correspond to a cleavage between Lysine 16 and Leucine 17 of the Aβ domain of APP (Fig. 19 D and **E**). Thus, the major peak ending at glutamine 15 might be a c-terminal metastable truncation product by an unknown carboxypeptidase activity independent of ADAM10. Another explanation would be a sequential cleavage of ADAM10. Depending on which hypothesis holds true, the ratio between the minor and the major peak should be altered in the first case or unaltered in the latter case. In-

deed, the ratio between minor and major peak shifted in favor of the minor peak at 4824.43 Da upon a shorter, four hour incubation period.

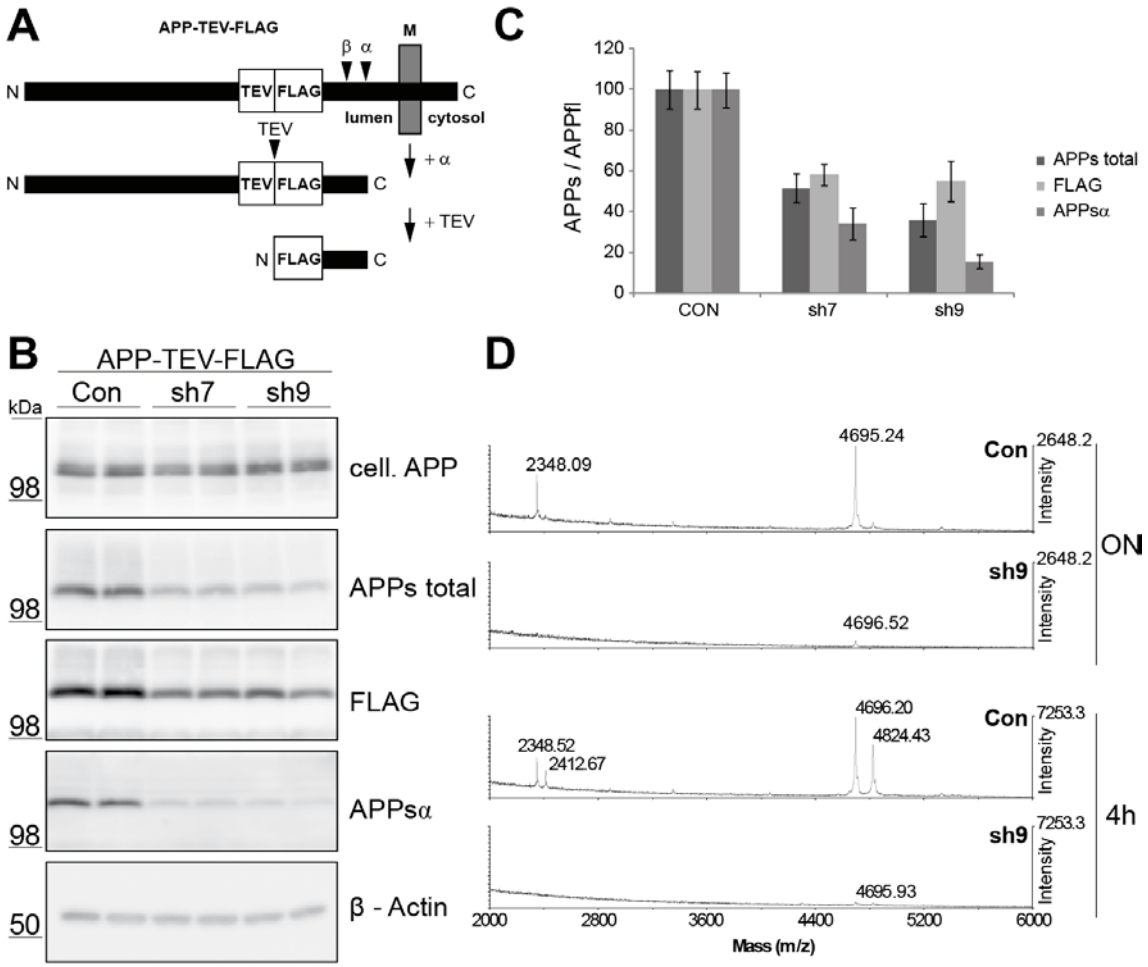

E

Peptide	Charge	Meas. Mass (Da)	Calc. Mass (Da)	Dev. (Da)	Sample
GDYKDDDDKSGLTNIKTEEISEVKMDAEFRHDSGYEVHHQ	+1	4695.24	4695.11	+0.13	ON Con
" "	+2	2348.09	2349,06	-0.97	ON Con
" "	+1	4696.52	4695,11	+1.41	ON sh9
GDYKDDDDKSGLTNIKTEEISEVKMDAEFRHDSGYEVHHQK	+1	4824.43	4823.21	+1.22	4h Con
GDYKDDDDKSGLTNIKTEEISEVKMDAEFRHDSGYEVHHQ	+1	4696.20	4695.11	+1.09	4h Con
GDYKDDDDKSGLTNIKTEEISEVKMDAEFRHDSGYEVHHQK	+2	2412.67	2413.11	-0.44	4h Con
GDYKDDDDKSGLTNIKTEEISEVKMDAEFRHDSGYEVHHQ	+2	2348.52	2349.06	-0.54	4h Con
" "	+1	4695.93	4695.11	+0.82	4h sh9

Figure 19 Determination of the ADAM10 cleavage site in APP:. (A) Strategy used to isolate the peptide which contains the APP-cleavage site: FLAG-IP of APPs, followed by TEV-cleavage and a second round of FLAG-IP. (B) Shows the analysis of APP-TEV-FLAG processing to ensure proper APP processing in the presence of the TEV-FLAG tag incorporated upstream of the juxtamembrane region of APP. (**C**) Quantification of three independent experiments of B. (D) Maldi-TOF analysis of the APP cleavage peptide in control cells and ADAM10 knockdown cells. (E) Calculated, measured masses and corresponding peptide sequences.

This speaks for the explanation model of an unknown carboxypeptidase activity with an initial ADAM10 mediated cleavage between Lysine 16 and Leucine 17 of the Aβ domain.

3.5 Establishment of the method Secretome Protein Enrichment with Click Sugars - SPECS

Identification and quantification of protease substrates with mass spectrometry on a secretome-wide scale is in principle possible comparing control cells with cells carrying a protease knockout. Quantification in mass spectrometry can be achieved using isotope labeling techniques like SILAC, ITRAQ or label-free quantification. Nevertheless, proteolytically released or secreted proteins in conditioned media so far remained inaccessible to mass spectrometric analysis due to several reasons. First, cellular proteins are diluted in conditioned media. Second, supplementation of *in vitro* cell culture media with fetal calf serum (FCS) or B27 in the case of primary cortical neurons is desirable for cell viability, normal cell physiology and regular ectodomain shedding but introduces a rich source of contaminating proteins. Both supplements contain high concentrations of albumin and a plethora of other abundant proteins in the case of FCS outranging the concentration of cellular proteins by several orders of magnitude. Furthermore, cytosolic cellular proteins are released into conditioned media upon apoptosis. Due to these reasons, ordinary conditioned media are complex protein mixtures with only trace amounts of proteins released upon secretion or ectodomain shedding. The hierarchical composition of low abundant like shedded proteins and high abundant proteins like exogenous albumin can be described as the dynamic range of a proteome. Both detection and sample preparation in mass spectrometry are confronted by the dynamic range problem due to technical reasons. This explains why mass spectrometry aided detection of proteins released by secretion or proteolysis is hampered both by the release of cytosolic proteins upon apoptosis and the addition of protein based growth supplements like FCS. The strong need for a method in mass spectrometry which is able to discriminate between exogenous serum proteins and cytosolic proteins on the one hand and proteolytically released and secreted proteins on the other hand prompted me to develop a novel enrichment method for glycoproteins. This method is based on metabolic glycan labeling, subsequent glycan biotinylation mediated by click chemistry and streptavidin pull down of the biotinylated proteins (Fig 20 a and 20 b). It takes advantage of glycosylation being a posttranslational modification exhibited by the majority of secretory and membrane proteins which in turn enables their specific enrich-

ment. In fact, it allows discrimination between de novo synthesized secreted or proteolytically released glycoproteins and all other proteins in conditioned media.

First, the technical feasibility of the SPECS technique was validated in primary cortical neurons. To exclude interference of metabolic glycan labeling with proper ectodomain shedding of membrane proteins, $1.5x10^6$ primary cortical neurons were cultured in the presence or absence of 50 µM percacetylated amino sugar derivate tetraacetyl-N-acetylazido-Mannosamine (ManNAz) for 24 hours. Under both conditions, neurons were concurrently treated with DMSO as a solvent control or 2 µM of the BACE1 inhibitor C3. Afterwards, all conditioned media samples were treated with 2 µM Dibenzylcylcooctyne-PEG12-Biotin to perform click chemistry mediated biotinylation of labeled glycoproteins. As APP and APLP2 are both well characterized BACE1 substrates, conditioned media and cell lysates were analyzed for these two type-I membrane proteins. As expected for a BACE1 substrate, the levels of shedded APP and APLP2 ectodomain were reduced in the conditioned media of C3-treated neurons (Fig 20 c). Simultaneously, the full length precursors of both APP and APLP2 accumulated in the lysate. An immunoblot against the neo epitope of the BACE1-cleaved ectodomain of APP, sAPPβ, indirectly confirmed the complete pharmacological inhibition of BACE1. Moreover no obvious impairment of ectodomain shedding could be observed in the presence of ManNAz (Fig 20 c).

A specific biotin signal in the streptavidin-HRP blot (STREP-HRP) was only obtained if neurons were cultured in the presence of ManNAz. Besides a discreet immunoreactive smear which spanned the whole lane, four specific intense bands could be detected under control conditions. The highest and the lowest of these four bands disappeared upon treatment with C3 which gave a first qualitative insight into the alteration of the neuronal secretome upon C3 treatment.

Finally, after click chemistry reaction, comparable volumes of conditioned clicked medium and a representative streptavidin-pull of conditioned clicked medium were compared to each other to determine pull-down efficiency and purification factor. Therefore, we compared the levels of sAPPtotal in the Western Blot and bovine serum albumin (BSA) in the coomassie staining between direct load and pull-down. APP was enriched 2fold and BSA decreased 50fold which in the end multiplies to a relative enrichment of sAPPtotal of 100fold (Fig 20 d).

The unaltered shedding upon ManNAz treatment as well as the relative enrichment factor of 100 of the streptavidin pull down proofed that the technology could in principle work. Consequentially, the cell numbers were scaled up to obtain purified amounts which can be detected by mass spectrometry.

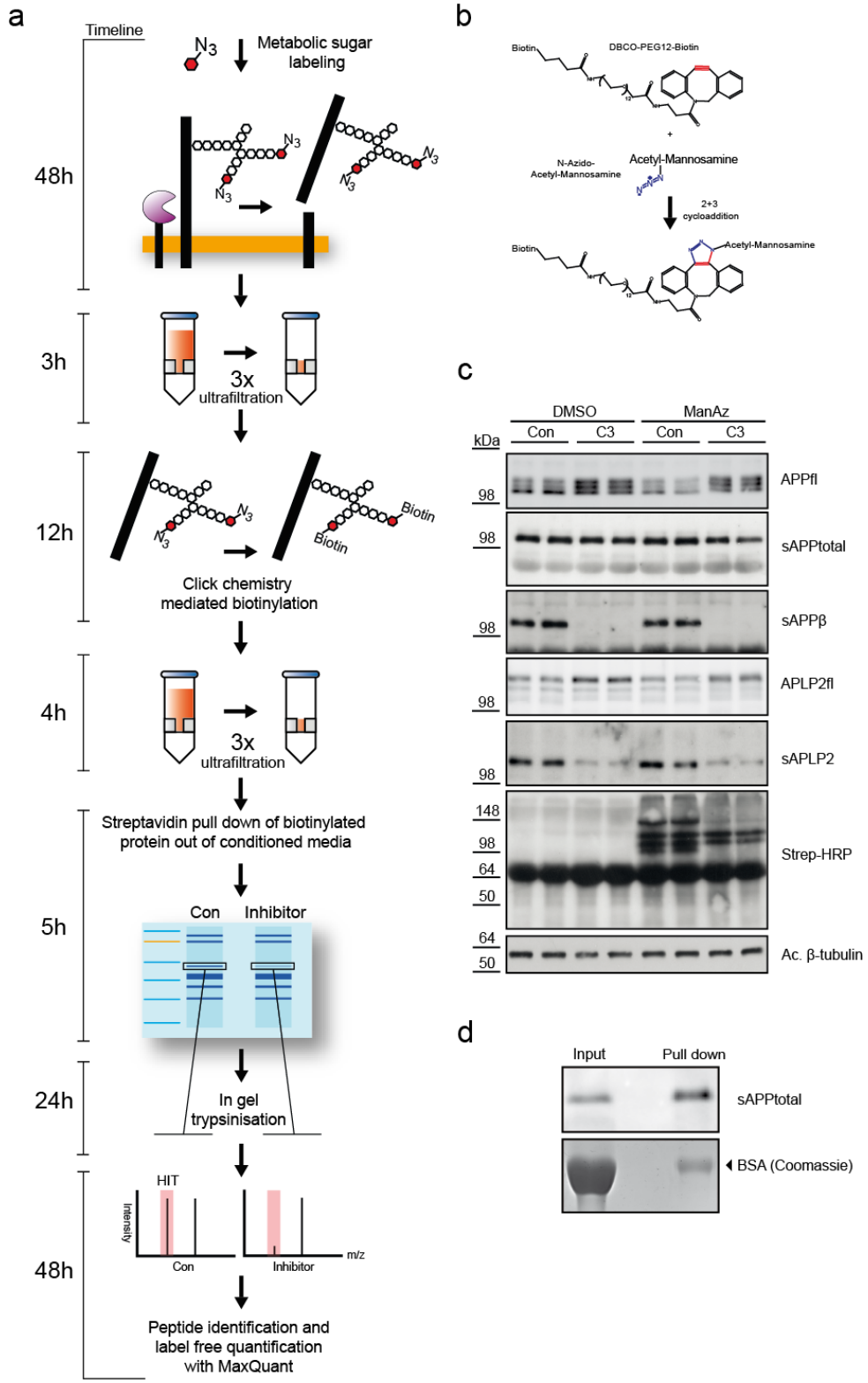

Figure 20 Workflow of the SPECS method and validation: (a) The SPECS workflow consists of metabolic labeling of cells, collection and ultrafiltration of supernatants, subsequent click reaction, a second round of ultrafiltration, streptavidin pull down, separation of pulled proteins on a SDS gel. in-gel trypsinisation and finally peptide identification and quantification with MaxQuant. (b) Click reaction between the strained alkyne DBCO-PEG12-Biotin and the azide of the sugar N-Azido-Acetyl-mannosamine. (c) Western Blot analysis of APP and APLP2 shedding as well as the Biotin signal in the presence or absence of the sugar N-Azidoacetylmannosamine. (d) Enrichment of APPs-total and BSA depletion in the immune precipitation (IP) compared to the input resulted in a relative enrichment of 100fold.

3.6 Determination of the HEK293T and the neuronal secretome

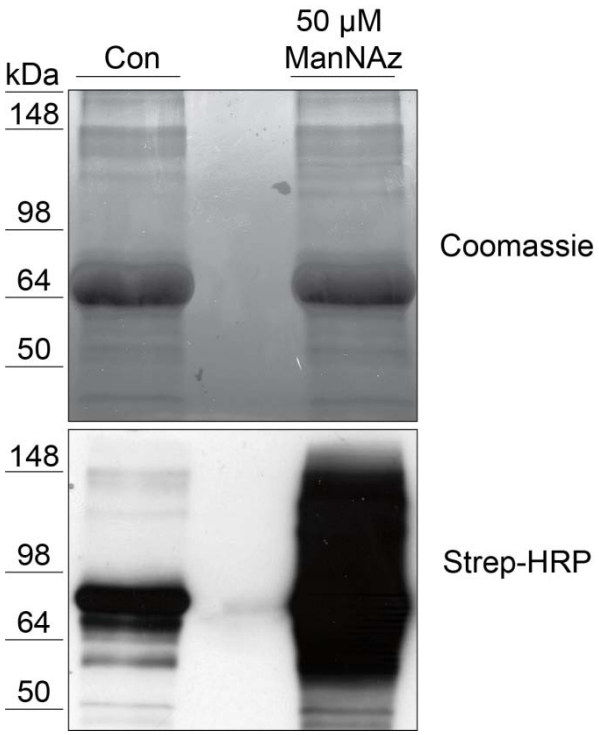

Figure 21 Streptavidin pull down of clicked glycoproteins of HEK293T cells: Comparison of the streptavidin pull-down of 293T cells cultured in the presence or absence of tetraacetyl-N-Azido-acetylmannosamine (ManNAz). A clear enrichment of biotin signal can be observed upon culture in the presence of ManNAz while the difference in the coomassie gel is only slightly apparent.

The secretome of immortalized human embryonic kidney cells (HEK293T) was analyzed first due to fast propagation and easy maintenance of HEK293T cells in comparison to neurons. $40x10^6$ HEK293T cells were cultured in 20 ml of DMEM + 5% (v/v) FCS in the presence or absence of 50 µM ManNAz. Media were finally treated as pointed out in the material and methods section. A very critical point in the whole protocol is the elution of biotinylated proteins from the streptavidin matrix. The streptavidin-biotin complex forms the strongest non-covalent bond in nature with a dissociation constant of 10^{-14} (Chaiet and Wolf, 1964). Even cooking in the presence of ordinary sample buffer is not able to quantitatively dissolve this bond. Only the addition of excess amounts of biotin and the use of urea in the sample buffer enable quantitative elution of biotinylated proteins from the streptavidin matrix. Proteins were separated via SDS-page (see 2.3.4). Though three subsequent washes were performed with 2% SDS in PBS, bovine serum albumin was still the most prominent protein in a representative coomassie stained gel of a streptavidin pull-down of biotinylated proteins after the click reaction. Nevertheless, qualitative differences in the staining between HEK293T cells treated with DMSO as a solvent control and HEK293T cells cultured in

the presence of 50 µM ManNAz could be observed. A blot against biotin with streptavidin HRP showed an even more drastic picture. A strong streptavidin-HRP reactive smear could only be detected in case of ManNAz while the pull-down of control cells showed only a few distinct bands. This was the first evidence for an efficient pull-down of biotinylated glycoproteins. To identify the proteins which were specifically enriched by this approach, tryptic peptides were retrieved from the gel via in-gel trypsinisation () and measured on a LTQ-Velos Orbitrap. Comparing respective streptavidin pull-downs of HEK293T conditioned media showed a clear enrichment of glycoproteins up to 1000-fold upon culture of HEK293T cells in the presence of of ManNAz. Filtering a total of 900 identified proteins with the following filters (at least 3fold enriched in ManNAz conditioned media compared to control media, at least 2 unique peptides, annotated as glycoprotein according to UNIPROT database) yielded 254 glycoproteins which were specifically detected in conditioned media of ManNAz-treated HEK293T cells. These 254 glycoproteins composed of 94 type-I membrane proteins, 36 type-II membrane proteins, 7 polytopic membrane proteins, 5 GPI-anchored proteins and 112 secreted proteins (Fig 23). With 142 membrane proteins more than half of all identified proteins constitute the sheddome of HEK293T cells (see Appendix). Even ectodomains of polytopic membrane proteins like Latrophilin 1, 2 and 3 were detected in the conditioned media. The ectodomain of Latrophilin 1 has already been described to undergo ectodomain shedding in previous studies (Silva et al., 2009; Volynski et al., 2004).

After the HEK293T analysis, the sheddome and secretome of neurons was analyzed due to the greater physiological relevance of neurons with regard to Alzheimer's disease. Therefore, $40x10^6$ primary E15/16 neurons were cultured in 20 ml of neurobasal medium supplemented with 2% B27 and 50 µM ManNAz. Simultaneously, these neurons were either treated with DMSO as a solvent control or with 2 µM of the BACE1 inhibitor C3. Under control conditions 283 proteins were identified in at least four out of five experiments, which comprised of 120 type-I membrane proteins, 34 type-II membrane proteins, 13 polytopic membrane proteins, 19 GPI-anchored proteins and 97 secreted proteins (See Appendix). Like in HEK293T cells, ectodomain peptides were detected of polytopic membrane proteins like Latrophilins.

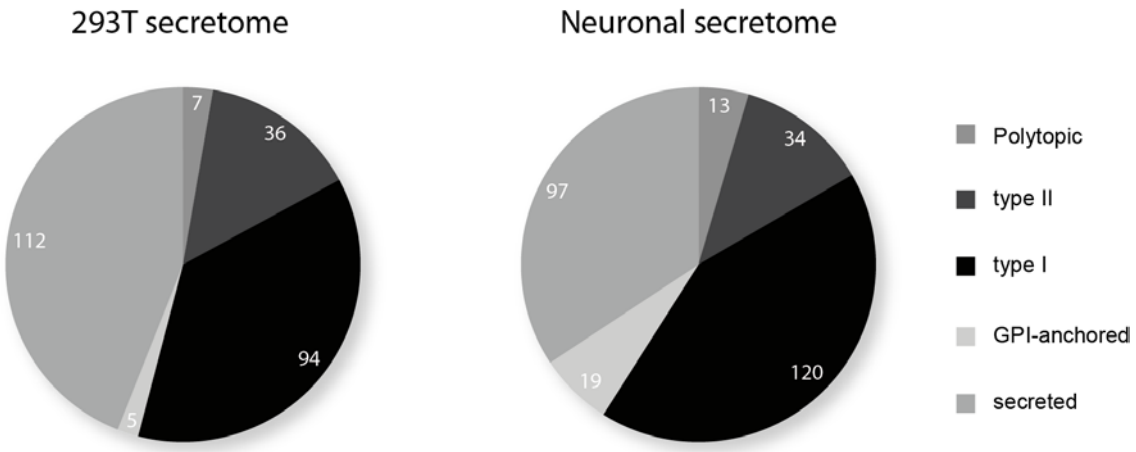

Figure 22 Identified proteins of the different glycoprotein classes in the HEK293T and the neuronal secretome: Shows the numbers of the different types of proteins identified in HEK293T cells and primary cortical neurons in a pie chart. The majority of shedded proteins are type I membrane proteins while another big group are secreted proteins. Minor groups are type II, GPI-anchored and polytopic membrane proteins.

3.7 Identification of the BACE1 sheddome in primary cortical neurons with the SPECS method

To identify novel BACE1 substrates, 40 million neurons were respectively cultured in the presence of DMSO plus 50 µM ManNAz or the BACE1 inhibitor C3 plus 50 µM ManNAz. Glycoproteins in the conditioned media were purified with the SPECS method. Afterwards SPECS purified proteins were separated on a SDS gel and finally trypsinized. The tryptic peptides were measured on a LTQ-Velos Orbitrap and afterwards identified and quantified via label-free quantification with the MaxQuant suite. Comparing the quantitative changes of unique protein groups between C3-treated neurons and DMSO-treated neurons (control) allowed the identification of new BACE1 substrates in primary cortical neurons. Based on the assumption that a membrane protein undergoes BACE1 mediated shedding, the concentration of this protein should be decreased in case of BACE1 inhibition. Indeed, using the SPECS method the well-characterized BACE1 substrates APP, APLP1 and APLP2 were identified. This confirmed the predictive power of the SPECS method. Membrane proteins with mild, moderate and strong shedding inhibition were detected. Seizure protein 6 like 1 (Sez6L1) and its homolog Seizure protein 6 (SEZ6) were reduced down to 4% and 8% respectively in a similar manner like APLP1. L1 (21%), the close homolog of L1 (CHL1) (35%) and Contactin-2 (64%) showed a more moderate impairment of ectodomain shedding upon BACE1 inhibition while proteins like TMEM132A were only mildly reduced. Besides membrane proteins, secretory proteins were identified which showed a decrease like Neogenin or receptor-type tyrosine-protein phosphatase sigma (see table 17). These results show that the SPECS method has a very strong potential in identifying

novel protease substrates due to its accurate relative quantification between two different experimental conditions. This is exemplified here for BACE1 in primary cortical neurons.

Table 15 Membrane proteins showing reduced shedding upon BACE1 inhibitor C3 treatment

Protein Name	IPI (a)	Mean (b)	SEM (c)	VS (d)	Pept. (e)	Protein Type(f)
Seizure protein 6 like 1	IPI00674241	0.04	0.01	1.28E-02	13	Type I
Seizure protein 6	IPI00380749	0.08	0.03	3.08E-02	19	Type I
Amyloid like Precursor Protein 1	IPI00129249	0.11	0.02	2.32E-02	27	Type I
VWFA and cache domain-containing protein 1	IPI00350425	0.12	0.12	1.31E-01	6	Type I
Golgi apparatus protein 1	IPI00122399	0.21	0.05	6.69E-02	11	Type I
L1	IPI00785371	0.21	0.03	3.79E-02	24	Type I
Leucine-rich repeat neuronal protein 1	IPI00126070	0.25	0.06	7.69E-02	7	Type I
Plexin domain-containing protein 2	IPI00471179	0.25	0.10	1.38E-01	3	Type I
Neurotrimin	IPI00417005	0.33	0.14	2.08E-01	6	GPI
Close homolog of L1	IPI00831546	0.35	0.05	7.25E-02	49	Type I
Peptidyl-glycine alpha-amidating monooxygenase	IPI00323974	0.36	0.12	1.83E-01	23	Type I
Alpha-1,4-N-acetylhexosaminyltransferase EXTL2	IPI00112900	0.36	0.16	2.47E-01	5	Type II
Protocadherin gamma A11	IPI00129686	0.42	0.15	2.56E-01	7	Type I
Amyloid like Precursor Protein 2	IPI00121338	0.43	0.09	1.57E-01	20	Type I
ST3GAL-I sialyltransferase	IPI00108849	0.44	0.17	2.98E-01	3	Type II
Latrophilin-1	IPI00918724	0.45	0.10	1.79E-01	19	Polytopic
Neuroligin 4	IPI00858277	0.45	0.08	1.38E-01	22	Type I
Semaphorin-6D	IPI00396759	0.47	0.09	1.70E-01	3	Type I
Lysosomal membrane glycoprotein 1	IPI00469218	0.48	0.16	3.14E-01	2	Type I
Neurexin I-alpha	IPI00468539	0.51	0.04	7.94E-02	30	Type I
Protocadherin-20	IPI00222278	0.52	0.16	3.22E-01	10	Type I
Latrophilin-3	IPI00411157	0.53	0.10	2.09E-01	7	Polytopic
Latrophilin-2	IPI00876558	0.56	0.10	2.17E-01	10	Polytopic
Sodium/potassium-dependent ATPase subunit beta-1	IPI00121550	0.57	0.14	3.33E-01	3	Type II
Delta and Notch-like epidermal growth factor-related receptor	IPI00170342	0.57	0.09	2.19E-01	3	Type I
Interferon alpha/beta receptor 2	IPI00395209	0.58	0.12	2.84E-01	4	Type I
Neuroligin-2	IPI00468605	0.58	0.11	2.55E-01	16	Type I
Seizure 6-like protein 2	IPI00128454	0.60	0.14	3.41E-01	13	Type I
Leucine-rich repeat and fibronectin type-III domain-containing protein 2	IPI00330152	0.62	0.13	3.37E-01	4	Type I
CX3C membrane-anchored chemokine	IPI00127811	0.64	0.11	2.97E-01	4	Type I
Contactin-2	IPI00119970	0.64	0.06	1.81E-01	39	GPI
Amyloid Precursor Protein	IPI00114389	0.67	0.08	2.44E-01	30	Type I
Neuroligin-1	IPI00309113	0.73	0.08	2.86E-01	13	Type I
Transmembrane protein 132A	IPI00464151	0.82	0.06	3.45E-01	38	Type I

Table 16 Soluble proteins reduced under C3 treatment

Protein Name	IPI (a)	Mean (b)	SEM (C)	VS (d)	Pept (e)	Protein Type(f)
Activin beta-B chain	IPI00355134	0.14	0.08	8.87E-02	7	Secreted
Adamts3	IPI00672899	0.30	0.18	2.53E-01	7	Secreted
Insulin-like growth factor-binding protein 2	IPI00313327	0.41	0.12	2.10E-01	2	Secreted
Extracellular matrix protein 1	IPI00889948	0.49	0.13	2.63E-01	5	Secreted
Neuronal olfactomedin-related ER localized protein	IPI00136712	0.50	0.12	2.28E-01	10	Secreted
Reelin	IPI00121421	0.85	0.04	2.87E-01	21	Secreted

Table 17 Selection of proteins unaltered under C3 treatment

Protein Name	IPI (a)	Mean (b)	SEM (c)	VS (d)	Pept (e)	Protein Type(f)
Hepatocyte growth factor receptor	IPI00130420	0.829	0.13	7.60E-01	8	Type I
Neogenin	IPI00129159	0.898	0.09	8.56E-01	33	Type I
Protocadherin gamma C3	IPI00129613	0.81	0.13	6.86E-01	12	Type I
Receptor-type tyrosine-protein phosphatase sigma	IPI00230067	0.90	0.19	1.90E+00	20	Type I
Leucine-rich repeat-containing protein 4B	IPI00381059	0.913	0.18	2.13E+00	20	Type I
Netrin receptor DCC	IPI00137347	1.00	0.18	1.38E+02	31	Type I
Prostaglandin F2 receptor negative regulator	IPI00515319	0.85	0.15	1.04E+00	29	Type I
Neural cell adhesion molecule 1	IPI00122971	0.986	0.16	1.12E+01	28	Type I

Table 15/16 Identification of BACE1 substrates of a comparative quantitative analysis of SPECS purified neuronal secretomes of DMSO and C3 treated neurons: Identified shedded and secreted proteins which show quantitative changes upon C3 inhibition legend: (a) IPI accession number of the protein, (b) Mean ratio between BACE1 inhibitor treatment (C3) and control (DMSO) conditions of the summed unique peptide intensities identified for a unique protein group for five biological replicates (C3/DMSO) shows remaining ectodomain levels upon BACE1 inhibition. SPECS values for remaining shedding of APP (0.67), APLP1 (0.11) and APLP2 (0.42) corresponds well to literature. In neurons APLP1 is mainly cleaved by BACE1 (Sala Frigerio et al., 2010), whereas APLP2 shedding is mediated to about 60% by BACE1(Hogl et al., 2011). In contrast, total APP shedding was only mildly inhibited with C3, because it is known that inhibition of BACE1 cleavage of APP is accompanied by an increase in the ADAM10-mediated cleavage, resulting in only a moderate inhibition of total APP shedding upon BACE1 inhibition (May et al., 2011a; Vassar et al., 1999). (c) Standard error of the mean for five biological replicates, (e) Variance score was calculated for all proteins. Proteins with a variation score ≤ 0,35 were considered as proteins with a consistent change under BACE1 inhibition (f) Protein type: Secreted: Secreted, soluble protein, Type I: type I membrane protein, Type II: type II membrane protein, Polytopic: membrane protein with multiple transmembrane domains, GPI: GPI-anchored membrane protein.

Table 17 Selection of unaltered proteins upon C3 treatment in the comparative quantitative SPECS analysis: Proteins were selected which did not show any significant change in the SPECS analysis. These proteins serve as negative control.

3.8 Validation of CHL1, L1CAM, Sez6 and Contactin-2 as new BACE1 substrates by Western Blot analysis

To further corroborate the initial mass spectrometry-based SPECS analysis for novel physiological BACE1 substrates in primary cortical neurons, selected proteins with strong, moderate and mild inhibition of shedding were analyzed via Western Blot in more detail. Therefore $1.5x10^6$ E15/E16 neurons were treated either with DMSO as solvent control or with C3 for BACE1 inhibition. Ectodomain shedding of Seizure Protein 6 (Sez6) was reduced down to 12%. Sez6 has been described to be involved in dendritic arbor formation as well as maturation of synapses (Gunnersen et al., 2007; Miyazaki et al., 2006). Ectodomain shedding of L1 was reduced down to 23% and for Close homolog of L1 (CHL1) down to 49%. Both proteins have been described to undergo ectodomain shedding (Maretzky et al., 2005; Naus et al., 2004). Ectodomain shedding was mildly reduced down to 56% in case of the GPI-anchored protein Contactin-2 which has been implicated in the positioning of potassium channels in the juxtaparanode region (Gu and Gu, 2011; Poliak et al., 2003; Traka et al., 2003) (Fig 23

A, B). These results are in line with the results that were obtained via the SPECS method which respectively measured 8%, 21%, 35% and 64% (Fig B, upper panel). At the same time the full length precursors of the investigated proteins accumulated in the lysate (Fig 23 A, Fig 23 B, lower panel). The extent of accumulation did not correlate in a linear fashion with the decrease of ectodomain shedding, exemplified by Contactin-2 (Cont-2) and CHL1 whose ectodomain shedding was only moderately reduced while their respective full-length precursors showed the strongest accumulation (CHL1, 2.45fold) (Contactin-2, 2.2fold) in the cell besides APLP1 (4.2fold) while Sez6 accumulated only 1.65fold though ectodomain shedding was reduced down to 12%. Ectodomain shedding of all three APP family members was investigated which are known to be BACE1 substrates. The ectodomain shedding of APP was only mildly reduced down to 90% which is in line with previous studies (Sala Frigerio et al., 2010). APLP2 showed a moderate decrease down to 55%. In case of APLP1, ectodomain shedding was reduced down to 15%. All three APP family members showed the expected accumulation in the lysate (Fig 23 B). As the observed behavior of APP, APLP1 and APLP2 fits well with previous studies (Hogl et al., 2011; Sala Frigerio et al., 2010) and with the results of the SPECS method, all three proteins served as internal quality controls for the SPECS method. To exclude potential BACE1 inhibitor off-target effects and to proof BACE1 cleavage *in vivo*, soluble ectodomains and full length proteins of Sez6, L1, CHL1 and Contactin-2 were compared in brain homogenates between wild type and BACE1 knockout mice at day 7 postnatal. Corresponding to the BACE1 inhibitor experiment, the reduction of ectodomain shedding was most pronounced in case of Sez6 (down to 9%). While L1CAM shedding was reduced down to 34%, CHL1 shedding was only mildly reduced down to 60%. Contactin-2 shedding could not be evaluated in the brain homogenates as part of the GPI-anchored full length Contactin-2 had been released into the soluble fraction during sample workup. The membrane-tethered precursor of Sez6 and CHL1 respectively accumulated 1.5 and 2.3-fold while L1 accumulated with 1.2 fold only mildly. In sharp contrast, Contactin-2 exhibited again the strongest accumulation among all novel BACE1 substrates with 2.8 fold though shedding was only mildly reduced (Fig 24 A, lower panel). Western Blots for full length protein of N-Cadherin and PTPRF showed no accumulation in the lysate for both proteins and thus confirmed indirectly the unaltered ectodomain shedding under BACE1 inhibition which had been measured with the SPECS method (Fig 24 B). Both proteins served as negative controls. Furthermore the whole APP family was analyzed via Western blot. The measured shedding reduction of APP (down to 85%), APLP1 (down to 17%) and APLP2 (down to 46%) was in line with the results of the SPECS method as well as with results from previous studies (Fig 24 B). All three proteins served as

positive controls for the analysis of BACE1 knockout mice. A blot for BACE1 confirmed the genotype of BACE1 knockout as well as of the wild type brains. While immunoreactivity could be observed for BACE1 in the wild type brains, there was no signal in the BACE1 knockout brains (Fig 24 A). The Western Blot results of dissociated E15/E16 neurons treated with the BACE1 inhibitor C3 and the wild type and knock out brain homogenates corroborated the results obtained with the SPECS method in a qualitative and quantitative manner for the already known BACE1 substrates APP, APLP1 and APLP2 and the four novel BACE1 substrates L1, Close homolog to L1 (CHL1), Contactin-2 and Seizure protein 6. Furthermore by analyzing the soluble and the detergent fraction of brains obtained from young wild type and BACE1 knockout animals, BACE1 cleavage of these substrates could also be proofed *in vivo*. BACE1-mediated cleavage of these substrates points to a function of BACE1 in neurite outgrowth, synaptic maturation and intercellular communication especially between neurons and oligodendroglia. A more detailed analysis of the function of BACE1-mediated shedding of these proteins as well as the assessment of the biologic functions of the cleaved ectodomains of these substrates have to be done to finally understand the physiological function of BACE1 in the central nervous system.

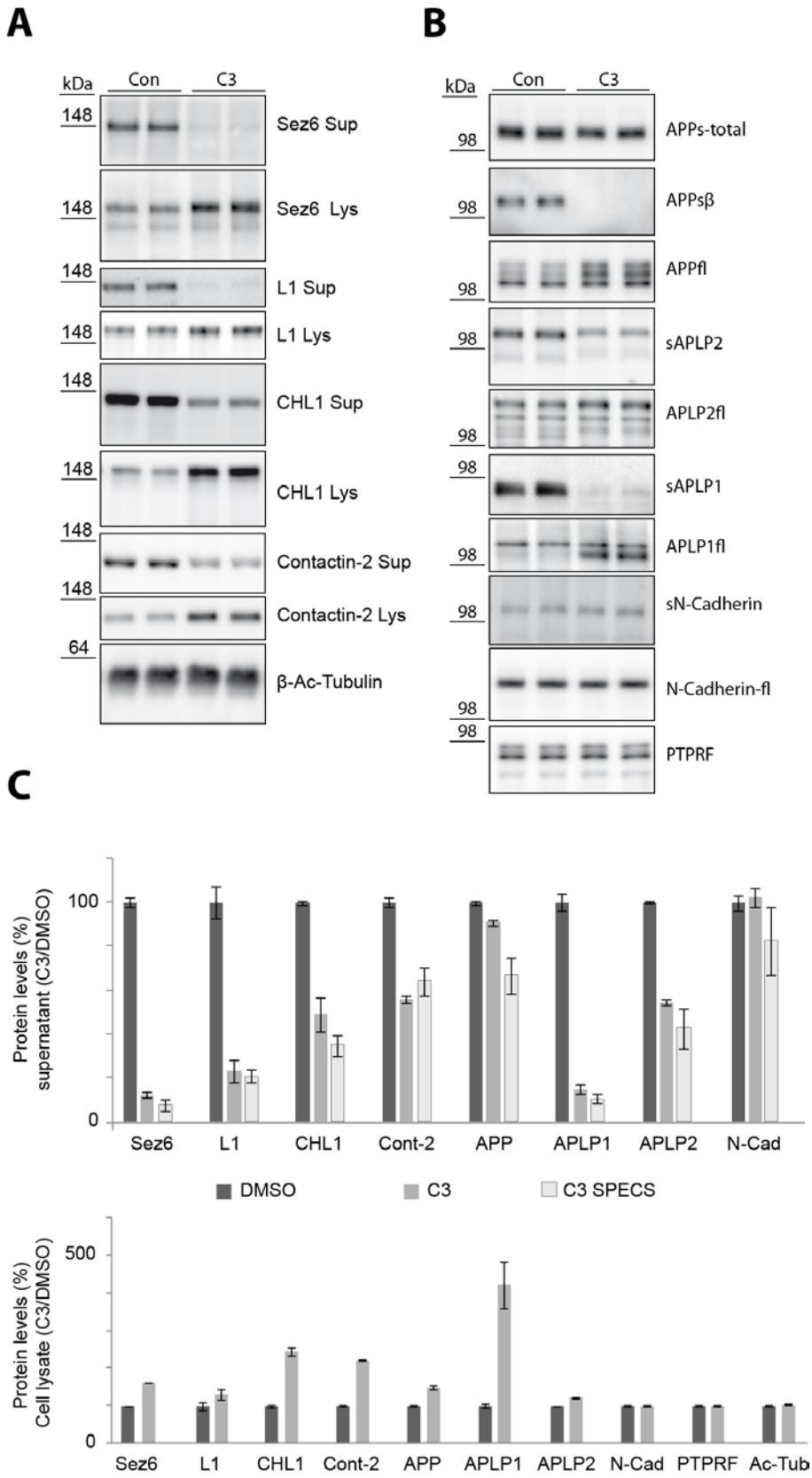

Figure 23 Validation of SPECS results for APP family and four novel BACE1 substrates shows the validation of identified BACE1 substrates with the SPECS method via Western Blot in C3 treated neurons. (**A**) Novel BACE1 substrates were Seizure protein 6 (SEZ6), CHL1, L1 and Contactin-2. (**B**) APP, APLP1 and APLP2 served as positive controls as these are kown BACE1 substrates. N-Cadherin and PTPRF showed no change in the SPECS analysis and therefore were included as negative controls. (**C**) Quantifiaction of the soluble ectodomans including the value obtained from the SPECS method. Quantifaction of the membrane precursors shows an accumulation.

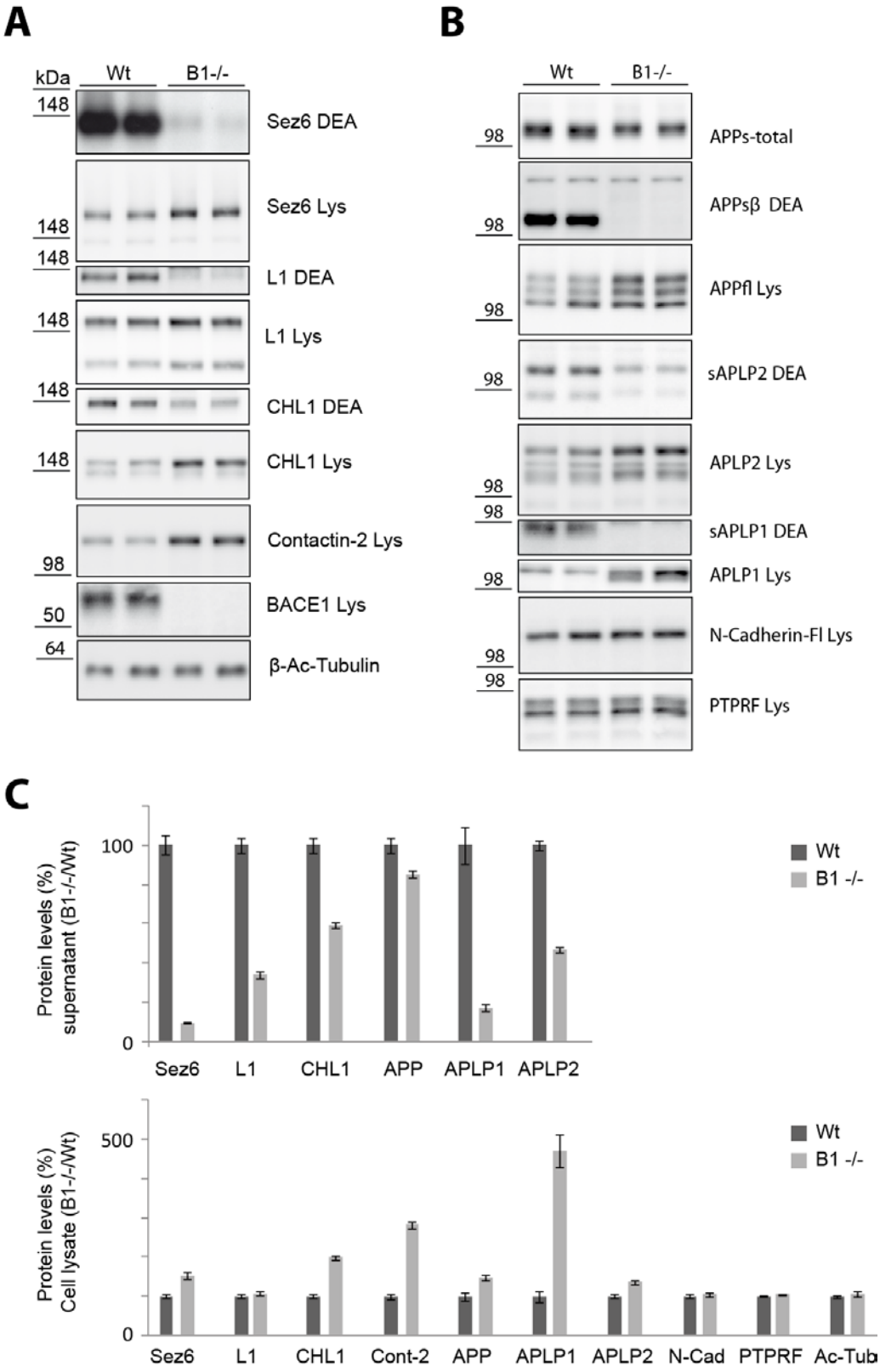

Figure 24 Validation of APP family and novel BACE1 substrates in BACE1 knockout brains (A) Analysis of Sez6, CHL1, L1 and Contactin-2 shedding in BACE1 knockout (B1-/-) and wildtype (Wt) brains. (B) APP, APLP1 and APLP2 served as positive controls while N-Cadherin and PTPRF served as negative controls. (**C**) Quantification of the shedding the accumulation of the membrane-attached precursors in wildtype and knockout brains.

4 Discussion

Identifying α-secretase in primary cortical neurons and the BACE1 substratome this study provides a more detailed insight into the biology of APP proteases. Though proteolytic processing of APP has been extensively studied over the last two decades, the underlying biology is not well understood. The biology of the APP proteases beyond APP processing is even more nebulous. Moreover, the identity of APP α-secretase was either controversially discussed or missing until now. The first part of the discussion deals with the establishment of the necessary methods that finally enabled the determination of APP α-secretase in primary cortical neurons, which will be discussed in the second part of the discussion. The third part will deal with the introduction of a new methodology which enables the proteome-wide unbiased identification of protease substrates and its application to identify physiological substrates of APP β-secretase BACE-1 in primary cortical neurons.

APP ectodomain shedding by α- and β-secretase activity releases the whole APP ectodomain while meprin-β mediated APP ectodomain cleaveage yields two smaller n-terminal fragments (Anderson et al., 1991; Haass et al., 1992a; Haass et al., 1992b; Jefferson et al., 2011). While β-secretase activity has been shown to be encoded by the aspartyl protease BACE1, the identity of α-secretase remained controversial. Several members of the "**A d**isintegrin **a**nd **m**etalloprotease" (ADAM) family have been proposed as APP alpha secretase (Allinson et al., 2004; Asai et al., 2003; Koike et al., 1999; Slack et al., 2001). This study tried to answer the question which metalloprotease activity facilitates the liberation of APPsα from the APP full length precursor in primary cortical neurons. The identification of the responsible protease like in case of β-secretase will serve a deeper biological understanding of α-secretase activity and a deeper functional characterization of the protease biology by identifying other substrates besides APP. The identification of α-secretase is also important with regard to a discussed therapeutic strategy which takes advantage of APP alpha secretase cleavage activation to the expense of APP β-secretase cleavage to prevent Aβ generation (Endres and Fahrenholz, 2011; Lichtenthaler et al., 2011; Tippmann et al., 2009). From a therapeutic perspective, identification of α-secretase will pave the way for the development of specific inhibitors and their assessment with regard to side-effects.

4.1.1 Modified lentiviral vectors allow knockdown and overexpression of membrane proteins

As the identity of α-secretase should be determined in primary cortical neurons first the technical problems of gene transfer into primary cortical neurons had to be overcome. Lipotransfection of primary cortical neurons yields only low transfection efficiencies of 1% to 5% (Karra and Dahm, 2010) which is desirable for single cell analysis. However, to enable biochemical studies in primary cortical neurons gene transfer efficiencies close to 100% are needed. Recombinant lentiviruses are transfer vehicles which provide gene transfer efficiencies close to 100% combined with low cytotoxicity (Zufferey et al., 1997). For this study, lentiviral vectors were used as these combine several advantages over other virus systems (Bouard et al., 2009). In comparison to other viruses, lentiviruses stably integrate into the genome, have a reasonable packaging capacity of around 7-8 kb and offer high *in vitro* infectivity and stable transgene expression. The employed lentivirus is based on a lentiviral second generation packaging system that combines high lentiviral titers with excellent biosafety (Zufferey et al., 1997). The system works by simultaneous transfection of three plasmids. The first plasmid codes for the viral envelope glycoprotein of the vesicular stomatitis virus (VSV-G) which covers the viral particle instead of its native envelope protein gp160. This strategy is called pseudotyping and extends the tropism of lentiviral particles to other cell types (Akkina et al., 1996; Naldini et al., 1996). The second plasmid codes for the structural protein gag and the viral polymerase (pol) and integrase (int). The third plasmid is a defective viral transfer vector which is devoid of the coding sequences of viral proteins. It only contains the long terminal repeats (LTR), a packaging signal and the desired expression cassette. Therefore, the resulting viruses are replication deficient as the viral proteins are no more expressed under control of the viral promoter and are no more packaged as genetic information into lentiviral particles. The transfer vectors utilized to meet the demands of this study can be divided into three groups: Constitutive transgene expression vectors, conditional transgene expression vectors which even do not express the transgene of interest in the producer cells and RNAi vectors based on either H1 or U6 promoter driven small hairpin RNA (shRNA) expression. Here, I will focus on the development and modification of RNAi vectors and of conditional transgene expression vectors as these were essential tools to address the questions about APP α-secretase. All lentiviral shRNA expressing transfer vectors in this thesis are either based on the pLKO 1.1 vector or the pLVTHM vector which have been described elsewhere (Stewart et al., 2003; Wiznerowicz and Trono, 2003). The plKO 1.1 vector contains a U6 promoter while the pLVTHM vector contains a H1 promoter. The U6 promoter outperforms the H1 promoter in terms of transcript production (Boden et

al., 2003). For this reason, while using pLVTHM in the beginning for all knockdown experiments, this vector was later replaced by the plKO2mod-EGFP-WPRE vector as standard RNAi mediating vector. shRNA expression with this vector allowed to silence the expression of genes like ADAM17 whose expression was resilient to H1 promoter driven shRNAs. This vector is a modified version of the pLKO1.1 vector. To meet our specific needs, a multiple cloning site for shRNAs was inserted, Puromycin was exchanged for GFP and a Woodchuck hepatitis virus responsive element (WPRE) was added to improve the expression of the GFP transgene (Donello et al., 1998) (see Fig. 11 A). This modified vector system in the end allowed us to efficiently silence genes while monitoring transduction efficiency via GFP fluorescence (Fig. 11 B).

Furthermore lentiviral gene transfer of plasma membrane proteins, in particular type-I, type-II and GPI-anchored membrane proteins, was another technical problem which needed to be solved. At first sight, this seems to be a simple problem: “If it works with GFP why shouldn’t it work with a membrane protein like APP?”. However, lentiviruses belong to the family of retroviruses which transport their genetic information in form of RNA. As recombinant retroviruses are produced in cells this consequentially leads to the translation of the first coding sequence (CDS) of a given retroviral RNA. Cytotoxic transgenes and type-I, -II and GPI-anchored membrane transgenes cannot be efficiently transferred with lentiviruses as they interfere with the virus genesis either by affecting cell viability in the first case or by disturbing proper pseudotyping of lentiviral particles in the latter case (see also Fig. 12). The new lentiviral expression system had to fulfill the criteria of no transgene expression in the producer cells and robust transgene expression in the target cells. For this purpose I made use of the Gal4/UAS system. Gal4-VP16 is a strong transcriptional activator and binds to a specific consensus sequence (Sadowski et al., 1988). In combination with these Gal4 binding so-called upstream activating sequences (UAS) and a minimal promoter, it enables transgene expression in drosphila, zebrafish, mouse and other organisms (Akitake et al., 2011; Baier and Scott, 2009; Benzekhroufa et al., 2009; Shaw et al., 2009). The initial system was based on a bidirectional expression cassette with DsRed and the gene of interest under control of 14 UAS repeats (Paquet et al., 2009). This expression cassette was inserted into a lentiviral transfer vector to generate DsRed and APP-TEV-FLAG coexpressing cells which were later used to determine the APP-cleavage site of APP α-secretase. As Gal4VP16 and the UAS-transgene viruses are produced separately, no GAL4-VP16 driven transgene expression should occur in the UAS-transgene virus expressing producer cells. However, as lentiviruses are RNA viruses, the first CDS is translated. This was also the case in the bidirectional system which in the end led to low transduction efficiencies. A temporary workaround solved this problem by

FACS-sorting the cells according to their DsRed fluorescence to obtain a homogenous APP-TEV-FLAG expressing population. The problem of expression in the producer cells was finally solved by placing either Puromycin or GFP upstream of a unidirectional UAS element followed by the gene of interest (see Fig 13). Placing GFP and Puromycin upstream of the UAS element has two beneficial effects because it blocks translation of the GOI both in packaging cells and target cells. In target cells, the absence of leaky expression of the GOI in the absence of Gal4-VP16 can finally be exploited for the improvement of background expression in the context of inducible expression systems which exist for Gal4-VP16 in form of an ecdysone receptor fusion protein as well (Esengil et al., 2007). Others have also constructed lentiviral expression systems either based on the tet or the Gal4 system in order to enhance transgene expression in beta-cells of the pancreas or to drive cell-specific inducible transgene expression in the rat brain (Benzekhroufa et al., 2009; Liu et al., 2008; Shaw et al., 2009). However, these studies did not take into account the possibility that the transgene expression itself can disturb lentiviral particle production. Hence, the lentiviruses produced and used in these studies suffered from lower titers and a higher background expression due to the already described phenomenon of transgene expression by cellular promoters (see also Fig 15). Though the described system here offers a good solution to the problems of membrane transgenes it is not necessarily ideal because UAS sequences can be silenced due to their repetitive nature. A solution to UAS silencing might be the use of a non-repetitive UAS element or higher expression of Gal4-VP16 which in the end would allow long-term expression (Akitake et al., 2011; Goll et al., 2009).

4.1.2 ADAM10 is the physiologically relevant alpha secretase of APP

After the establishment of the necessary methods to address the question of α-secretase identity APP processing was investigated in more detail. Strong motivations to answer this question are a deeper insight into the underlying biology as well as a proposed Alzheimer's disease therapeutic strategy which exploits modulation of α-secretase to the expense of β-secretase activity to prevent Aβ formation. So far the identity of α-secretase has been heavily debated. The most frequently proposed candidates in literature have been ADAM9, ADAM10 and ADAM17. Why is there so much confusion about the identity of alpha secretase? For all three proteases knockdown as well as knockout studies have been performed. Unfortunately, these studies led to different, conflicting results. ADAM9 knockout mice show no overt phenotype during their whole life time. In contrast, a knockout of ADAM10 is lethal at day E9.5 while the majority of ADAM17 deficient mice die between day E17 and P1 (Hartmann et al., 2002;

Peschon et al., 1998; Weskamp et al., 2002). APP processing was not affected in E18.5 hippocampal neurons of ADAM9 knockout mice. Moreover, APP was not consistently reduced in ADAM10-deficient fibroblasts generated from ADAM10 knockout mouse fetuses while in ADAM17 deficient fibroblast only the PMA stimulated APP-shedding was abolished. Though all three studies were performed with knockout animals, two studies lacked primary cells due to the essential role of ADAM10 and ADAM17 in development and differentiation. An important role for differentiation, in particular in the nervous system, has been shown for ADAM10 in a recent study (Jorissen et al., 2010) which is discussed to be dependent on a lack of Notch processing. Lack of Notch processing in ADAM10 knockout mice is a good explanation for early embryogenic lethality as processing of Notch by ADAM10 has been shown by several other studies (Gibb et al., 2010; van Tetering et al., 2009; Wen et al., 1997). RNAi studies against ADAM9, ADAM10 and ADAM17 did not contribute to a final clarification of alpha secretase identity as these had to grapple with technical problems like RNAi mediated off-target effects (Asai et al., 2003; Camden et al., 2005; Taylor et al., 2009). Moreover, these studies were exclusively performed in tumor cell lines and lacked an antibody which exclusively detected APPsα. None of these studies led to a complete abolishment of α-secretase activity.

These inconsistent results led to the tenor that all three proteases contributed to sAPPα shedding and hence would be able to compensate for each other. However, this is contradicted by other membrane proteins like CD23, transforming growth factor α (TGFα) or N-Cadherin which seem to be exclusively shedded by one protease (Reiss et al., 2005; Sahin et al., 2004; Weskamp et al., 2006).

I finally decided to address the question about the identity of alpha secretase in primary neurons because these are the most relevant cells with regard to Alzheimer's disease. In the context of this study, monoclonal antibodies were generated in collaboration with Elisabeth Kremmer against the human and murine APPsα epitopes (EVHHQK and EVRHQK) according to a seminal publication in 1991 which determined the APP alpha cleavage site by cyanobromide digests of sAPP products of PC12 cells (Anderson et al., 1991). APPsα-specific antibodies were generated due to reasons. First, a big proportion of APP is cleaved at the alternative β' cleavage site in rodent cells (Buxbaum et al., 1998b; Wang et al., 1996). Second, the obtained APPsα-specific antibodies 4B4 and 7A6 both recognize exclusively APPsα thus outperforming antibodies like 6E10 or WO2 which additionally detect the alternative BACE1 β'-cleavage product (Ida et al., 1996; Kuhn et al., 2010; Miles et al., 2008). Bearing these antibodies in our hand, the final analysis on APP α-secretase in primary cortical neurons was started.

Therefore, E15/E16 primary cortical neurons were infected with lentiviral particles coding either for a scrambled, non-targeting shRNA or shRNAs targeting ADAM9, ADAM10 or ADAM17 expression. A lot of emphasis was placed on the initial screening of the finally used shRNAs to mitigate off-target effects as good as it was technically possible. Off-target effects are a major concern in RNAi driven research and thus should be handled with care in every study working with RNAi (Jackson and Linsley, 2010). The shRNAs had to fulfill the criterion that expression of a protease targeting shRNA was neither supposed to affect the expression of the other investigated proteases nor to be cytotoxic. The final analysis of the APP cleavage products APPsα, APPsβ and Aβ identified ADAM10 to be the sole APPsα secretase while ADAM9 and ADAM17 knockdown had no effect on APPsα. Both ADAM10 shRNAs led to a variable increase in APPsβ and Aβ. This might speak for a competition between ADAM10 and BACE1. This competition was also observed in a transgenic Alzheimer model which beforehand had been crossed to an ADAM10 overexpression mouse model. Upon overexpression of ADAM10, APPsα was increased while APPsβ and Aβ were decreased. Moreover, this consequentially ameliorated plaque pathology and behavioral deficits in these mice (Postina et al., 2004). However, as already exemplified for BACE1, ADAM10 overexpression might lead to mislocalisation and premature activation of ADAM10 (Gibb et al., 2010; Huse et al., 2002). This consequently could enable ADAM10 to compete with BACE1 for APP as a substrate. In contrast, within the limits of endogenous BACE1 expression even activation of ADAM10 does not necessarily lead to a reduction of APPsβ. Mice treated with the retincoic acid agonist acitretin showed increased levels of APPsα but no decrease in APPsβ levels in brain homogenates (Tippmann et al., 2009). However, these mice showed decreased levels of Aβ40 and Aβ42 in the brain which is the desired aim of all Aβ lowering approaches. Whether this results from APPsβ reduction or upregulation of Aβ degrading enzymes remains open to further investigation. Moreover, the ADAM10-specific cleavage product of APP was analyzed by mass spectrometry (see Fig. 19). The whole APP ectodomain is heterogeneously glycosylated and very large which consequently would perturb accurate mass spectrometry measurements that allow cleavage site determination. A solution was the usage of an APP construct which contained a TEV protease cleavage site followed by a FLAG epitope 33 amino acids upstream of the ADAM10 cleavage site. Cleavage with TEV and FLAG immunoprecipitation allowed purification of the c-terminal ADAM10 cleavage product. This in the end enabled determination of the ADAM10-specific cleavage site whose generation was blocked upon expression of an ADAM10 specific shRNA which fits well with previous studies (Anderson et al., 1991; Lammich et al., 1999). Finally, APP processing was also analyzed in a conditional

knockout model of ADAM10 in E15/E16 primary cortical neurons. Therefore, primary cortical neurons from mice carrying loxP site flanked ADAM10 loci were infected with Cre recombinase. The deletion of exon 9 led to an almost complete knockout of ADAM10 (see Fig. 18). The knockout coincided with an almost complete loss of APPsα shedding. In contrast to the shRNA mediated knockdown of ADAM10, BACE1 did not seem to compensate for the loss of ADAM10 cleavage in this experimental set up. APPsβ levels were not elevated. Moreover, a slight accumulation of mature APP in the cell lysate and a mild reduction of total secreted APP could be observed. These findings are strongly suggestive for an off-target effect of both ADAM10 targeting shRNAs on BACE1 expression. Nevertheless, both experimental approaches confirm ADAM10 as the sole alpha secretase in primary cortical neurons. On the contrary, BACE1 knockout and inhibition lead to a strong increase in APPsα generation (Luo et al., 2001; Nishitomi et al., 2006; Skovronsky et al., 2000). How can this unilateral behavior of compensation be explained? There are three possible explanations. First, APP sequentially traffics through the BACE1 and ADAM10 compartment in the designated order. In case of a BACE1 knockout, more APP can traffic to the ADAM10 compartment to be finally processed there. Vice versa, an ADAM10 knockout would not lead to increased APP processing by BACE1 if internalized unprocessed plasma membrane APP does not contribute to BACE1 dependent APP processing. This theory is corroborated by the findings that endogenous mature BACE1 as well as the bulk of Aβ40 localize to the late trans golgi network (TGN) (Hartmann et al., 1997; Xu et al., 1997; Yan et al., 2001) while mature ADAM10 localizes to the plasma membrane (Wild-Bode et al., 2006). A second possible scenario is the saturation of BACE1 with substrate. Thus BACE1 would not be able to process additional APP full length protein provided by missing ADAM10 processing. However, a saturation of BACE1 is rather unlikely as a recent study could show that endogenous APP processing is unaffected in BACE1 heterozygous knockout mice in which a halved BACE1 expression still sustains the same levels of Aβ generation compared to wild type mice (Nishitomi et al., 2006). A third explanation would be the minor 10% contribution of ADAM10 to APP total shedding which upon knockout is not measurable due to the major 90% contribution of BACE1 to total APP shedding in primary cortical neurons. In summary, based on the data presented ADAM10 can be designated as the sole constitutive α-secretase in primary cortical neurons which has been as well confirmed by another study (Jorissen et al., 2010; Kuhn et al., 2010). ADAM10 thus should be in focus of α-secretase activity modulating drug research. In the meantime, the unilateral compensation of APP processing by ADAM10 will need further investigation to finally understand the underlying biology.

Furthermore it will become important to investigate the substrate spectrum of ADAM10 to predict the side-effects of ADAM10 activation.

4.1.3 Secretome Protein enrichment with click sugars enables identification of novel BACE1 substrates in primary cortical neurons

After clarification of α-secretase identity, I focused on the physiological function of BACE1. BACE1-mediated ectodomain shedding of APP is the initial and rate-limiting step of Aβ production (Sinha et al., 1999; Vassar et al., 1999; Yan et al., 1999). The amyloid cascade hypothesis considers Aβ as the central player in the molecular pathological changes driving Alzheimer's disease pathology (Hardy and Selkoe, 2002; Hardy and Higgins, 1992). Pioneer phenotypic studies of BACE1 knockout mice described no obvious phenotype (Cai et al., 2001; Luo et al., 2001; Roberds et al., 2001). Therefore, BACE1 inhibition is still considered to be one of the most favored therapeutic strategies of the pharmaceutical industry to prevent Alzheimer's disease. BACE1 inhibition will obviously only be possible if it does not cause severe side-effects. A recent study about an orally available BACE1 inhibitor short-term treatment showed robust reduction of Aβ with no obvious side-effects (May et al., 2011b). However, only long term treatments will allow to anticipating side-effects in the central nervous system. Meanwhile, in contrast to initial BACE1 knockout mice studies recent studies draw a more complex picture of the neurophysiologic deficits of BACE1 knockout mice. BACE1 knockout mice show behavioral deficits like reduced anxiety levels, reduced swim speed, an impaired spatial working memory, increased postnatal lethality within the first 20 days after birth, hyperactivity and a higher susceptibility for seizures (Dominguez et al., 2005; Hitt et al., 2010; Laird et al., 2005). Electrophysiological studies revealed presynaptic deficits in mossy fibers of the CA1 and CA3 region in the hippocampus which both are assumed to originate from a dysfunction in presynaptic Ca^{2+} regulation (Wang et al., 2008). A subset of BACE1 knockout mice experienced epileptic seizures which were accompanied by spike-wave complexes in the electroencephalogram (EEG) (Hitt et al., 2010; Hu et al., 2010). Moreover, BACE1 knockout mice showed increased paired-pulse facilitation ratios which also speak for a presynaptic deficit. The presynaptic deficit would correlate with the purported anterograde axonal transport and localization of BACE1 in presynaptic boutons (Kamal et al., 2001; Laird et al., 2005). However, this is under debate (Lazarov et al., 2005).

Besides the behavioral and electrophysiological studies it is necessary to understand the underlying molecular mechanisms. As the physiological function of a prote-

ase is defined by its substrates, a deeper functional insight can be gained by their identification. With APP, APLP1, APLP2, Sialyltransferase ST6GAL1, PSGL-1, Neuregulin I type III, , IL-1R2, the β2 subunit of voltage-gated sodium channels, LRP only few BACE1 substrates have been so far proposed (Eggert et al., 2004; Haass et al., 1992b; Hu et al., 2006; Kim et al., 2007; Kitazume et al., 2003; Kuhn et al., 2007; Li and Sudhof, 2004; Lichtenthaler et al., 2003; Sala Frigerio et al., 2010; von Arnim et al., 2005; Willem et al., 2006). With regard to the physiological consequence and relevance, Neuregulin-1 type III is the only substrate whose lack of BACE1-mediated processing could be linked to a hypomyelination phenotype in the peripheral nerve system (PNS) (Hu et al., 2006; Willem et al., 2006). BACE1 liberates the EGF soluble domain of Neuregulin-1 type III and thus controls the myelin sheet thickness of axons originating from dorsal root ganglia by inducing myelination (Velanac et al., 2012). Nevertheless, the lack of BACE1-mediated processing of Neuregulin 1 type III in the PNS offers no satisfactory explanation for the multifaceted phenotype of BACE1 knockout mice. A proteomic study identified over 65 candidate BACE1 substrates in BACE1 overexpressing tumor cells (Hemming et al., 2009). However, overexpression of BACE1 can lead to artificial localization of BACE1 and hence to aberrant substrate cleavage (Huse et al., 2002; Yan et al., 2001). To circumvent this problem, this study introduced a new method called **S**ecretome **p**rotein **e**nrichment with **c**lick **s**ugars (SPECS) which enables proteome-wide identification and quantification of proteolytically liberated as well as secreted glycoproteins under endogenous expression conditions of BACE1 in primary cortical neurons. SPECS offers an unbiased alternative to candidate-based approaches for protease substrate identification. This enabled the identification of a lot of novel BACE1 substrates in primary cortical neurons. SPECS combines glycoprotein enrichment via metabolic labeling with azido sugars and copper-free click chemistry-mediated biotinylation with subsequent mass spectrometry driven detection and label-free quantification of these proteins. The majority of secreted and membrane proteins are glycosylated (Zielinska et al., 2010). Furthermore glycosylation is a good discrimination criterion to distinguish between cytosolic and membrane proteins. Hence, glycoproteins were metabolically labeled with an azide group by feeding primary cortical neurons with tetraacetyl-*N*-azidoacetyl-mannosamine. Metabolic labeling with azidogroup containing amino sugars has already been described to be well-tolerated *in vivo* and *in vitro* (Baskin et al., 2007; Dube et al., 2006; Laughlin et al., 2008). For in vitro click chemistry mediated biotinylation, Dibenzocyclooctyne(DBCO)-PEG12- Biotin was used (Ning et al., 2008) which outperforms Difluorcycloocytyne due to a combination of easier synthesis with equal reaction kinetics (Baskin et al., 2007). Furthermore, modification of the aromatic rings of Dibenzocyclooctyne can be exploited for further

reactivity enhancment or fluorescent properties upon cycloaddition which in the end would allow real-time monitoring of the click reaction (Jewett and Bertozzi, 2011). The long polyethylenglycol linker offers good accessability for both Biotin binding to Streptavidin as well as the click reaction of the strained alkyne moiety DBCO.

Usage of SPECS enabled identification of 283 glycoproteins in neurons and 254 glycoproteins in HEK293T cells which we defined as their secretomes. For certain these secretomes are far from being complete due to the following limitations of the technique. First, the usage of azidosugars for metabolic labeling restricts the enriched proteins to glycoproteins. Though the majority of secreted and plasma membrane proteins is glycosylated, still a small proportion of proteins will not be detected. Second, the purification though quantitative precipitates only 1/20 of all labeled glycoproteins due to the low capacity of Streptavidin beads. Hence, low abundance proteins are underrepresented in the sample. Moreover unspecific binding of proteins to the utilized streptavidin matrix is a problem as these unspecifically bound proteins are eluted under the harsh elution conditions needed to break the biotin streptavidin bond (see Fig. 21).

Nevertheless, comparing shedded and secreted proteins of non-treated with BACE1 inhibitor treated neurons via SPECS resulted in 34 BACE1 substrates with strong, moderate and mild reduction of ectodomain shedding. The well-known BACE1 substrates APP (67%), APLP1 (11%) and APLP2 (43%) were all identified and properly quantified according to results of previous studies and thus served as an internal validation of the method (Hogl et al., 2011; Sala Frigerio et al., 2010). Seizure protein 6 (4%) and Seizure protein 6 like 1 (8%) showed the strongest reduction in shedding while the third member of the Sez6 family Seizure protein 6 like 2 showed only a moderate reduction down to 60%. The triple knockout of the Sez6 family leads to impaired synaptic maturation in the cerebellum which resulted in a clumsy motoric behavior (Miyazaki et al., 2006). Sez6 seems to play an important role in proper dendritic arbor specification and development of excitatory synapses (Gunnersen et al., 2007). That study proposes a balanced interplay between membrane bound and soluble Sez6. The authors propose alternative splicing of Sez6 to be causative for the simultaneous presence of a membrane-bound and a soluble form of Sez6. However, Sez6 seems to be a very good substrate for BACE1. Sez6 was identified as a BACE1 substrate with the SPECS method which was further corroborated by Western Blot analysis with a polyclonal antibody (Gunnersen et al., 2007) in BACE1 inhibitor treated neurons and BACE1 knockout brain homogenates. While soluble Sez6 ectodomain was completely abolished upon BACE1 inhibition or knockout, no evidence was found for protein products of alternative transcripts. Both the genetic and the pharmacological inhibition of BACE1 suppressed BACE1-mediated shedding of Sez6. Thus, BACE1 might regulate

the interplay between membrane-bound and soluble Sez6 and hence regulate specification of the dendritic arbor and maturation of excitatory synapses. Besides the Sez6 family, other proteins with strong shedding inhibition L1CAM (21%), CHL1 (35%) and mild shedding inhibition Contactin-2 (64%) were identified via SPECS. This was further corroborated by respective immunoblots against L1CAM, CHL1 and Contactin-2 in BACE1 inhibitor treated neurons and BACE1 knockout brain homogenates. The quantified shedding reduction in Western Blot corresponded well with the quantified values in the SPECS experiment. This again proofed that SPECS allows proper quantification and prediction of protease substrates. L1CAM and CHL1 belong to the L1 family which is comprised of L1, CHL1, NrCam and Neurofascin (Schmid and Maness, 2008). CHL1 interacts most likely with integrins of the radial glia and is necessary for positioning of deep layer pyramidal neurons in the posterior neo cortex by facilitating radial migration of neuronal precursors. Moreover, CHL1 seems to be indispensible for proper positioning of apical dendrites (Demyanenko et al., 2004). Recently, it has also been implied to be necessary for proper thalamocortical projections from the thalamic ventrobasal nucleus to the somatosensory cortex (Wright et al., 2007). The knockout of L1 resembles a lot of features of the human CRASH syndrome which is caused by C-terminal truncation mutations of the L1 protein (Yamasaki et al., 1997). L1 is supposed to play a role in dendritic morphogenesis as an L1 knockout leads to abnormal dendritic architecture, dilated ventricles, a decreased number of hippocampal neurons and a dysgenesis of the corpus callosum (Demyanenko et al., 1999). Inefficient migration of dopaminergic neurons in L1 knockout mice leads to their abnormal distribution. This finding would also fit to the reduced dopamine content and turnover in the striatum observed in BACE1 knockout mice (Harrison et al., 2003). Nevertheless, BACE1 knockout mice have a fairly normal brain anatomy and the human CRASH syndrome is caused by c-terminal truncation mutations which might imply that most L1 functions are mediated by the full length form (Luo et al., 2001).

Another novel substrate identified by SPECS is Contactin-2 which is involved in the molecular organization of myelin. It localizes delayed rectifier potassium channels to the juxtaparaondal region of nodes of ranvier in myelinated axons and separates these from sodium channels in the nodal region. The localization of potassium channels is achieved by a homophilic interaction of neuronal Contactin-2 with oligodendroglial Contactin-2 and a heterophilic interaction with CaspR2 in neurons (Gu and Gu, 2011; Poliak et al., 2003; Traka et al., 2003). Though Contactin-2 shedding is only reduced to 64%, it accumulated almost threefold in the brain upon BACE1 knockout. As a presynaptic deficit has been described in electrophysiological studies of BACE1 knockout

mice, it will be interesting to see whether the distribution of potassium channels in the axonal compartment is altered (Wang et al., 2008).

The described functions of some selected BACE1 substrates already show the phenotypic complexity of BACE1 knockout mice. This phenotypic complexity will aggravate linkage identification between deficient processing of a given substrate and a certain phenotype observed in BACE1 knockout mice. Further in vivo studies as well as a deeper understanding of the interactions between different membrane proteins are needed to fully understand the phenotype of BACE1 knockout mice.

4.1.4 ADAM10 and BACE1 in light of a future therapeutic perspective

With regard to ADAM10 activation or BACE1 inhibition as future therapeutic options in Alzheimer's disease, the results obtained might lead to the conclusion that neither ADAM10 activation nor BACE1 inhibition are viable strategies to prevent Alzheimer's disease. Though ADAM10 is the α-secretase in primary cortical neurons, ADAM10 seems not to compete with BACE1 for APP as a substrate. This could hint into the direction of another metalloprotease which is competing with BACE1 for APP. However, the identity of this protease so far is not known.

On the other hand, the identification of novel BACE1 substrates in conjunction with the described phenotypes of BACE1 knockout mice provides evidence that BACE1 inhibition in the long run might induce side effects. Thus, it would be better to develop substrate targeting compounds which modulate substrate proteolytic processing by binding to the substrate cleavage region. This could in turn block the binding of the protease. Consequentially the drug would only affect the processing of a single substrate instead of all substrates of a given protease if the protease is targeted with an inhibitor.

5 Outlook

The novel method secretome protein enrichment with click sugars (SPECS) enables the proteome-wide identification of cellular secretomes and thus led to the identification of novel BACE1 substrates in primary cortical neurons in this study. SPECS is not limited to neurons but will also be applicable in other cell types in the brain like oligodendrocytes, astrocytes and to other cell types in the body like immune cells or hepatocytes. In the future SPECS might also be used in organotypic slice cultures or even *in vivo*. However, therefore novel strategies of metabolic labeling have to be developed. Amino sugars per se cannot penetrate mammalian cells (Wang et al., 2009a). As a consequence the OH-groups of amino sugars utilized for metabolic labeling are peracetylated to increase sugar lipophilicity which in turn allows their passive diffusion into the cell. Once the amino sugar has reached the cytosol it is trapped by deacetylation via cellular esterases. For *in vivo* applications of SPECS however a more selective labeling approach is necessary which would allow cell specific metabolic labeling *in vivo.* In sharp contrast, peracetylated amino sugar analogs are mainly metabolized at the injection site. Targeted metabolic labeling could be achieved by ectopic expression of a non-existent specific amino sugar transporter thus eliminating the need for amino sugar peracetylation. Tissue-specific promoter driven expression of this transporter would for example allow the investigation of cellular responses of immune cells upon an immunological stimulus or the creation of proteomic inventories of substructures in the mouse.

SPECS is not limited to the investigation of cellular secretomes but can also be applied to glycoprotein enrichment from cellular lysates or the plasma membrane. This might enable the quantification of membrane proteins at the cell surface. Furthermore in conjunction with a labeling enzyme like biotin ligase targeted to specific cellular compartments SPECS might enable to investigate these compartments for their specific protein content (Thyagarajan and Ting, 2010). These could be the postsynaptic or the presynaptic compartment, lysosomes or autophagosomes. Furthermore SPECS might be used for the identification of novel biomarkers in different diseases as it allows the systematic identification of surface glycoproteins in tumor cells.

Furthermore, there is still room for improvement in the SPECS method. So far, only 5% to 10% of all metabolically labeled and biotinylated proteins can be purified via streptavidin pull down. Furthermore, nonspecifically bound proteins are eluted under the harsh elution conditions. A solution to this problem might be the combined use of

the biotin derivative desthiobiotin and the Streptactin matrix. Captured glycoproteins could be mildy released via elution with 2-(4-hydroxyphenylazo) benzoic acid (HABA) which is able to displace Desthiobiotin from the Streptactin matrix (Maier et al., 1998; Zwicker et al., 1999). Another approach would be the functionalization of a hydrophilic polymer with strained alkyne moieties to click azide-bearing glycoproteins directly to the polymer. This could in turn be purified either by precipitation or centrifugation through a filter which retains the polymer protein complexes. This outlook shows the potential of glycoprotein labeling for a lot of scientific questions in the future.

6 Summary

The data presented in this thesis deal with method development in different areas and furthermore novel biological insights into protease biology of BACE1 and ADAM10 with regard to APP processing and beyond APP processing.

First of all within the scope of my thesis, the identity of α-secretase should be determined. α-secretase promotes anti-amyloidogenic processing of APP cleaving within the amyloid β domain of APP which leads to the liberations of the APPsα ectodomain. However, the identity of α-secretase has been controversially discussed in the last decade. Several candidates like ADAM9, ADAM10 and ADAM17 as well as compensation among these proteases have been proposed which resulted from technical limitations like RNAi off-target effects, the studied cellular system or embryonic lethality of a gene knockout like in case for ADAM10. The results presented in this thesis clearly proof that ADAM10 is the sole long-thought APP α-secretase in primary cortical neurons while ADAM9 and ADAM17 do not play a role in APPsα generation in primary cortical neurons. Additionally, loss of APPsα processing upon ADAM10 knockdown or knockout is not compensated by other metalloproteases. These results put an end to the long discussion about APP α-secretase identity. Additionally, constitutively active ADAM10 does not to compete with β-secretase for APP as a substrate. However, ADAM10 activation has been considered a viable strategy to promote anti-amyloidogenic processing of APP and thus preventing Aβ generation. For this reason, pinpointing the identity of alpha secretase to ADAM10 is valuable information for the future development of alpha secretase modulating drugs.

Within the scope of my thesis I developed novel lentiviral vectors which can be used for the efficient expression of toxic and membrane transgenes in any desired cell type. These viral transfer responder vectors show no expression of the gene of interest in the producer cells due to a translational block and a silent promoter. Upon cotransduction with a transcriptional activator in the target cells strong and robust expression is achieved by the responder vector. This system allowed the expression of APP-TEV-FLAG which in the end allowed the determination of APP ADAM10 cleavage site via MALDI-TOF mass spectrometry. Furthermore, this lentiviral overexpression system will enable the study of membrane protein interactions, trafficking and other biological processes in primary cells like for example neurons.

The knowledge of BACE1 protease biology beyond APP processing is rather marginal. The lack of knowledge of BACE1 substrates stemmed mainly from technical limi-

tations. Meanwhile, mass spectrometry-driven proteomics are a serious alternative to classical analysis techniques for the identification of protease substrates. However, mass spectrometry is not selective during the measurement process which comprises of peptide ionization and their measurement. Hence, abundant proteins are more prone to be detected than sparse proteins. For example glycoproteins are less abundant than cytosolic proteins. To make these proteins more visible to mass spectrometry based detection specific glycoprotein enrichment methods are required. Hence, I developed the Secretome protein enrichment with click sugars (SPECS) method which is based on metabolic labeling of glycoproteins with azido sugars and their subsequent biotinylation via a strain promoted 2+3 cycloaddition. Both enables exclusive purification of de novo synthesized cellular glycoproteins in the presence of serum. This in the end enabled the qualitative identification and quantification of the neuronal secretome with 283 glycoproteins which could be robustly detected in five biological replicates. This list is a resource for researchers which are interested in studying secreted or shedded extracellular proteins to study signaling, proteolytic processing of surface membrane proteins or extracellular matrix interactions. Furthermore, quantitatively comparing two experimental conditions of neurons either treated with the BACE1 inhibitor C3 or DMSO as a solvent control via mass spectrometry allowed the identification of 34 novel putative BACE1 substrates. Among these 34 BACE1 substrates the known substrates APP, APLP1 and APLP2 could be found which already validated the technique. Besides the known BACE1 substrates, out of 34 putative new BACE1 substrates the four novel substrates Sez6, L1, CHL1 and Contactin-2 could be confirmed in C3 treated neurons and in homogenates of BACE1 knockout brains via Western Blot. The quantified Western blot results were in accordance with the quantitative measurements of the SPECS method which shows the quantitative accuracy of the SPECS method. Finally, purification and identification of the HEK293T secretome exemplifies that the SPECS method is not restricted to neurons but can also be extended to different kind of cell lines or even tissues.

The novel identified substrates of BACE1 require a careful reassessment of BACE1 inhibition as a potential therapeutic strategy to prevent amyloidogenic processing of APP and thus the development of Alzheimer's disease with regard to potential side-effects. These side-effects may arise from the inhibited processing of novel BACE1 substrates. A strategy targeting the substrates directly instead of the converting protease might circumvent many of these problems though this strategy might be more challenging with regard to drug design.

7 Index

(2011). The amyloid cascade hypothesis has misled the pharmaceutical industry. Biochemical Society transactions *39*, 920-923.
Agard, N.J., Prescher, J.A., and Bertozzi, C.R. (2004). A strain-promoted [3 + 2] azide-alkyne cycloaddition for covalent modification of biomolecules in living systems. Journal of the American Chemical Society *126*, 15046-15047.
Akitake, C.M., Macurak, M., Halpern, M.E., and Goll, M.G. (2011). Transgenerational analysis of transcriptional silencing in zebrafish. Developmental biology *352*, 191-201.
Akkina, R.K., Walton, R.M., Chen, M.L., Li, Q.X., Planelles, V., and Chen, I.S. (1996). High-efficiency gene transfer into CD34+ cells with a human immunodeficiency virus type 1-based retroviral vector pseudotyped with vesicular stomatitis virus envelope glycoprotein G. Journal of virology *70*, 2581-2585.
Alexandru, A., Jagla, W., Graubner, S., Becker, A., Bauscher, C., Kohlmann, S., Sedlmeier, R., Raber, K.A., Cynis, H., Ronicke, R.*, et al.* (2011). Selective hippocampal neurodegeneration in transgenic mice expressing small amounts of truncated Abeta is induced by pyroglutamate-Abeta formation. The Journal of neuroscience : the official journal of the Society for Neuroscience *31*, 12790-12801.
Allinson, T.M., Parkin, E.T., Condon, T.P., Schwager, S.L., Sturrock, E.D., Turner, A.J., and Hooper, N.M. (2004). The role of ADAM10 and ADAM17 in the ectodomain shedding of angiotensin converting enzyme and the amyloid precursor protein. European journal of biochemistry / FEBS *271*, 2539-2547.
Almaraz, R.T., Aich, U., Khanna, H.S., Tan, E., Bhattacharya, R., Shah, S., and Yarema, K.J. (2011). Metabolic oligosaccharide engineering with N-Acyl functionalized ManNAc analogs: Cytotoxicity, metabolic flux, and glycan-display considerations. Biotechnology and bioengineering.
Alzheimer, A., Stelzmann, R.A., Schnitzlein, H.N., and Murtagh, F.R. (1995). An English translation of Alzheimer's 1907 paper, "Uber eine eigenartige Erkankung der Hirnrinde". Clin Anat *8*, 429-431.
Anders, A., Gilbert, S., Garten, W., Postina, R., and Fahrenholz, F. (2001). Regulation of the alpha-secretase ADAM10 by its prodomain and proprotein convertases. The FASEB journal : official publication of the Federation of American Societies for Experimental Biology *15*, 1837-1839.
Anderson, J.P., Esch, F.S., Keim, P.S., Sambamurti, K., Lieberburg, I., and Robakis, N.K. (1991). Exact cleavage site of Alzheimer amyloid precursor in neuronal PC-12 cells. Neuroscience letters *128*, 126-128.
Asai, M., Hattori, C., Szabo, B., Sasagawa, N., Maruyama, K., Tanuma, S., and Ishiura, S. (2003). Putative function of ADAM9, ADAM10, and ADAM17 as APP alpha-secretase. Biochemical and biophysical research communications *301*, 231-235.
Aydin, D., Weyer, S.W., and Muller, U.C. (2011). Functions of the APP gene family in the nervous system: insights from mouse models. Experimental brain research Experimentelle Hirnforschung Experimentation cerebrale.
Bai, G., and Pfaff, S.L. (2011). Protease regulation: the Yin and Yang of neural development and disease. Neuron *72*, 9-21.
Baier, H., and Scott, E.K. (2009). Genetic and optical targeting of neural circuits and behavior--zebrafish in the spotlight. Current opinion in neurobiology *19*, 553-560.
Ballard, C., Gauthier, S., Corbett, A., Brayne, C., Aarsland, D., and Jones, E. (2011). Alzheimer's disease. Lancet *377*, 1019-1031.
Baskin, J.M., Prescher, J.A., Laughlin, S.T., Agard, N.J., Chang, P.V., Miller, I.A., Lo, A., Codelli, J.A., and Bertozzi, C.R. (2007). Copper-free click chemistry for dynamic in

vivo imaging. Proceedings of the National Academy of Sciences of the United States of America *104*, 16793-16797.
Bateman, R.J., Siemers, E.R., Mawuenyega, K.G., Wen, G., Browning, K.R., Sigurdson, W.C., Yarasheski, K.E., Friedrich, S.W., Demattos, R.B., May, P.C.*, et al.* (2009). A gamma-secretase inhibitor decreases amyloid-beta production in the central nervous system. Annals of neurology *66*, 48-54.
Benzekhroufa, K., Liu, B.H., Teschemacher, A.G., and Kasparov, S. (2009). Targeting central serotonergic neurons with lentiviral vectors based on a transcriptional amplification strategy. Gene therapy *16*, 681-688.
Black, R.A., Rauch, C.T., Kozlosky, C.J., Peschon, J.J., Slack, J.L., Wolfson, M.F., Castner, B.J., Stocking, K.L., Reddy, P., Srinivasan, S.*, et al.* (1997). A metalloproteinase disintegrin that releases tumour-necrosis factor-alpha from cells. Nature *385*, 729-733.
Boden, D., Pusch, O., Lee, F., Tucker, L., Shank, P.R., and Ramratnam, B. (2003). Promoter choice affects the potency of HIV-1 specific RNA interference. Nucleic acids research *31*, 5033-5038.
Bouard, D., Alazard-Dany, D., and Cosset, F.L. (2009). Viral vectors: from virology to transgene expression. British journal of pharmacology *157*, 153-165.
Braak, E., and Braak, H. (1997). Alzheimer's disease: transiently developing dendritic changes in pyramidal cells of sector CA1 of the Ammon's horn. Acta neuropathologica *93*, 323-325.
Braak, H., Alafuzoff, I., Arzberger, T., Kretzschmar, H., and Del Tredici, K. (2006). Staging of Alzheimer disease-associated neurofibrillary pathology using paraffin sections and immunocytochemistry. Acta neuropathologica *112*, 389-404.
Braak, H., and Braak, E. (1991). Demonstration of amyloid deposits and neurofibrillary changes in whole brain sections. Brain Pathol *1*, 213-216.
Brown, M.S., and Goldstein, J.L. (1999). A proteolytic pathway that controls the cholesterol content of membranes, cells, and blood. Proceedings of the National Academy of Sciences of the United States of America *96*, 11041-11048.
Bu, G. (2009). Apolipoprotein E and its receptors in Alzheimer's disease: pathways, pathogenesis and therapy. Nature reviews Neuroscience *10*, 333-344.
Buxbaum, J.D., Liu, K.N., Luo, Y., Slack, J.L., Stocking, K.L., Peschon, J.J., Johnson, R.S., Castner, B.J., Cerretti, D.P., and Black, R.A. (1998a). Evidence that tumor necrosis factor alpha converting enzyme is involved in regulated alpha-secretase cleavage of the Alzheimer amyloid protein precursor. The Journal of biological chemistry *273*, 27765-27767.
Buxbaum, J.D., Thinakaran, G., Koliatsos, V., O'Callahan, J., Slunt, H.H., Price, D.L., and Sisodia, S.S. (1998b). Alzheimer amyloid protein precursor in the rat hippocampus: transport and processing through the perforant path. The Journal of neuroscience : the official journal of the Society for Neuroscience *18*, 9629-9637.
Cai, H., Wang, Y., McCarthy, D., Wen, H., Borchelt, D.R., Price, D.L., and Wong, P.C. (2001). BACE1 is the major beta-secretase for generation of Abeta peptides by neurons. Nature neuroscience *4*, 233-234.
Camden, J.M., Schrader, A.M., Camden, R.E., Gonzalez, F.A., Erb, L., Seye, C.I., and Weisman, G.A. (2005). P2Y2 nucleotide receptors enhance alpha-secretase-dependent amyloid precursor protein processing. The Journal of biological chemistry *280*, 18696-18702.
Cao, X., and Sudhof, T.C. (2001). A transcriptionally [correction of transcriptively] active complex of APP with Fe65 and histone acetyltransferase Tip60. Science *293*, 115-120.
Capell, A., Steiner, H., Willem, M., Kaiser, H., Meyer, C., Walter, J., Lammich, S., Multhaup, G., and Haass, C. (2000). Maturation and pro-peptide cleavage of beta-secretase. The Journal of biological chemistry *275*, 30849-30854.
Castellano, J.M., Kim, J., Stewart, F.R., Jiang, H., DeMattos, R.B., Patterson, B.W., Fagan, A.M., Morris, J.C., Mawuenyega, K.G., Cruchaga, C.*, et al.* (2011). Human

apoE isoforms differentially regulate brain amyloid-beta peptide clearance. Science translational medicine *3*, 89ra57.
Chaiet, L., and Wolf, F.J. (1964). The Properties of Streptavidin, a Biotin-Binding Protein Produced by Streptomycetes. Archives of biochemistry and biophysics *106*, 1-5.
Chang, P.V., Chen, X., Smyrniotis, C., Xenakis, A., Hu, T., Bertozzi, C.R., and Wu, P. (2009). Metabolic labeling of sialic acids in living animals with alkynyl sugars. Angew Chem Int Ed Engl *48*, 4030-4033.
Chen, G., and Zhang, X. (2010). New insights into S2P signaling cascades: regulation, variation, and conservation. Protein science : a publication of the Protein Society *19*, 2015-2030.
Chin, J., Palop, J.J., Puolivali, J., Massaro, C., Bien-Ly, N., Gerstein, H., Scearce-Levie, K., Masliah, E., and Mucke, L. (2005). Fyn kinase induces synaptic and cognitive impairments in a transgenic mouse model of Alzheimer's disease. The Journal of neuroscience : the official journal of the Society for Neuroscience *25*, 9694-9703.
Citron, M., Oltersdorf, T., Haass, C., McConlogue, L., Hung, A.Y., Seubert, P., Vigo-Pelfrey, C., Lieberburg, I., and Selkoe, D.J. (1992). Mutation of the beta-amyloid precursor protein in familial Alzheimer's disease increases beta-protein production. Nature *360*, 672-674.
Corder, E.H., Saunders, A.M., Strittmatter, W.J., Schmechel, D.E., Gaskell, P.C., Small, G.W., Roses, A.D., Haines, J.L., and Pericak-Vance, M.A. (1993). Gene dose of apolipoprotein E type 4 allele and the risk of Alzheimer's disease in late onset families. Science *261*, 921-923.
Cynis, H., Scheel, E., Saido, T.C., Schilling, S., and Demuth, H.U. (2008). Amyloidogenic processing of amyloid precursor protein: evidence of a pivotal role of glutaminyl cyclase in generation of pyroglutamate-modified amyloid-beta. Biochemistry *47*, 7405-7413.
Dahlgren, K.N., Manelli, A.M., Stine, W.B., Jr., Baker, L.K., Krafft, G.A., and LaDu, M.J. (2002). Oligomeric and fibrillar species of amyloid-beta peptides differentially affect neuronal viability. The Journal of biological chemistry *277*, 32046-32053.
Davies, P., and Maloney, A.J. (1976). Selective loss of central cholinergic neurons in Alzheimer's disease. Lancet *2*, 1403.
De Strooper, B., Annaert, W., Cupers, P., Saftig, P., Craessaerts, K., Mumm, J.S., Schroeter, E.H., Schrijvers, V., Wolfe, M.S., Ray, W.J.*, et al.* (1999). A presenilin-1-dependent gamma-secretase-like protease mediates release of Notch intracellular domain. Nature *398*, 518-522.
De Strooper, B., Saftig, P., Craessaerts, K., Vanderstichele, H., Guhde, G., Annaert, W., Von Figura, K., and Van Leuven, F. (1998). Deficiency of presenilin-1 inhibits the normal cleavage of amyloid precursor protein. Nature *391*, 387-390.
DeBose-Boyd, R.A., Brown, M.S., Li, W.P., Nohturfft, A., Goldstein, J.L., and Espenshade, P.J. (1999). Transport-dependent proteolysis of SREBP: relocation of site-1 protease from Golgi to ER obviates the need for SREBP transport to Golgi. Cell *99*, 703-712.
Demuro, A., Mina, E., Kayed, R., Milton, S.C., Parker, I., and Glabe, C.G. (2005). Calcium dysregulation and membrane disruption as a ubiquitous neurotoxic mechanism of soluble amyloid oligomers. The Journal of biological chemistry *280*, 17294-17300.
Demyanenko, G.P., Schachner, M., Anton, E., Schmid, R., Feng, G., Sanes, J., and Maness, P.F. (2004). Close homolog of L1 modulates area-specific neuronal positioning and dendrite orientation in the cerebral cortex. Neuron *44*, 423-437.
Demyanenko, G.P., Tsai, A.Y., and Maness, P.F. (1999). Abnormalities in neuronal process extension, hippocampal development, and the ventricular system of L1 knockout mice. The Journal of neuroscience : the official journal of the Society for Neuroscience *19*, 4907-4920.
Dettmer, U., Kuhn, P.H., Abou-Ajram, C., Lichtenthaler, S.F., Kruger, M., Kremmer, E., Haass, C., and Haffner, C. (2010). Transmembrane protein 147 (TMEM147) is a novel

component of the Nicalin-NOMO protein complex. The Journal of biological chemistry *285*, 26174-26181.
Devaraj, N.K., Weissleder, R., and Hilderbrand, S.A. (2008). Tetrazine-based cycloadditions: application to pretargeted live cell imaging. Bioconjugate chemistry *19*, 2297-2299.
Dominguez, D., Tournoy, J., Hartmann, D., Huth, T., Cryns, K., Deforce, S., Serneels, L., Camacho, I.E., Marjaux, E., Craessaerts, K.*, et al.* (2005). Phenotypic and biochemical analyses of BACE1- and BACE2-deficient mice. The Journal of biological chemistry *280*, 30797-30806.
Dommerholt, J., Schmidt, S., Temming, R., Hendriks, L.J., Rutjes, F.P., van Hest, J.C., Lefeber, D.J., Friedl, P., and van Delft, F.L. (2010). Readily accessible bicyclononynes for bioorthogonal labeling and three-dimensional imaging of living cells. Angew Chem Int Ed Engl *49*, 9422-9425.
Donello, J.E., Loeb, J.E., and Hope, T.J. (1998). Woodchuck hepatitis virus contains a tripartite posttranscriptional regulatory element. Journal of virology *72*, 5085-5092.
Dovey, H.F., John, V., Anderson, J.P., Chen, L.Z., de Saint Andrieu, P., Fang, L.Y., Freedman, S.B., Folmer, B., Goldbach, E., Holsztynska, E.J.*, et al.* (2001). Functional gamma-secretase inhibitors reduce beta-amyloid peptide levels in brain. Journal of neurochemistry *76*, 173-181.
Dube, D.H., Prescher, J.A., Quang, C.N., and Bertozzi, C.R. (2006). Probing mucin-type O-linked glycosylation in living animals. Proceedings of the National Academy of Sciences of the United States of America *103*, 4819-4824.
Edbauer, D., Winkler, E., Regula, J.T., Pesold, B., Steiner, H., and Haass, C. (2003). Reconstitution of gamma-secretase activity. Nature cell biology *5*, 486-488.
Eggert, S., Paliga, K., Soba, P., Evin, G., Masters, C.L., Weidemann, A., and Beyreuther, K. (2004). The proteolytic processing of the amyloid precursor protein gene family members APLP-1 and APLP-2 involves alpha-, beta-, gamma-, and epsilon-like cleavages: modulation of APLP-1 processing by n-glycosylation. The Journal of biological chemistry *279*, 18146-18156.
Endres, K., and Fahrenholz, F. (2011). Regulation of alpha-secretase ADAM10 expression and activity. Experimental brain research Experimentelle Hirnforschung Experimentation cerebrale.
Ertekin-Taner, N. (2007). Genetics of Alzheimer's disease: a centennial review. Neurologic clinics *25*, 611-667, v.
Esch, F.S., Keim, P.S., Beattie, E.C., Blacher, R.W., Culwell, A.R., Oltersdorf, T., McClure, D., and Ward, P.J. (1990). Cleavage of amyloid beta peptide during constitutive processing of its precursor. Science *248*, 1122-1124.
Esengil, H., Chang, V., Mich, J.K., and Chen, J.K. (2007). Small-molecule regulation of zebrafish gene expression. Nature chemical biology *3*, 154-155.
Esler, W.P., Kimberly, W.T., Ostaszewski, B.L., Diehl, T.S., Moore, C.L., Tsai, J.Y., Rahmati, T., Xia, W., Selkoe, D.J., and Wolfe, M.S. (2000). Transition-state analogue inhibitors of gamma-secretase bind directly to presenilin-1. Nature cell biology *2*, 428-434.
Esterhazy, D., Stutzer, I., Wang, H., Rechsteiner, M.P., Beauchamp, J., Dobeli, H., Hilpert, H., Matile, H., Prummer, M., Schmidt, A.*, et al.* (2011). Bace2 is a beta cell-enriched protease that regulates pancreatic beta cell function and mass. Cell metabolism *14*, 365-377.
Eto, K., Huet, C., Tarui, T., Kupriyanov, S., Liu, H.Z., Puzon-McLaughlin, W., Zhang, X.P., Sheppard, D., Engvall, E., and Takada, Y. (2002). Functional classification of ADAMs based on a conserved motif for binding to integrin alpha 9beta 1: implications for sperm-egg binding and other cell interactions. The Journal of biological chemistry *277*, 17804-17810.
Ferri, C.P., Prince, M., Brayne, C., Brodaty, H., Fratiglioni, L., Ganguli, M., Hall, K., Hasegawa, K., Hendrie, H., Huang, Y.*, et al.* (2005). Global prevalence of dementia: a Delphi consensus study. Lancet *366*, 2112-2117.

Fluhrer, R., Grammer, G., Israel, L., Condron, M.M., Haffner, C., Friedmann, E., Bohland, C., Imhof, A., Martoglio, B., Teplow, D.B.*, et al.* (2006). A gamma-secretase-like intramembrane cleavage of TNFalpha by the GxGD aspartyl protease SPPL2b. Nature cell biology *8*, 894-896.
Fluhrer, R., and Haass, C. (2007). Signal peptide peptidases and gamma-secretase: cousins of the same protease family? Neuro-degenerative diseases *4*, 112-116.
Fluhrer, R., Steiner, H., and Haass, C. (2009). Intramembrane proteolysis by signal peptide peptidases: a comparative discussion of GXGD-type aspartyl proteases. The Journal of biological chemistry *284*, 13975-13979.
Francis, R., McGrath, G., Zhang, J., Ruddy, D.A., Sym, M., Apfeld, J., Nicoll, M., Maxwell, M., Hai, B., Ellis, M.C.*, et al.* (2002). aph-1 and pen-2 are required for Notch pathway signaling, gamma-secretase cleavage of betaAPP, and presenilin protein accumulation. Developmental cell *3*, 85-97.
Freeman, M. (2009). Rhomboids: 7 years of a new protease family. Seminars in cell & developmental biology *20*, 231-239.
Friedmann, E., Hauben, E., Maylandt, K., Schleeger, S., Vreugde, S., Lichtenthaler, S.F., Kuhn, P.H., Stauffer, D., Rovelli, G., and Martoglio, B. (2006). SPPL2a and SPPL2b promote intramembrane proteolysis of TNFalpha in activated dendritic cells to trigger IL-12 production. Nature cell biology *8*, 843-848.
Gallyas, F. (1971). Silver staining of Alzheimer's neurofibrillary changes by means of physical development. Acta morphologica Academiae Scientiarum Hungaricae *19*, 1-8.
Ghiso, J., Matsubara, E., Koudinov, A., Choi-Miura, N.H., Tomita, M., Wisniewski, T., and Frangione, B. (1993). The cerebrospinal-fluid soluble form of Alzheimer's amyloid beta is complexed to SP-40,40 (apolipoprotein J), an inhibitor of the complement membrane-attack complex. The Biochemical journal *293 (Pt 1)*, 27-30.
Gibb, D.R., El Shikh, M., Kang, D.J., Rowe, W.J., El Sayed, R., Cichy, J., Yagita, H., Tew, J.G., Dempsey, P.J., Crawford, H.C.*, et al.* (2010). ADAM10 is essential for Notch2-dependent marginal zone B cell development and CD23 cleavage in vivo. The Journal of experimental medicine *207*, 623-635.
Gibb, D.R., Saleem, S.J., Chaimowitz, N.S., Mathews, J., and Conrad, D.H. (2011). The emergence of ADAM10 as a regulator of lymphocyte development and autoimmunity. Molecular immunology *48*, 1319-1327.
Glenner, G.G., and Wong, C.W. (1984). Alzheimer's disease: initial report of the purification and characterization of a novel cerebrovascular amyloid protein. Biochemical and biophysical research communications *120*, 885-890.
Goate, A., Chartier-Harlin, M.C., Mullan, M., Brown, J., Crawford, F., Fidani, L., Giuffra, L., Haynes, A., Irving, N., James, L.*, et al.* (1991). Segregation of a missense mutation in the amyloid precursor protein gene with familial Alzheimer's disease. Nature *349*, 704-706.
Goedert, M., Wischik, C.M., Crowther, R.A., Walker, J.E., and Klug, A. (1988). Cloning and sequencing of the cDNA encoding a core protein of the paired helical filament of Alzheimer disease: identification as the microtubule-associated protein tau. Proceedings of the National Academy of Sciences of the United States of America *85*, 4051-4055.
Golabek, A., Marques, M.A., Lalowski, M., and Wisniewski, T. (1995). Amyloid beta binding proteins in vitro and in normal human cerebrospinal fluid. Neuroscience letters *191*, 79-82.
Golde, T.E., Estus, S., Younkin, L.H., Selkoe, D.J., and Younkin, S.G. (1992). Processing of the amyloid protein precursor to potentially amyloidogenic derivatives. Science *255*, 728-730.
Goll, M.G., Anderson, R., Stainier, D.Y., Spradling, A.C., and Halpern, M.E. (2009). Transcriptional silencing and reactivation in transgenic zebrafish. Genetics *182*, 747-755.
Green, R.C., Schneider, L.S., Amato, D.A., Beelen, A.P., Wilcock, G., Swabb, E.A., and Zavitz, K.H. (2009). Effect of tarenflurbil on cognitive decline and activities of daily

living in patients with mild Alzheimer disease: a randomized controlled trial. JAMA : the journal of the American Medical Association *302*, 2557-2564.
Gu, C., and Gu, Y. (2011). Clustering and activity tuning of Kv1 channels in myelinated hippocampal axons. The Journal of biological chemistry *286*, 25835-25847.
Gunnersen, J.M., Kim, M.H., Fuller, S.J., De Silva, M., Britto, J.M., Hammond, V.E., Davies, P.J., Petrou, S., Faber, E.S., Sah, P.*, et al.* (2007). Sez-6 proteins affect dendritic arborization patterns and excitability of cortical pyramidal neurons. Neuron *56*, 621-639.
Haass, C., Koo, E.H., Mellon, A., Hung, A.Y., and Selkoe, D.J. (1992a). Targeting of cell-surface beta-amyloid precursor protein to lysosomes: alternative processing into amyloid-bearing fragments. Nature *357*, 500-503.
Haass, C., Lemere, C.A., Capell, A., Citron, M., Seubert, P., Schenk, D., Lannfelt, L., and Selkoe, D.J. (1995). The Swedish mutation causes early-onset Alzheimer's disease by beta-secretase cleavage within the secretory pathway. Nature medicine *1*, 1291-1296.
Haass, C., Schlossmacher, M.G., Hung, A.Y., Vigo-Pelfrey, C., Mellon, A., Ostaszewski, B.L., Lieberburg, I., Koo, E.H., Schenk, D., Teplow, D.B.*, et al.* (1992b). Amyloid beta-peptide is produced by cultured cells during normal metabolism. Nature *359*, 322-325.
Haass, C., and Selkoe, D.J. (1993). Cellular processing of beta-amyloid precursor protein and the genesis of amyloid beta-peptide. Cell *75*, 1039-1042.
Haass, C., and Selkoe, D.J. (2007). Soluble protein oligomers in neurodegeneration: lessons from the Alzheimer's amyloid beta-peptide. Nature reviews Molecular cell biology *8*, 101-112.
Hadler-Olsen, E., Fadnes, B., Sylte, I., Uhlin-Hansen, L., and Winberg, J.O. (2011). Regulation of matrix metalloproteinase activity in health and disease. The FEBS journal *278*, 28-45.
Hang, H.C., Yu, C., Kato, D.L., and Bertozzi, C.R. (2003). A metabolic labeling approach toward proteomic analysis of mucin-type O-linked glycosylation. Proceedings of the National Academy of Sciences of the United States of America *100*, 14846-14851.
Hanson, S.R., Hsu, T.L., Weerapana, E., Kishikawa, K., Simon, G.M., Cravatt, B.F., and Wong, C.H. (2007). Tailored glycoproteomics and glycan site mapping using saccharide-selective bioorthogonal probes. Journal of the American Chemical Society *129*, 7266-7267.
Hardy, J., and Selkoe, D.J. (2002). The amyloid hypothesis of Alzheimer's disease: progress and problems on the road to therapeutics. Science *297*, 353-356.
Hardy, J.A., and Higgins, G.A. (1992). Alzheimer's disease: the amyloid cascade hypothesis. Science *256*, 184-185.
Harold, D., Abraham, R., Hollingworth, P., Sims, R., Gerrish, A., Hamshere, M.L., Pahwa, J.S., Moskvina, V., Dowzell, K., Williams, A.*, et al.* (2009). Genome-wide association study identifies variants at CLU and PICALM associated with Alzheimer's disease. Nature genetics *41*, 1088-1093.
Harrison, S.M., Harper, A.J., Hawkins, J., Duddy, G., Grau, E., Pugh, P.L., Winter, P.H., Shilliam, C.S., Hughes, Z.A., Dawson, L.A.*, et al.* (2003). BACE1 (beta-secretase) transgenic and knockout mice: identification of neurochemical deficits and behavioral changes. Molecular and cellular neurosciences *24*, 646-655.
Hartmann, D., de Strooper, B., Serneels, L., Craessaerts, K., Herreman, A., Annaert, W., Umans, L., Lubke, T., Lena Illert, A., von Figura, K.*, et al.* (2002). The disintegrin/metalloprotease ADAM 10 is essential for Notch signalling but not for alpha-secretase activity in fibroblasts. Human molecular genetics *11*, 2615-2624.
Hartmann, T., Bieger, S.C., Bruhl, B., Tienari, P.J., Ida, N., Allsop, D., Roberts, G.W., Masters, C.L., Dotti, C.G., Unsicker, K.*, et al.* (1997). Distinct sites of intracellular production for Alzheimer's disease A beta40/42 amyloid peptides. Nature medicine *3*, 1016-1020.

Heber, S., Herms, J., Gajic, V., Hainfellner, J., Aguzzi, A., Rulicke, T., von Kretzschmar, H., von Koch, C., Sisodia, S., Tremml, P.*, et al.* (2000). Mice with combined gene knock-outs reveal essential and partially redundant functions of amyloid precursor protein family members. The Journal of neuroscience : the official journal of the Society for Neuroscience *20*, 7951-7963.
Hemming, M.L., Elias, J.E., Gygi, S.P., and Selkoe, D.J. (2009). Identification of beta-secretase (BACE1) substrates using quantitative proteomics. PloS one *4*, e8477.
Herms, J., Anliker, B., Heber, S., Ring, S., Fuhrmann, M., Kretzschmar, H., Sisodia, S., and Muller, U. (2004). Cortical dysplasia resembling human type 2 lissencephaly in mice lacking all three APP family members. The EMBO journal *23*, 4106-4115.
Higgins, G.A., and Jacobsen, H. (2003). Transgenic mouse models of Alzheimer's disease: phenotype and application. Behavioural pharmacology *14*, 419-438.
Hitt, B.D., Jaramillo, T.C., Chetkovich, D.M., and Vassar, R. (2010). BACE1-/- mice exhibit seizure activity that does not correlate with sodium channel level or axonal localization. Molecular neurodegeneration *5*, 31.
Hogl, S., Kuhn, P.H., Colombo, A., and Lichtenthaler, S.F. (2011). Determination of the proteolytic cleavage sites of the amyloid precursor-like protein 2 by the proteases ADAM10, BACE1 and gamma-secretase. PloS one *6*, e21337.
Hollingworth, P., Harold, D., Sims, R., Gerrish, A., Lambert, J.C., Carrasquillo, M.M., Abraham, R., Hamshere, M.L., Pahwa, J.S., Moskvina, V.*, et al.* (2011). Common variants at ABCA7, MS4A6A/MS4A4E, EPHA1, CD33 and CD2AP are associated with Alzheimer's disease. Nature genetics *43*, 429-435.
Hook, V., Funkelstein, L., Lu, D., Bark, S., Wegrzyn, J., and Hwang, S.R. (2008). Proteases for processing proneuropeptides into peptide neurotransmitters and hormones. Annual review of pharmacology and toxicology *48*, 393-423.
Hosoda, R., Saido, T.C., Otvos, L., Jr., Arai, T., Mann, D.M., Lee, V.M., Trojanowski, J.Q., and Iwatsubo, T. (1998). Quantification of modified amyloid beta peptides in Alzheimer disease and Down syndrome brains. Journal of neuropathology and experimental neurology *57*, 1089-1095.
Hu, X., Hicks, C.W., He, W., Wong, P., Macklin, W.B., Trapp, B.D., and Yan, R. (2006). Bace1 modulates myelination in the central and peripheral nervous system. Nature neuroscience *9*, 1520-1525.
Hu, X., Zhou, X., He, W., Yang, J., Xiong, W., Wong, P., Wilson, C.G., and Yan, R. (2010). BACE1 deficiency causes altered neuronal activity and neurodegeneration. The Journal of neuroscience : the official journal of the Society for Neuroscience *30*, 8819-8829.
Huse, J.T., Liu, K., Pijak, D.S., Carlin, D., Lee, V.M., and Doms, R.W. (2002). Beta-secretase processing in the trans-Golgi network preferentially generates truncated amyloid species that accumulate in Alzheimer's disease brain. The Journal of biological chemistry *277*, 16278-16284.
Huse, J.T., Pijak, D.S., Leslie, G.J., Lee, V.M., and Doms, R.W. (2000). Maturation and endosomal targeting of beta-site amyloid precursor protein-cleaving enzyme. The Alzheimer's disease beta-secretase. The Journal of biological chemistry *275*, 33729-33737.
Iba, K., Albrechtsen, R., Gilpin, B., Frohlich, C., Loechel, F., Zolkiewska, A., Ishiguro, K., Kojima, T., Liu, W., Langford, J.K.*, et al.* (2000). The cysteine-rich domain of human ADAM 12 supports cell adhesion through syndecans and triggers signaling events that lead to beta1 integrin-dependent cell spreading. The Journal of cell biology *149*, 1143-1156.
Ida, N., Hartmann, T., Pantel, J., Schroder, J., Zerfass, R., Forstl, H., Sandbrink, R., Masters, C.L., and Beyreuther, K. (1996). Analysis of heterogeneous A4 peptides in human cerebrospinal fluid and blood by a newly developed sensitive Western blot assay. The Journal of biological chemistry *271*, 22908-22914.
Iqbal, K., Grundke-Iqbal, I., Zaidi, T., Merz, P.A., Wen, G.Y., Shaikh, S.S., Wisniewski, H.M., Alafuzoff, I., and Winblad, B. (1986). Defective brain microtubule assembly in Alzheimer's disease. Lancet *2*, 421-426.

Ittner, L.M., Ke, Y.D., Delerue, F., Bi, M., Gladbach, A., van Eersel, J., Wolfing, H., Chieng, B.C., Christie, M.J., Napier, I.A*., et al.* (2010). Dendritic function of tau mediates amyloid-beta toxicity in Alzheimer's disease mouse models. Cell *142*, 387-397.

Iwatsubo, T., Saido, T.C., Mann, D.M., Lee, V.M., and Trojanowski, J.Q. (1996). Full-length amyloid-beta (1-42(43)) and amino-terminally modified and truncated amyloid-beta 42(43) deposit in diffuse plaques. The American journal of pathology *149*, 1823-1830.

Jackson, A.L., and Linsley, P.S. (2010). Recognizing and avoiding siRNA off-target effects for target identification and therapeutic application. Nature reviews Drug discovery *9*, 57-67.

Jefferson, T., Causevic, M., auf dem Keller, U., Schilling, O., Isbert, S., Geyer, R., Maier, W., Tschickardt, S., Jumpertz, T., Weggen, S*., et al.* (2011). Metalloprotease meprin beta generates nontoxic N-terminal amyloid precursor protein fragments in vivo. The Journal of biological chemistry *286*, 27741-27750.

Jervis, G.A. (1948). Early senile dementia in mongoloid idiocy. The American journal of psychiatry *105*, 102-106.

Jewett, J.C., and Bertozzi, C.R. (2010). Cu-free click cycloaddition reactions in chemical biology. Chemical Society reviews *39*, 1272-1279.

Jewett, J.C., and Bertozzi, C.R. (2011). Synthesis of a fluorogenic cyclooctyne activated by Cu-free click chemistry. Organic letters *13*, 5937-5939.

Jiang, Q., Lee, C.Y., Mandrekar, S., Wilkinson, B., Cramer, P., Zelcer, N., Mann, K., Lamb, B., Willson, T.M., Collins, J.L*., et al.* (2008). ApoE promotes the proteolytic degradation of Abeta. Neuron *58*, 681-693.

Jin, M., Shepardson, N., Yang, T., Chen, G., Walsh, D., and Selkoe, D.J. (2011). Soluble amyloid beta-protein dimers isolated from Alzheimer cortex directly induce Tau hyperphosphorylation and neuritic degeneration. Proceedings of the National Academy of Sciences of the United States of America *108*, 5819-5824.

Jorissen, E., Prox, J., Bernreuther, C., Weber, S., Schwanbeck, R., Serneels, L., Snellinx, A., Craessaerts, K., Thathiah, A., Tesseur, I*., et al.* (2010). The disintegrin/metalloproteinase ADAM10 is essential for the establishment of the brain cortex. The Journal of neuroscience : the official journal of the Society for Neuroscience *30*, 4833-4844.

Kamal, A., Almenar-Queralt, A., LeBlanc, J.F., Roberts, E.A., and Goldstein, L.S. (2001). Kinesin-mediated axonal transport of a membrane compartment containing beta-secretase and presenilin-1 requires APP. Nature *414*, 643-648.

Kang, J., Lemaire, H.G., Unterbeck, A., Salbaum, J.M., Masters, C.L., Grzeschik, K.H., Multhaup, G., Beyreuther, K., and Muller-Hill, B. (1987). The precursor of Alzheimer's disease amyloid A4 protein resembles a cell-surface receptor. Nature *325*, 733-736.

Karra, D., and Dahm, R. (2010). Transfection techniques for neuronal cells. The Journal of neuroscience : the official journal of the Society for Neuroscience *30*, 6171-6177.

Kayed, R., Head, E., Thompson, J.L., McIntire, T.M., Milton, S.C., Cotman, C.W., and Glabe, C.G. (2003). Common structure of soluble amyloid oligomers implies common mechanism of pathogenesis. Science *300*, 486-489.

Kim, D.Y., Carey, B.W., Wang, H., Ingano, L.A., Binshtok, A.M., Wertz, M.H., Pettingell, W.H., He, P., Lee, V.M., Woolf, C.J*., et al.* (2007). BACE1 regulates voltage-gated sodium channels and neuronal activity. Nature cell biology *9*, 755-764.

Kitazume, S., Tachida, Y., Oka, R., Kotani, N., Ogawa, K., Suzuki, M., Dohmae, N., Takio, K., Saido, T.C., and Hashimoto, Y. (2003). Characterization of alpha 2,6-sialyltransferase cleavage by Alzheimer's beta -secretase (BACE1). The Journal of biological chemistry *278*, 14865-14871.

Kleifeld, O., Doucet, A., auf dem Keller, U., Prudova, A., Schilling, O., Kainthan, R.K., Starr, A.E., Foster, L.J., Kizhakkedathu, J.N., and Overall, C.M. (2010). Isotopic labeling of terminal amines in complex samples identifies protein N-termini and protease cleavage products. Nature biotechnology *28*, 281-288.

Koike, H., Tomioka, S., Sorimachi, H., Saido, T.C., Maruyama, K., Okuyama, A., Fujisawa-Sehara, A., Ohno, S., Suzuki, K., and Ishiura, S. (1999). Membrane-anchored metalloprotease MDC9 has an alpha-secretase activity responsible for processing the amyloid precursor protein. The Biochemical journal *343 Pt 2*, 371-375.
Kojima, N., Ishibashi, H., Obata, K., and Kandel, E.R. (1998). Higher seizure susceptibility and enhanced tyrosine phosphorylation of N-methyl-D-aspartate receptor subunit 2B in fyn transgenic mice. Learn Mem *5*, 429-445.
Kuhn, P.H., Marjaux, E., Imhof, A., De Strooper, B., Haass, C., and Lichtenthaler, S.F. (2007). Regulated intramembrane proteolysis of the interleukin-1 receptor II by alpha-, beta-, and gamma-secretase. The Journal of biological chemistry *282*, 11982-11995.
Kuhn, P.H., Wang, H., Dislich, B., Colombo, A., Zeitschel, U., Ellwart, J.W., Kremmer, E., Rossner, S., and Lichtenthaler, S.F. (2010). ADAM10 is the physiologically relevant, constitutive alpha-secretase of the amyloid precursor protein in primary neurons. The EMBO journal *29*, 3020-3032.
Kukar, T., and Golde, T.E. (2008). Possible mechanisms of action of NSAIDs and related compounds that modulate gamma-secretase cleavage. Current topics in medicinal chemistry *8*, 47-53.
Laird, F.M., Cai, H., Savonenko, A.V., Farah, M.H., He, K., Melnikova, T., Wen, H., Chiang, H.C., Xu, G., Koliatsos, V.E*., et al.* (2005). BACE1, a major determinant of selective vulnerability of the brain to amyloid-beta amyloidogenesis, is essential for cognitive, emotional, and synaptic functions. The Journal of neuroscience : the official journal of the Society for Neuroscience *25*, 11693-11709.
Lambert, J.C., Heath, S., Even, G., Campion, D., Sleegers, K., Hiltunen, M., Combarros, O., Zelenika, D., Bullido, M.J., Tavernier, B*., et al.* (2009). Genome-wide association study identifies variants at CLU and CR1 associated with Alzheimer's disease. Nature genetics *41*, 1094-1099.
Lambert, M.P., Barlow, A.K., Chromy, B.A., Edwards, C., Freed, R., Liosatos, M., Morgan, T.E., Rozovsky, I., Trommer, B., Viola, K.L*., et al.* (1998). Diffusible, nonfibrillar ligands derived from Abeta1-42 are potent central nervous system neurotoxins. Proceedings of the National Academy of Sciences of the United States of America *95*, 6448-6453.
Lammich, S., Kojro, E., Postina, R., Gilbert, S., Pfeiffer, R., Jasionowski, M., Haass, C., and Fahrenholz, F. (1999). Constitutive and regulated alpha-secretase cleavage of Alzheimer's amyloid precursor protein by a disintegrin metalloprotease. Proceedings of the National Academy of Sciences of the United States of America *96*, 3922-3927.
Laughlin, S.T., Baskin, J.M., Amacher, S.L., and Bertozzi, C.R. (2008). In vivo imaging of membrane-associated glycans in developing zebrafish. Science *320*, 664-667.
Lazarov, O., Morfini, G.A., Lee, E.B., Farah, M.H., Szodorai, A., DeBoer, S.R., Koliatsos, V.E., Kins, S., Lee, V.M., Wong, P.C*., et al.* (2005). Axonal transport, amyloid precursor protein, kinesin-1, and the processing apparatus: revisited. The Journal of neuroscience : the official journal of the Society for Neuroscience *25*, 2386-2395.
Lazarov, V.K., Fraering, P.C., Ye, W., Wolfe, M.S., Selkoe, D.J., and Li, H. (2006). Electron microscopic structure of purified, active gamma-secretase reveals an aqueous intramembrane chamber and two pores. Proceedings of the National Academy of Sciences of the United States of America *103*, 6889-6894.
Levy-Lahad, E., Wasco, W., Poorkaj, P., Romano, D.M., Oshima, J., Pettingell, W.H., Yu, C.E., Jondro, P.D., Schmidt, S.D., Wang, K*., et al.* (1995a). Candidate gene for the chromosome 1 familial Alzheimer's disease locus. Science *269*, 973-977.
Levy-Lahad, E., Wijsman, E.M., Nemens, E., Anderson, L., Goddard, K.A., Weber, J.L., Bird, T.D., and Schellenberg, G.D. (1995b). A familial Alzheimer's disease locus on chromosome 1. Science *269*, 970-973.
Li, Q., and Sudhof, T.C. (2004). Cleavage of amyloid-beta precursor protein and amyloid-beta precursor-like protein by BACE 1. The Journal of biological chemistry *279*, 10542-10550.

Lichtenthaler, S.F., Dominguez, D.I., Westmeyer, G.G., Reiss, K., Haass, C., Saftig, P., De Strooper, B., and Seed, B. (2003). The cell adhesion protein P-selectin glycoprotein ligand-1 is a substrate for the aspartyl protease BACE1. The Journal of biological chemistry *278*, 48713-48719.
Lichtenthaler, S.F., Haass, C., and Steiner, H. (2011). Regulated intramembrane proteolysis--lessons from amyloid precursor protein processing. Journal of neurochemistry *117*, 779-796.
Liu, B., Wang, S., Brenner, M., Paton, J.F., and Kasparov, S. (2008). Enhancement of cell-specific transgene expression from a Tet-Off regulatory system using a transcriptional amplification strategy in the rat brain. The journal of gene medicine *10*, 583-592.
Loffler, J., and Huber, G. (1992). Beta-amyloid precursor protein isoforms in various rat brain regions and during brain development. Journal of neurochemistry *59*, 1316-1324.
Luchansky, S.J., Argade, S., Hayes, B.K., and Bertozzi, C.R. (2004). Metabolic functionalization of recombinant glycoproteins. Biochemistry *43*, 12358-12366.
Luo, X., and Yan, R. (2010). Inhibition of BACE1 for therapeutic use in Alzheimer's disease. International journal of clinical and experimental pathology *3*, 618-628.
Luo, Y., Bolon, B., Kahn, S., Bennett, B.D., Babu-Khan, S., Denis, P., Fan, W., Kha, H., Zhang, J., Gong, Y*., et al.* (2001). Mice deficient in BACE1, the Alzheimer's beta-secretase, have normal phenotype and abolished beta-amyloid generation. Nature neuroscience *4*, 231-232.
Ma, H., Lesne, S., Kotilinek, L., Steidl-Nichols, J.V., Sherman, M., Younkin, L., Younkin, S., Forster, C., Sergeant, N., Delacourte, A*., et al.* (2007). Involvement of beta-site APP cleaving enzyme 1 (BACE1) in amyloid precursor protein-mediated enhancement of memory and activity-dependent synaptic plasticity. Proceedings of the National Academy of Sciences of the United States of America *104*, 8167-8172.
Mahley, R.W. (1988). Apolipoprotein E: cholesterol transport protein with expanding role in cell biology. Science *240*, 622-630.
Maier, T., Drapal, N., Thanbichler, M., and Bock, A. (1998). Strep-tag II affinity purification: an approach to study intermediates of metalloenzyme biosynthesis. Analytical biochemistry *259*, 68-73.
Marcade, M., Bourdin, J., Loiseau, N., Peillon, H., Rayer, A., Drouin, D., Schweighoffer, F., and Desire, L. (2008). Etazolate, a neuroprotective drug linking GABA(A) receptor pharmacology to amyloid precursor protein processing. Journal of neurochemistry *106*, 392-404.
Maretzky, T., Schulte, M., Ludwig, A., Rose-John, S., Blobel, C., Hartmann, D., Altevogt, P., Saftig, P., and Reiss, K. (2005). L1 is sequentially processed by two differently activated metalloproteases and presenilin/gamma-secretase and regulates neural cell adhesion, cell migration, and neurite outgrowth. Molecular and cellular biology *25*, 9040-9053.
Martin, B.R., and Cravatt, B.F. (2009). Large-scale profiling of protein palmitoylation in mammalian cells. Nature methods *6*, 135-138.
Martin, L., Fluhrer, R., Reiss, K., Kremmer, E., Saftig, P., and Haass, C. (2008). Regulated intramembrane proteolysis of Bri2 (Itm2b) by ADAM10 and SPPL2a/SPPL2b. The Journal of biological chemistry *283*, 1644-1652.
Masters, C.L., Multhaup, G., Simms, G., Pottgiesser, J., Martins, R.N., and Beyreuther, K. (1985a). Neuronal origin of a cerebral amyloid: neurofibrillary tangles of Alzheimer's disease contain the same protein as the amyloid of plaque cores and blood vessels. The EMBO journal *4*, 2757-2763.
Masters, C.L., Simms, G., Weinman, N.A., Multhaup, G., McDonald, B.L., and Beyreuther, K. (1985b). Amyloid plaque core protein in Alzheimer disease and Down syndrome. Proceedings of the National Academy of Sciences of the United States of America *82*, 4245-4249.
May, P.C., Dean, R.A., Lowe, S.L., Martenyi, F., Sheehan, S.M., Boggs, L.N., Monk, S.A., Mathes, B.M., Mergott, D.J., Watson, B.M*., et al.* (2011a). Robust Central Reduction of Amyloid-beta in Humans with an Orally Available, Non-Peptidic beta-

Secretase Inhibitor. The Journal of neuroscience : the official journal of the Society for Neuroscience *31*, 16507-16516.
May, P.C., Dean, R.A., Lowe, S.L., Martenyi, F., Sheehan, S.M., Boggs, L.N., Monk, S.A., Mathes, B.M., Mergott, D.J., Watson, B.M.*, et al.* (2011b). Robust central reduction of amyloid-beta in humans with an orally available, non-peptidic beta-secretase inhibitor. The Journal of neuroscience : the official journal of the Society for Neuroscience *31*, 16507-16516.
Miles, L.A., Wun, K.S., Crespi, G.A., Fodero-Tavoletti, M.T., Galatis, D., Bagley, C.J., Beyreuther, K., Masters, C.L., Cappai, R., McKinstry, W.J.*, et al.* (2008). Amyloid-beta-anti-amyloid-beta complex structure reveals an extended conformation in the immunodominant B-cell epitope. Journal of molecular biology *377*, 181-192.
Milla, M.E., Leesnitzer, M.A., Moss, M.L., Clay, W.C., Carter, H.L., Miller, A.B., Su, J.L., Lambert, M.H., Willard, D.H., Sheeley, D.M.*, et al.* (1999). Specific sequence elements are required for the expression of functional tumor necrosis factor-alpha-converting enzyme (TACE). The Journal of biological chemistry *274*, 30563-30570.
Miyazaki, T., Hashimoto, K., Uda, A., Sakagami, H., Nakamura, Y., Saito, S.Y., Nishi, M., Kume, H., Tohgo, A., Kaneko, I.*, et al.* (2006). Disturbance of cerebellar synaptic maturation in mutant mice lacking BSRPs, a novel brain-specific receptor-like protein family. FEBS letters *580*, 4057-4064.
Moss, M.L., Jin, S.L., Milla, M.E., Bickett, D.M., Burkhart, W., Carter, H.L., Chen, W.J., Clay, W.C., Didsbury, J.R., Hassler, D.*, et al.* (1997). Cloning of a disintegrin metalloproteinase that processes precursor tumour-necrosis factor-alpha. Nature *385*, 733-736.
Mullan, M., Crawford, F., Axelman, K., Houlden, H., Lilius, L., Winblad, B., and Lannfelt, L. (1992). A pathogenic mutation for probable Alzheimer's disease in the APP gene at the N-terminus of beta-amyloid. Nature genetics *1*, 345-347.
Muller, U., Cristina, N., Li, Z.W., Wolfer, D.P., Lipp, H.P., Rulicke, T., Brandner, S., Aguzzi, A., and Weissmann, C. (1994). Behavioral and anatomical deficits in mice homozygous for a modified beta-amyloid precursor protein gene. Cell *79*, 755-765.
Myers, R.H., Schaefer, E.J., Wilson, P.W., D'Agostino, R., Ordovas, J.M., Espino, A., Au, R., White, R.F., Knoefel, J.E., Cobb, J.L.*, et al.* (1996). Apolipoprotein E epsilon4 association with dementia in a population-based study: The Framingham study. Neurology *46*, 673-677.
Naj, A.C., Jun, G., Beecham, G.W., Wang, L.S., Vardarajan, B.N., Buros, J., Gallins, P.J., Buxbaum, J.D., Jarvik, G.P., Crane, P.K.*, et al.* (2011). Common variants at MS4A4/MS4A6E, CD2AP, CD33 and EPHA1 are associated with late-onset Alzheimer's disease. Nature genetics *43*, 436-441.
Naldini, L., Blomer, U., Gallay, P., Ory, D., Mulligan, R., Gage, F.H., Verma, I.M., and Trono, D. (1996). In vivo gene delivery and stable transduction of nondividing cells by a lentiviral vector. Science *272*, 263-267.
Naus, S., Richter, M., Wildeboer, D., Moss, M., Schachner, M., and Bartsch, J.W. (2004). Ectodomain shedding of the neural recognition molecule CHL1 by the metalloprotease-disintegrin ADAM8 promotes neurite outgrowth and suppresses neuronal cell death. The Journal of biological chemistry *279*, 16083-16090.
Nikolaev, A., McLaughlin, T., O'Leary, D.D., and Tessier-Lavigne, M. (2009). APP binds DR6 to trigger axon pruning and neuron death via distinct caspases. Nature *457*, 981-989.
Ning, X., Guo, J., Wolfert, M.A., and Boons, G.J. (2008). Visualizing metabolically labeled glycoconjugates of living cells by copper-free and fast huisgen cycloadditions. Angew Chem Int Ed Engl *47*, 2253-2255.
Nishitomi, K., Sakaguchi, G., Horikoshi, Y., Gray, A.J., Maeda, M., Hirata-Fukae, C., Becker, A.G., Hosono, M., Sakaguchi, I., Minami, S.S.*, et al.* (2006). BACE1 inhibition reduces endogenous Abeta and alters APP processing in wild-type mice. Journal of neurochemistry *99*, 1555-1563.

Nitsch, R.M., Slack, B.E., Wurtman, R.J., and Growdon, J.H. (1992). Release of Alzheimer amyloid precursor derivatives stimulated by activation of muscarinic acetylcholine receptors. Science *258*, 304-307.
Nordstedt, C., Gandy, S.E., Alafuzoff, I., Caporaso, G.L., Iverfeldt, K., Grebb, J.A., Winblad, B., and Greengard, P. (1991). Alzheimer beta/A4 amyloid precursor protein in human brain: aging-associated increases in holoprotein and in a proteolytic fragment. Proceedings of the National Academy of Sciences of the United States of America *88*, 8910-8914.
Norstrom, E.M., Zhang, C., Tanzi, R., and Sisodia, S.S. (2010). Identification of NEEP21 as a ss-amyloid precursor protein-interacting protein in vivo that modulates amyloidogenic processing in vitro. The Journal of neuroscience : the official journal of the Society for Neuroscience *30*, 15677-15685.
Osenkowski, P., Li, H., Ye, W., Li, D., Aeschbach, L., Fraering, P.C., Wolfe, M.S., and Selkoe, D.J. (2009). Cryoelectron microscopy structure of purified gamma-secretase at 12 A resolution. Journal of molecular biology *385*, 642-652.
Paquet, D., Bhat, R., Sydow, A., Mandelkow, E.M., Berg, S., Hellberg, S., Falting, J., Distel, M., Koster, R.W., Schmid, B.*, et al.* (2009). A zebrafish model of tauopathy allows in vivo imaging of neuronal cell death and drug evaluation. The Journal of clinical investigation *119*, 1382-1395.
Paterna, J.C., Moccetti, T., Mura, A., Feldon, J., and Bueler, H. (2000). Influence of promoter and WHV post-transcriptional regulatory element on AAV-mediated transgene expression in the rat brain. Gene therapy *7*, 1304-1311.
Peschon, J.J., Slack, J.L., Reddy, P., Stocking, K.L., Sunnarborg, S.W., Lee, D.C., Russell, W.E., Castner, B.J., Johnson, R.S., Fitzner, J.N.*, et al.* (1998). An essential role for ectodomain shedding in mammalian development. Science *282*, 1281-1284.
Poliak, S., Salomon, D., Elhanany, H., Sabanay, H., Kiernan, B., Pevny, L., Stewart, C.L., Xu, X., Chiu, S.Y., Shrager, P.*, et al.* (2003). Juxtaparanodal clustering of Shaker-like K+ channels in myelinated axons depends on Caspr2 and TAG-1. The Journal of cell biology *162*, 1149-1160.
Postina, R., Schroeder, A., Dewachter, I., Bohl, J., Schmitt, U., Kojro, E., Prinzen, C., Endres, K., Hiemke, C., Blessing, M.*, et al.* (2004). A disintegrin-metalloproteinase prevents amyloid plaque formation and hippocampal defects in an Alzheimer disease mouse model. The Journal of clinical investigation *113*, 1456-1464.
Prescher, J.A., Dube, D.H., and Bertozzi, C.R. (2004). Chemical remodelling of cell surfaces in living animals. Nature *430*, 873-877.
Puente, X.S., Sanchez, L.M., Overall, C.M., and Lopez-Otin, C. (2003). Human and mouse proteases: a comparative genomic approach. Nature reviews Genetics *4*, 544-558.
Rasool, C.G., Svendsen, C.N., and Selkoe, D.J. (1986). Neurofibrillary degeneration of cholinergic and noncholinergic neurons of the basal forebrain in Alzheimer's disease. Annals of neurology *20*, 482-488.
Reiss, K., Maretzky, T., Ludwig, A., Tousseyn, T., de Strooper, B., Hartmann, D., and Saftig, P. (2005). ADAM10 cleavage of N-cadherin and regulation of cell-cell adhesion and beta-catenin nuclear signalling. The EMBO journal *24*, 742-752.
Reiss, K., and Saftig, P. (2009). The "a disintegrin and metalloprotease" (ADAM) family of sheddases: physiological and cellular functions. Seminars in cell & developmental biology *20*, 126-137.
Reitz, C., Brayne, C., and Mayeux, R. (2011). Epidemiology of Alzheimer disease. Nature reviews Neurology *7*, 137-152.
Renzi, F., Zhang, X., Rice, W.J., Torres-Arancivia, C., Gomez-Llorente, Y., Diaz, R., Ahn, K., Yu, C., Li, Y.M., Sisodia, S.S.*, et al.* (2011). Structure of gamma-secretase and its trimeric pre-activation intermediate by single-particle electron microscopy. The Journal of biological chemistry *286*, 21440-21449.
Ring, S., Weyer, S.W., Kilian, S.B., Waldron, E., Pietrzik, C.U., Filippov, M.A., Herms, J., Buchholz, C., Eckman, C.B., Korte, M.*, et al.* (2007). The secreted beta-amyloid precursor protein ectodomain APPs alpha is sufficient to rescue the anatomical,

behavioral, and electrophysiological abnormalities of APP-deficient mice. The Journal of neuroscience : the official journal of the Society for Neuroscience *27*, 7817-7826.
Roberds, S.L., Anderson, J., Basi, G., Bienkowski, M.J., Branstetter, D.G., Chen, K.S., Freedman, S.B., Frigon, N.L., Games, D., Hu, K.*, et al.* (2001). BACE knockout mice are healthy despite lacking the primary beta-secretase activity in brain: implications for Alzheimer's disease therapeutics. Human molecular genetics *10*, 1317-1324.
Robert, S., Maillet, M., Morel, E., Launay, J.M., Fischmeister, R., Mercken, L., and Lezoualc'h, F. (2005). Regulation of the amyloid precursor protein ectodomain shedding by the 5-HT4 receptor and Epac. FEBS letters *579*, 1136-1142.
Rostovtsev, V.V., Green, L.G., Fokin, V.V., and Sharpless, K.B. (2002). A stepwise huisgen cycloaddition process: copper(I)-catalyzed regioselective "ligation" of azides and terminal alkynes. Angew Chem Int Ed Engl *41*, 2596-2599.
Ryan, S.D., Whitehead, S.N., Swayne, L.A., Moffat, T.C., Hou, W., Ethier, M., Bourgeois, A.J., Rashidian, J., Blanchard, A.P., Fraser, P.E.*, et al.* (2009). Amyloid-beta42 signals tau hyperphosphorylation and compromises neuronal viability by disrupting alkylacylglycerophosphocholine metabolism. Proceedings of the National Academy of Sciences of the United States of America *106*, 20936-20941.
Sadowski, I., Ma, J., Triezenberg, S., and Ptashne, M. (1988). GAL4-VP16 is an unusually potent transcriptional activator. Nature *335*, 563-564.
Sahin, U., Weskamp, G., Kelly, K., Zhou, H.M., Higashiyama, S., Peschon, J., Hartmann, D., Saftig, P., and Blobel, C.P. (2004). Distinct roles for ADAM10 and ADAM17 in ectodomain shedding of six EGFR ligands. The Journal of cell biology *164*, 769-779.
Saido, T.C., Yamao-Harigaya, W., Iwatsubo, T., and Kawashima, S. (1996). Amino- and carboxyl-terminal heterogeneity of beta-amyloid peptides deposited in human brain. Neuroscience letters *215*, 173-176.
Sala Frigerio, C., Fadeeva, J.V., Minogue, A.M., Citron, M., Van Leuven, F., Staufenbiel, M., Paganetti, P., Selkoe, D.J., and Walsh, D.M. (2010). beta-Secretase cleavage is not required for generation of the intracellular C-terminal domain of the amyloid precursor family of proteins. The FEBS journal *277*, 1503-1518.
Saxon, E., and Bertozzi, C.R. (2000). Cell surface engineering by a modified Staudinger reaction. Science *287*, 2007-2010.
Schagger, H., and von Jagow, G. (1987). Tricine-sodium dodecyl sulfate-polyacrylamide gel electrophoresis for the separation of proteins in the range from 1 to 100 kDa. Analytical biochemistry *166*, 368-379.
Schellenberg, G.D., Bird, T.D., Wijsman, E.M., Orr, H.T., Anderson, L., Nemens, E., White, J.A., Bonnycastle, L., Weber, J.L., Alonso, M.E.*, et al.* (1992). Genetic linkage evidence for a familial Alzheimer's disease locus on chromosome 14. Science *258*, 668-671.
Schilling, S., Zeitschel, U., Hoffmann, T., Heiser, U., Francke, M., Kehlen, A., Holzer, M., Hutter-Paier, B., Prokesch, M., Windisch, M.*, et al.* (2008). Glutaminyl cyclase inhibition attenuates pyroglutamate Abeta and Alzheimer's disease-like pathology. Nature medicine *14*, 1106-1111.
Schlenzig, D., Manhart, S., Cinar, Y., Kleinschmidt, M., Hause, G., Willbold, D., Funke, S.A., Schilling, S., and Demuth, H.U. (2009). Pyroglutamate formation influences solubility and amyloidogenicity of amyloid peptides. Biochemistry *48*, 7072-7078.
Schmechel, D.E., Saunders, A.M., Strittmatter, W.J., Crain, B.J., Hulette, C.M., Joo, S.H., Pericak-Vance, M.A., Goldgaber, D., and Roses, A.D. (1993). Increased amyloid beta-peptide deposition in cerebral cortex as a consequence of apolipoprotein E genotype in late-onset Alzheimer disease. Proceedings of the National Academy of Sciences of the United States of America *90*, 9649-9653.
Schmid, R.S., and Maness, P.F. (2008). L1 and NCAM adhesion molecules as signaling coreceptors in neuronal migration and process outgrowth. Current opinion in neurobiology *18*, 245-250.
Seabrook, G.R., Smith, D.W., Bowery, B.J., Easter, A., Reynolds, T., Fitzjohn, S.M., Morton, R.A., Zheng, H., Dawson, G.R., Sirinathsinghji, D.J.*, et al.* (1999). Mechanisms

contributing to the deficits in hippocampal synaptic plasticity in mice lacking amyloid precursor protein. Neuropharmacology *38*, 349-359.
Seals, D.F., and Courtneidge, S.A. (2003). The ADAMs family of metalloproteases: multidomain proteins with multiple functions. Genes & development *17*, 7-30.
Searfoss, G.H., Jordan, W.H., Calligaro, D.O., Galbreath, E.J., Schirtzinger, L.M., Berridge, B.R., Gao, H., Higgins, M.A., May, P.C., and Ryan, T.P. (2003). Adipsin, a biomarker of gastrointestinal toxicity mediated by a functional gamma-secretase inhibitor. The Journal of biological chemistry *278*, 46107-46116.
Seshadri, S., Fitzpatrick, A.L., Ikram, M.A., DeStefano, A.L., Gudnason, V., Boada, M., Bis, J.C., Smith, A.V., Carassquillo, M.M., Lambert, J.C*., et al.* (2010). Genome-wide analysis of genetic loci associated with Alzheimer disease. JAMA : the journal of the American Medical Association *303*, 1832-1840.
Shaw, K.L., Pais, E., Ge, S., Hardee, C., Skelton, D., Hollis, R.P., Crooks, G.M., and Kohn, D.B. (2009). Lentiviral vectors with amplified beta cell-specific gene expression. Gene therapy *16*, 998-1008.
Shen, J., Bronson, R.T., Chen, D.F., Xia, W., Selkoe, D.J., and Tonegawa, S. (1997). Skeletal and CNS defects in Presenilin-1-deficient mice. Cell *89*, 629-639.
Sherman, C.A., and Higgins, G.A. (1992). Regulated splicing of the amyloid precursor protein gene during postnatal development of the rat basal forebrain. Brain research Developmental brain research *66*, 63-69.
Siemers, E.R., Dean, R.A., Friedrich, S., Ferguson-Sells, L., Gonzales, C., Farlow, M.R., and May, P.C. (2007). Safety, tolerability, and effects on plasma and cerebrospinal fluid amyloid-beta after inhibition of gamma-secretase. Clinical neuropharmacology *30*, 317-325.
Silva, J.P., Lelianova, V., Hopkins, C., Volynski, K.E., and Ushkaryov, Y. (2009). Functional cross-interaction of the fragments produced by the cleavage of distinct adhesion G-protein-coupled receptors. The Journal of biological chemistry *284*, 6495-6506.
Sinha, S., Anderson, J.P., Barbour, R., Basi, G.S., Caccavello, R., Davis, D., Doan, M., Dovey, H.F., Frigon, N., Hong, J*., et al.* (1999). Purification and cloning of amyloid precursor protein beta-secretase from human brain. Nature *402*, 537-540.
Sisodia, S.S., Koo, E.H., Beyreuther, K., Unterbeck, A., and Price, D.L. (1990). Evidence that beta-amyloid protein in Alzheimer's disease is not derived by normal processing. Science *248*, 492-495.
Skovronsky, D.M., Moore, D.B., Milla, M.E., Doms, R.W., and Lee, V.M. (2000). Protein kinase C-dependent alpha-secretase competes with beta-secretase for cleavage of amyloid-beta precursor protein in the trans-golgi network. The Journal of biological chemistry *275*, 2568-2575.
Slack, B.E., Ma, L.K., and Seah, C.C. (2001). Constitutive shedding of the amyloid precursor protein ectodomain is up-regulated by tumour necrosis factor-alpha converting enzyme. The Biochemical journal *357*, 787-794.
Srour, N., Lebel, A., McMahon, S., Fournier, I., Fugere, M., Day, R., and Dubois, C.M. (2003). TACE/ADAM-17 maturation and activation of sheddase activity require proprotein convertase activity. FEBS letters *554*, 275-283.
St George-Hyslop, P., Haines, J., Rogaev, E., Mortilla, M., Vaula, G., Pericak-Vance, M., Foncin, J.F., Montesi, M., Bruni, A., Sorbi, S*., et al.* (1992). Genetic evidence for a novel familial Alzheimer's disease locus on chromosome 14. Nature genetics *2*, 330-334.
St George-Hyslop, P.H., Tanzi, R.E., Polinsky, R.J., Haines, J.L., Nee, L., Watkins, P.C., Myers, R.H., Feldman, R.G., Pollen, D., Drachman, D*., et al.* (1987). The genetic defect causing familial Alzheimer's disease maps on chromosome 21. Science *235*, 885-890.
Stelzmann, R.A., Alzheimer, A., Schnitzlein, H.N., and Murtagh, F.R. (1995). An English translation of Alzheimer's 1907 paper, "Uber eine eigenartige Erkankung der Hirnrinde". Clin Anat *8*, 429-431.

Stewart, S.A., Dykxhoorn, D.M., Palliser, D., Mizuno, H., Yu, E.Y., An, D.S., Sabatini, D.M., Chen, I.S., Hahn, W.C., Sharp, P.A.*, et al.* (2003). Lentivirus-delivered stable gene silencing by RNAi in primary cells. RNA *9*, 493-501.
Strittmatter, W.J., Saunders, A.M., Schmechel, D., Pericak-Vance, M., Enghild, J., Salvesen, G.S., and Roses, A.D. (1993). Apolipoprotein E: high-avidity binding to beta-amyloid and increased frequency of type 4 allele in late-onset familial Alzheimer disease. Proceedings of the National Academy of Sciences of the United States of America *90*, 1977-1981.
Suenaga, N., Mori, H., Itoh, Y., and Seiki, M. (2005). CD44 binding through the hemopexin-like domain is critical for its shedding by membrane-type 1 matrix metalloproteinase. Oncogene *24*, 859-868.
Szabo, R., and Bugge, T.H. (2011). Membrane-anchored serine proteases in vertebrate cell and developmental biology. Annual review of cell and developmental biology *27*, 213-235.
Tam, E.M., Morrison, C.J., Wu, Y.I., Stack, M.S., and Overall, C.M. (2004). Membrane protease proteomics: Isotope-coded affinity tag MS identification of undescribed MT1-matrix metalloproteinase substrates. Proceedings of the National Academy of Sciences of the United States of America *101*, 6917-6922.
Taniguchi, Y., Kim, S.H., and Sisodia, S.S. (2003). Presenilin-dependent "gamma-secretase" processing of deleted in colorectal cancer (DCC). The Journal of biological chemistry *278*, 30425-30428.
Taylor, D.R., Parkin, E.T., Cocklin, S.L., Ault, J.R., Ashcroft, A.E., Turner, A.J., and Hooper, N.M. (2009). Role of ADAMs in the ectodomain shedding and conformational conversion of the prion protein. The Journal of biological chemistry *284*, 22590-22600.
Thyagarajan, A., and Ting, A.Y. (2010). Imaging activity-dependent regulation of neurexin-neuroligin interactions using trans-synaptic enzymatic biotinylation. Cell *143*, 456-469.
Tippmann, F., Hundt, J., Schneider, A., Endres, K., and Fahrenholz, F. (2009). Up-regulation of the alpha-secretase ADAM10 by retinoic acid receptors and acitretin. The FASEB journal : official publication of the Federation of American Societies for Experimental Biology *23*, 1643-1654.
Traka, M., Goutebroze, L., Denisenko, N., Bessa, M., Nifli, A., Havaki, S., Iwakura, Y., Fukamauchi, F., Watanabe, K., Soliven, B.*, et al.* (2003). Association of TAG-1 with Caspr2 is essential for the molecular organization of juxtaparanodal regions of myelinated fibers. The Journal of cell biology *162*, 1161-1172.
Uchihara, T. (2007). Silver diagnosis in neuropathology: principles, practice and revised interpretation. Acta neuropathologica *113*, 483-499.
Urban, S., and Dickey, S.W. (2011). The rhomboid protease family: a decade of progress on function and mechanism. Genome biology *12*, 231.
van Berkel, S.S., Dirks, A.T., Debets, M.F., van Delft, F.L., Cornelissen, J.J., Nolte, R.J., and Rutjes, F.P. (2007). Metal-free triazole formation as a tool for bioconjugation. Chembiochem : a European journal of chemical biology *8*, 1504-1508.
Van Broeckhoven, C., Backhovens, H., Cruts, M., De Winter, G., Bruyland, M., Cras, P., and Martin, J.J. (1992). Mapping of a gene predisposing to early-onset Alzheimer's disease to chromosome 14q24.3. Nature genetics *2*, 335-339.
van Tetering, G., van Diest, P., Verlaan, I., van der Wall, E., Kopan, R., and Vooijs, M. (2009). Metalloprotease ADAM10 is required for Notch1 site 2 cleavage. The Journal of biological chemistry *284*, 31018-31027.
Varga, B.R., Kallay, M., Hegyi, K., Beni, S., and Kele, P. (2011). A Non-Fluorinated Monobenzocyclooctyne for Rapid Copper-Free Click Reactions. Chemistry.
Vassar, R., Bennett, B.D., Babu-Khan, S., Kahn, S., Mendiaz, E.A., Denis, P., Teplow, D.B., Ross, S., Amarante, P., Loeloff, R.*, et al.* (1999). Beta-secretase cleavage of Alzheimer's amyloid precursor protein by the transmembrane aspartic protease BACE. Science *286*, 735-741.
Velanac, V., Unterbarnscheidt, T., Hinrichs, W., Gummert, M.N., Fischer, T.M., Rossner, M.J., Trimarco, A., Brivio, V., Taveggia, C., Willem, M.*, et al.* (2012). Bace1

processing of NRG1 type III produces a myelin-inducing signal but is not essential for the stimulation of myelination. Glia *60*, 203-217.
Volynski, K.E., Silva, J.P., Lelianova, V.G., Atiqur Rahman, M., Hopkins, C., and Ushkaryov, Y.A. (2004). Latrophilin fragments behave as independent proteins that associate and signal on binding of LTX(N4C). The EMBO journal *23*, 4423-4433.
von Arnim, C.A., Kinoshita, A., Peltan, I.D., Tangredi, M.M., Herl, L., Lee, B.M., Spoelgen, R., Hshieh, T.T., Ranganathan, S., Battey, F.D*., et al.* (2005). The low density lipoprotein receptor-related protein (LRP) is a novel beta-secretase (BACE1) substrate. The Journal of biological chemistry *280*, 17777-17785.
Vossel, K.A., Zhang, K., Brodbeck, J., Daub, A.C., Sharma, P., Finkbeiner, S., Cui, B., and Mucke, L. (2010). Tau reduction prevents Abeta-induced defects in axonal transport. Science *330*, 198.
Walsh, D.M., Klyubin, I., Fadeeva, J.V., Cullen, W.K., Anwyl, R., Wolfe, M.S., Rowan, M.J., and Selkoe, D.J. (2002). Naturally secreted oligomers of amyloid beta protein potently inhibit hippocampal long-term potentiation in vivo. Nature *416*, 535-539.
Wang, H., Song, L., Laird, F., Wong, P.C., and Lee, H.K. (2008). BACE1 knock-outs display deficits in activity-dependent potentiation of synaptic transmission at mossy fiber to CA3 synapses in the hippocampus. The Journal of neuroscience : the official journal of the Society for Neuroscience *28*, 8677-8681.
Wang, H., Song, L., Lee, A., Laird, F., Wong, P.C., and Lee, H.K. (2010). Mossy fiber long-term potentiation deficits in BACE1 knock-outs can be rescued by activation of alpha7 nicotinic acetylcholine receptors. The Journal of neuroscience : the official journal of the Society for Neuroscience *30*, 13808-13813.
Wang, R., Sweeney, D., Gandy, S.E., and Sisodia, S.S. (1996). The profile of soluble amyloid beta protein in cultured cell media. Detection and quantification of amyloid beta protein and variants by immunoprecipitation-mass spectrometry. The Journal of biological chemistry *271*, 31894-31902.
Wang, Z., Du, J., Che, P.L., Meledeo, M.A., and Yarema, K.J. (2009a). Hexosamine analogs: from metabolic glycoengineering to drug discovery. Current opinion in chemical biology *13*, 565-572.
Wang, Z., Wang, B., Yang, L., Guo, Q., Aithmitti, N., Songyang, Z., and Zheng, H. (2009b). Presynaptic and postsynaptic interaction of the amyloid precursor protein promotes peripheral and central synaptogenesis. The Journal of neuroscience : the official journal of the Society for Neuroscience *29*, 10788-10801.
Weggen, S., Eriksen, J.L., Das, P., Sagi, S.A., Wang, R., Pietrzik, C.U., Findlay, K.A., Smith, T.E., Murphy, M.P., Bulter, T*., et al.* (2001). A subset of NSAIDs lower amyloidogenic Abeta42 independently of cyclooxygenase activity. Nature *414*, 212-216.
Weidemann, A., Konig, G., Bunke, D., Fischer, P., Salbaum, J.M., Masters, C.L., and Beyreuther, K. (1989). Identification, biogenesis, and localization of precursors of Alzheimer's disease A4 amyloid protein. Cell *57*, 115-126.
Wen, C., Metzstein, M.M., and Greenwald, I. (1997). SUP-17, a Caenorhabditis elegans ADAM protein related to Drosophila KUZBANIAN, and its role in LIN-12/NOTCH signalling. Development *124*, 4759-4767.
Weskamp, G., Cai, H., Brodie, T.A., Higashyama, S., Manova, K., Ludwig, T., and Blobel, C.P. (2002). Mice lacking the metalloprotease-disintegrin MDC9 (ADAM9) have no evident major abnormalities during development or adult life. Molecular and cellular biology *22*, 1537-1544.
Weskamp, G., Ford, J.W., Sturgill, J., Martin, S., Docherty, A.J., Swendeman, S., Broadway, N., Hartmann, D., Saftig, P., Umland, S*., et al.* (2006). ADAM10 is a principal 'sheddase' of the low-affinity immunoglobulin E receptor CD23. Nature immunology *7*, 1293-1298.
Whitehouse, P.J., Price, D.L., Struble, R.G., Clark, A.W., Coyle, J.T., and Delon, M.R. (1982). Alzheimer's disease and senile dementia: loss of neurons in the basal forebrain. Science *215*, 1237-1239.

Wild-Bode, C., Fellerer, K., Kugler, J., Haass, C., and Capell, A. (2006). A basolateral sorting signal directs ADAM10 to adherens junctions and is required for its function in cell migration. The Journal of biological chemistry *281*, 23824-23829.
Willem, M., Garratt, A.N., Novak, B., Citron, M., Kaufmann, S., Rittger, A., DeStrooper, B., Saftig, P., Birchmeier, C., and Haass, C. (2006). Control of peripheral nerve myelination by the beta-secretase BACE1. Science *314*, 664-666.
Wimo, A., Jonsson, L., Gustavsson, A., McDaid, D., Ersek, K., Georges, J., Gulacsi, L., Karpati, K., Kenigsberg, P., and Valtonen, H. (2011). The economic impact of dementia in Europe in 2008-cost estimates from the Eurocode project. International journal of geriatric psychiatry *26*, 825-832.
Wirths, O., Breyhan, H., Cynis, H., Schilling, S., Demuth, H.U., and Bayer, T.A. (2009). Intraneuronal pyroglutamate-Abeta 3-42 triggers neurodegeneration and lethal neurological deficits in a transgenic mouse model. Acta neuropathologica *118*, 487-496.
Wittig G, K.A. (1961). Zur Existenz niedergliedriger Cycloalkine. Chem Berichte *94*, 3260-3275.
Wiznerowicz, M., and Trono, D. (2003). Conditional suppression of cellular genes: lentivirus vector-mediated drug-inducible RNA interference. Journal of virology *77*, 8957-8961.
Wolfe, M.S., De Los Angeles, J., Miller, D.D., Xia, W., and Selkoe, D.J. (1999a). Are presenilins intramembrane-cleaving proteases? Implications for the molecular mechanism of Alzheimer's disease. Biochemistry *38*, 11223-11230.
Wolfe, M.S., Xia, W., Ostaszewski, B.L., Diehl, T.S., Kimberly, W.T., and Selkoe, D.J. (1999b). Two transmembrane aspartates in presenilin-1 required for presenilin endoproteolysis and gamma-secretase activity. Nature *398*, 513-517.
Wolozin, B.L., Pruchnicki, A., Dickson, D.W., and Davies, P. (1986). A neuronal antigen in the brains of Alzheimer patients. Science *232*, 648-650.
Wright, A.G., Demyanenko, G.P., Powell, A., Schachner, M., Enriquez-Barreto, L., Tran, T.S., Polleux, F., and Maness, P.F. (2007). Close homolog of L1 and neuropilin 1 mediate guidance of thalamocortical axons at the ventral telencephalon. The Journal of neuroscience : the official journal of the Society for Neuroscience *27*, 13667-13679.
Xu, H., Sweeney, D., Wang, R., Thinakaran, G., Lo, A.C., Sisodia, S.S., Greengard, P., and Gandy, S. (1997). Generation of Alzheimer beta-amyloid protein in the trans-Golgi network in the apparent absence of vesicle formation. Proceedings of the National Academy of Sciences of the United States of America *94*, 3748-3752.
Yamasaki, M., Thompson, P., and Lemmon, V. (1997). CRASH syndrome: mutations in L1CAM correlate with severity of the disease. Neuropediatrics *28*, 175-178.
Yan, R., Bienkowski, M.J., Shuck, M.E., Miao, H., Tory, M.C., Pauley, A.M., Brashier, J.R., Stratman, N.C., Mathews, W.R., Buhl, A.E*., et al.* (1999). Membrane-anchored aspartyl protease with Alzheimer's disease beta-secretase activity. Nature *402*, 533-537.
Yan, R., Han, P., Miao, H., Greengard, P., and Xu, H. (2001). The transmembrane domain of the Alzheimer's beta-secretase (BACE1) determines its late Golgi localization and access to beta -amyloid precursor protein (APP) substrate. The Journal of biological chemistry *276*, 36788-36796.
Yang, L., Wang, Z., Wang, B., Justice, N.J., and Zheng, H. (2009). Amyloid precursor protein regulates Cav1.2 L-type calcium channel levels and function to influence GABAergic short-term plasticity. The Journal of neuroscience : the official journal of the Society for Neuroscience *29*, 15660-15668.
Yount, J.S., Moltedo, B., Yang, Y.Y., Charron, G., Moran, T.M., Lopez, C.B., and Hang, H.C. (2010). Palmitoylome profiling reveals S-palmitoylation-dependent antiviral activity of IFITM3. Nature chemical biology *6*, 610-614.
Yu, G., Nishimura, M., Arawaka, S., Levitan, D., Zhang, L., Tandon, A., Song, Y.Q., Rogaeva, E., Chen, F., Kawarai, T*., et al.* (2000). Nicastrin modulates presenilin-mediated notch/glp-1 signal transduction and betaAPP processing. Nature *407*, 48-54.

Zheng, H., Jiang, M., Trumbauer, M.E., Sirinathsinghji, D.J., Hopkins, R., Smith, D.W., Heavens, R.P., Dawson, G.R., Boyce, S., Conner, M.W*., et al.* (1995). beta-Amyloid precursor protein-deficient mice show reactive gliosis and decreased locomotor activity. Cell *81*, 525-531.
Zielinska, D.F., Gnad, F., Wisniewski, J.R., and Mann, M. (2010). Precision mapping of an in vivo N-glycoproteome reveals rigid topological and sequence constraints. Cell *141*, 897-907.
Zlokovic, B.V. (1996). Cerebrovascular transport of Alzheimer's amyloid beta and apolipoproteins J and E: possible anti-amyloidogenic role of the blood-brain barrier. Life sciences *59*, 1483-1497.
Zufferey, R., Donello, J.E., Trono, D., and Hope, T.J. (1999). Woodchuck hepatitis virus posttranscriptional regulatory element enhances expression of transgenes delivered by retroviral vectors. Journal of virology *73*, 2886-2892.
Zufferey, R., Nagy, D., Mandel, R.J., Naldini, L., and Trono, D. (1997). Multiply attenuated lentiviral vector achieves efficient gene delivery in vivo. Nature biotechnology *15*, 871-875.
Zwicker, N., Adelhelm, K., Thiericke, R., Grabley, S., and Hanel, F. (1999). Strep-tag II for one-step affinity purification of active bHLHzip domain of human c-Myc. BioTechniques *27*, 368-375.

8 Publication List

Determination of the proteolytic cleavage sites of the amyloid precursor-like protein 2 by the proteases ADAM10, BACE1 and γ-secretase.

Hogl S, **Kuhn PH**, Colombo A, Lichtenthaler SF.

PLoS One. 2011;6(6):e21337. Epub 2011 Jun 17

F-spondin regulates neuronal survival through activation of disabled-1 in the chicken ciliary ganglion.

Peterziel H, Sackmann T, Strelau J, **Kuhn PH**, Lichtenthaler SF, Marom K, Klar A, Unsicker K.

Mol Cell Neurosci. 2011 Feb;46(2):483-97. Epub 2010 Dec 9.

ADAM10 is the physiologically relevant, constitutive alpha-secretase of the amyloid precursor protein in primary neurons.

Kuhn PH, Wang H, Dislich B, Colombo A, Zeitschel U, Ellwart JW, Kremmer E, Rossner S, Lichtenthaler SF.

EMBO J. 2010 Sep 1;29(17):3020-32. Epub 2010 Jul 30.

Transmembrane protein 147 (TMEM147) is a novel component of the Nicalin-NOMO protein complex.

Dettmer U, **Kuhn PH**, Abou-Ajram C, Lichtenthaler SF, Krüger M, Kremmer E, Haass C, Haffner C.

J Biol Chem. 2010 Aug 20;285(34):26174-81. Epub 2010 Jun 10.

9 Acknowledgement

Ich danke meinen Eltern und meiner Familie für die kontinuierliche Unterstützung auf meinem Weg als Wissenschaftler und ein offenes Ohr, wenn ich schwierige Situationen zu meistern hatte. Des Weiteren danke ich meinem Betreuer Prof. Dr. Stefan Lichtenthaler für die gute Zusammenarbeit, den Willen, mir viele Freiräume in meiner Forschung einzuräumen und seiner Offenheit gegenüber neuen Technologien. Darüber hinaus danke ich meinen Arbeitskollegen, die zum Teil auch zu Freunden geworden sind, für die gute Arbeitsatmosphäre, harte aber faire wissenschaftliche Diskussionen und viele gemeinsame lustige, feuchtfröhliche Abende. Ich möchte diese Danksagung mit einem auf den erst Blick schlichtem Zitat beschließen, denn dies ist auch mein Leitmotiv in der Wissenschaft.

„*Sei naiv und mach ein Experiment*“ von Feodor Lynen